Buoy-based detection of low-energy cosmic-ray neutrons to monitor the influence of atmospheric, geomagnetic, and heliospheric effects

Martin Schrön[1], Daniel Rasche[2], Jannis Weimar[3], Markus Otto Köhli[4], Konstantin Herbst[5], Bertram Boehrer[6], Lasse Hertle[7], Simon Kögler[7], and Steffen Zacharias[8]

[1]Helmholtz Centre for Environmental Research GmbH - UFZ
[2]GFZ German Research Centre for Geosciences
[3]Physikalisches Institut, Heidelberg University
[4]Heidelberg University
[5]Christian-Albrechts-Universität zu Kiel
[6]UFZ - Helmholtz Centre for Environmental Research
[7]Helmholtz-Centre for Environmental Research - UFZ, Department for Monitoring and Exploration Technologies
[8]UFZ Helmholtz Centre for Environmental Research

December 21, 2023

Abstract

Cosmic radiation on Earth responds to heliospheric, geomagnetic, atmospheric, and lithospheric changes. In order to use its signal for soil hydrological monitoring, the signal of thermal and epithermal neutron detectors needs to be corrected for external influencing factors. However, theories about the neutron response to soil water, air pressure, air humidity, and incoming cosmic radiation are still under debate. To challenge these theories, we isolated the neutron response from almost any terrestrial changes by operating bare and moderated neutron detectors in a buoy on a lake in Germany from July 15 to December 02, 2014. We found that the count rate over water has been better predicted by a recent theory compared to the traditional approach. We further found strong linear correlation parameters to air pressure and air humidity for epithermal neutrons, while thermal neutrons responded differently. Correction for incoming radiation proved to be necessary for both thermal and epithermal neutrons, for which we tested different neutron monitors and correction methods. Here, the conventional approach worked best with the Jungfraujoch monitor in Switzerland, while the approach from a recent study was able to adequately rescale data from more remote neutron monitors. However, no approach was able to sufficiently remove the signal from a major Forbush decrease event, to which thermal and epithermal neutrons showed a comparatively strong response. The buoy detector experiment provided a unique dataset for empirical testing of traditional and new theories on CRNS. It could serve as a local alternative to reference data from remote neutron monitors.

Buoy-based detection of low-energy cosmic-ray neutrons to monitor the influence of atmospheric, geomagnetic, and heliospheric effects

Martin Schrön[1,*], Daniel Rasche[2,*], Jannis Weimar[3], Markus Köhli[3], Konstantin Herbst[4], Bertram Boehrer[5], Lasse Hertle[1], Simon Kögler[1], Steffen Zacharias[1]

[1]Helmholtz-Centre for Environmental Research - UFZ, Department for Monitoring and Exploration Technologies, Leipzig, Germany
[2]GFZ German Research Centre for Geosciences, Section Hydrology, Potsdam, Germany
[3]Physikalisches Institut, Heidelberg University, Im Neuenheimer Feld 226, 69120 Heidelberg, Germany
[4]Institute for Experimental and Applied Physics, University of Kiel, Kiel, Germany
[5]Helmholtz-Centre for Environmental Research - UFZ, Department for Limnology, Leipzig, Germany
[*]These authors contributed equally to this study

Key Points:

- Neutron detectors on a buoy were deployed in the center of a lake for five months.
- Thermal and epithermal signals correlated with air pressure, air humidity, and secondary cosmic rays from neutron monitors.
- Data was used to challenge traditional correction approaches and to serve as an alternative neutron monitor.

Corresponding author: Martin Schrön, martin.schroen@ufz.de

Abstract

Cosmic radiation on Earth responds to heliospheric, geomagnetic, atmospheric, and lithospheric changes. In order to use its signal for soil hydrological monitoring, the signal of thermal and epithermal neutron detectors needs to be corrected for external influencing factors. However, theories about the neutron response to soil water, air pressure, air humidity, and incoming cosmic radiation are still under debate. To challenge these theories, we isolated the neutron response from almost any terrestrial changes by operating a bare and a moderated neutron detector in a buoy on a lake in Germany from July 15 to December 02, 2014. We found that the count rate over water has been better predicted by a theory from Köhli et al. (2021) compared to the traditional approach from Desilets et al. (2010). We further found strong linear correlation parameters to air pressure ($\beta = 0.0077\,\mathrm{mb}^{-1}$) and air humidity ($\alpha = 0.0054\,\mathrm{m}^3/\mathrm{g}$) for epithermal neutrons, while thermal neutrons responded with $\alpha = 0.0023\,\mathrm{m}^3/\mathrm{g}$. Both approaches, from Rosolem et al. (2013) and from Köhli et al. (2021), were similarly able to remove correlations of epithermal neutrons to air humidity. Correction for incoming radiation proved to be necessary for both thermal and epithermal neutrons, for which we tested different neutron monitor stations and correction methods. Here, the approach from Zreda et al. (2012) worked best with the Jungfraujoch monitor in Switzerland, while the approach from McJannet and Desilets (2023) was able to adequately rescale data from more remote neutron monitors. However, no approach was able to sufficiently remove the signal from a major Forbush decrease event on September 13th, to which thermal and epithermal neutrons showed a comparatively strong response. The buoy detector experiment provided a unique dataset for empirical testing of traditional and new theories on CRNS. It could serve as a local alternative to reference data from remote neutron monitors.

Plain Language Summary

Earth's cosmic radiation near the ground is influenced by solar activity and atmospheric conditions but is also crucial for monitoring soil moisture and snow. To better understand how cosmic-ray neutron measurements should be corrected for meteorological effects, we operated a detector for low-energy neutrons in a buoy on a lake in Germany for five months in 2014. Since the water content in the surroundings is constant, we were able to isolate the signal from almost any ground-related disturbances. With this instrument, we challenged traditional and recent theories on the neutron response to water, air humidity, and to reference data from high-energy neutron monitors around the world. We found that in some cases, recent theories showed superior performance over traditional approaches. We also found a stronger response of the neutrons detected by the buoy to a major solar event than was observed by traditional neutron monitors. The concept of a neutron detector on a lake could be useful as a reference station for similar land-side detectors and help provide more reliable soil moisture products.

1 Introduction

The natural background radiation on Earth is mainly produced by the omnipresent and continuous exposure to galactic cosmic rays, which are modulated by solar activity, filtered by the geomagnetic field, and moderated by the Earth's atmosphere (Hess et al., 1961; Dorman, 2004; Usoskin et al., 2011). Since 1951, neutron monitors have been in operation at various places around the globe to continuously monitor high-energy cosmogenic neutrons as a proxy for space weather (Väisänen et al., 2021). About half a century ago, Kodama et al. (1975) revealed the potential of the lower energetic component of cosmic-ray neutrons for estimating water content in snow. Two decades after Kodama (1980) and Kodama et al. (1985) presented more experimental findings also related to soil moisture, Dorman (2004) proposed the broader use of this concept for hydrological applications. Yet, Zreda et al. (2008) were the first to introduce the methodological framework of Cosmic-Ray Neutron Sensing (CRNS) and to demonstrate its potential for large-scale monitoring of soil moisture. Soon after, Desilets et al. (2010) proposed an empirical but turned-out-to-be robust relationship to convert neutrons to soil moisture, followed by Zreda et al. (2012) presenting the concept and establishment of a continental CRNS network. To date, CRNS is a growing non-invasive and low-maintenance technique providing continuous hectare-scale root-zone soil moisture to inform and validate products of hydrological models (Baatz et al., 2014; Iwema et al., 2017; Patil et al., 2021) and remote sensing (Montzka et al., 2017; Döpper et al., 2022; Schmidt et al., 2024).

The ambient epithermal neutron radiation above the ground is of key interest for CRNS, as this energy band shows the highest sensitivity to hydrogen in soils (Desilets et al., 2010; Zreda et al., 2012; Köhli et al., 2015). Some CRNS probes additionally measure thermal neutrons as a potential proxy for soil chemistry, snow, biomass, or spatial heterogeneity (Tian et al., 2016; Jakobi et al., 2022; Rasche et al., 2021). In order to isolate the response of neutrons to the ground from external influences, CRNS data processing heavily relies on accurate corrections for changes in atmospheric shielding depth (i.e., air pressure), atmospheric hydrogen content (i.e., air humidity), and incoming cosmic rays (i.e., high-energy hadron flux). For epithermal neutrons, such corrections have been proposed based on literature about high-energy cosmic rays (Desilets et al., 2006; Zreda et al., 2012) or on dedicated simulations (Rosolem et al., 2013). However, no commonly accepted correction approaches exist for thermal neutrons, while the transferability of the epithermal correction functions is under debate (Andreasen et al., 2017; Jakobi et al., 2018, 2022; Rasche et al., 2021).

There is an ongoing debate about many aspects of CRNS theory and the traditional correction approaches since correlations to external signals were sometimes not removed sufficiently, and unexplained variations in the data remained. For example, Köhli et al. (2021) used new simulation approaches to explain neutron variations specifically in semi-arid regions, where limitations of the widely established approaches from Desilets et al. (2010) and Rosolem et al. (2013) became evident. However, the simulations from Köhli et al. (2021) were also insufficient to conclude on a final choice out of many offered correction models. Moreover, many authors have found inconsistencies in using the neutron monitor "Jungfraujoch" in Switzerland as a reference for the incoming cosmic-ray flux at different periods and locations on Earth (e.g. Hawdon et al., 2014; Schrön, 2017; Hands et al., 2021). The main reason is the dependence of the cosmic-ray flux on the geomagnetic field, which changes continuously in space and time (Belov et al., 2005; Kudela, 2012; Herbst et al., 2013). To account for that, authors suggested different correction approaches to rescale data from a neutron monitor site to a CRNS location (Hawdon et al., 2014; McJannet & Desilets, 2023), while their performance is yet to be tested. Nevertheless, more issues complicate the use of the neutron monitor network as a reference for CRNS stations across the world: the instruments measure different neutron energies than CRNS, they are sometimes prone to weather effects, the few neutron monitors have only scarce coverage on Earth, the data exhibits varying consistency and quality, and a single institute is responsible for the data provision and processing (Bütikofer, 1999; Aplin et al., 2005; Korotkov et al., 2011; Oh et al., 2013; Abunin et al., 2016; Ruffolo et al., 2016; Väisänen et al., 2021). Consequently, the future availability of incoming cosmic-ray reference data may not be guaranteed, which explains the current search for alternative concepts (e.g. Schrön et al., 2016; Fersch et al., 2020; Gugerli et al., 2022; Stevanato et al., 2022).

An empirical and objective evaluation of traditional and new theories on the neutron response to the ground, to the atmosphere, and to the magnetosphere, is a challenging endeavour. Any ground-based CRNS measurement inherently depends on the spatial and temporal variability of nearby hydrogen pools, such as soil moisture, biomass, ponding water, etc. (Iwema et al., 2021; Schrön et al., 2023). However, such variability can be considered negligible above lakes or other water bodies, were even rain events would not introduce a significant addition of water. Neutron measurements on a lake with a detector that has a comparable energy sensitivity to CRNS could provide a unique data set to investigate the local and "actual" influence of non-terrestrial variability on thermal and epithermal neutrons. In terrestrial CRNS applications, many of the external, ground-related influencing factors are often unknown and thus challenging to model, leading to uncertainties in the interpretation of the CRNS signal. A buoy detector on a lake, however, has a clear pure-water boundary condition and would allow for a more direct comparison of the observations with simulations of the sensor response. Moreover, a lake-base buoy CRNS detector might be even suitable as a reference monitor for the incoming cosmic-ray flux.

The advantage of water bodies beneath a neutron detector has been first reported by Krüger and Moraal (2010), who performed intercalibration measurements of high-energy neutron monitors all over the world by placing a miniature detector over a small nearby pool. CRNS detectors, however, are sensitive to the surrounding environment up to radii of 300 meters (Desilets & Zreda, 2013; Köhli et al., 2015). Hence, Franz et al. (2013) suggested short measurements on a lake to calibrate the pure-water limit of the sensor response, which was conducted using rafts for a few days by McJannet et al. (2014), Andreasen et al. (2017) and Rasche et al. (2023). The first long-term experiment of CRNS detectors on a lake was proposed and conducted in 2014 and later reported by Schrön et al. (2016) and Schrön (2017). The idea was further extended by Weimar (2022) with static and mobile measurements. The present study performs a first detailed analysis of the data set from 2014 and uses it to challenge traditional correction functions and recent CRNS theories.

The first hypothesis of this study is that state-of-the-art theories about the neutron-to-water relationship can predict the drop in neutron count rates from land to water. Here, we will challenge the widely established method from Desilets et al. (2010) and the more recent findings from Köhli et al. (2021). With any ground-related changes of water content removed, we further hypothesize that the hitherto established and partly debated correction functions for air pressure (Desilets et al., 2006; Zreda et al., 2012), air humidity (Rosolem et al., 2013; Köhli et al., 2021), and incoming cosmic radiation (Zreda et al., 2012; Hawdon et al., 2014; McJannet & Desilets, 2023) can adequately remove all remaining temporal variations during the study period. The performance of these approaches will also be tested for thermal neutrons, for which no study has yet confirmed their applicability. Finally, we propose using the buoy detector as an alternative for neutron monitors as a reference for incoming radiation, and test this hypothesis at a nearby CRNS research site.

2 Methods

2.1 Detection of cosmic radiation on Earth

Cosmic radiation mainly consists of protons and heavier ions, permanently penetrating the Earth's magnetic field and interacting with the Earth's atmosphere (Simpson, 1983). Their collision with nitrogen, carbon, or oxygen atoms in the air produces high-energy particle showers, which consist of neutrons, protons, muons, and other particles. Neutrons and protons can be detected by high-energy neutron monitors (NM) on Earth (Mavromichalaki et al., 2011; Väisänen et al., 2021). The muon component is regularly monitored by the global muon detector network (Rockenbach et al., 2014). Both their signals are a measure of the incoming cosmic radiation on Earth's surface and, as such, highly correlated to space weather and solar activity. Besides typical periodicities, such as the 22-year solar cycle, also irregular short-term events may change the incoming cosmic-ray flux significantly. Examples of these striking solar events are Forbush decreases (FD) or Ground-Level Enhancement (GLE). They are temporary reductions or enhancements of the cosmic ray flux observed on Earth, caused by the passage of a solar flare or coronal mass ejection (Laken et al., 2011; Mishev et al., 2014; Lingri et al., 2019; Hands et al., 2021).

As the cosmic-ray particles interact with the atmosphere, their signal on the ground additionally carries information on atmospheric conditions, such as air pressure, air humidity, and atmospheric temperature. For research on space weather, it is important to correct for such atmospheric factors, while research on the response of cosmic rays to the ground surface requires both atmospheric and heliospheric influences to be corrected for. To investigate these corrections empirically with ground-based sensors, however, it is necessary to exclude any ground-related influencing factors.

The interaction of high-energy cosmic rays with the ground usually produces lower energetic neutrons, which are, in turn, sensitive to environmental factors such as water content (Zreda et al., 2012). NMs make use of thick high-density polyethylene shields and lead producers to do both, reduce the influence of those low-energy neutrons that have already interacted with the ground, and tailor the sensitivity to direct high-energy cosmic radiation. Data from NMs available from the global Neutron Monitor database (`https://www.nmdb.eu`) is already corrected for atmospheric pressure and acts as a reference of incoming cosmic radiation on Earth for many adjacent research fields (Mavromichalaki et al., 2011). The distribution of NM stations across the globe aims at covering a range of geomagnetic locations, since the intensity and variability of cosmic rays are a function of the so-called vertical cutoff rigidity of the geomagnetic field, (R_c). This quantity relates to the alignment of the magnetic field lines, which acts as an energy filter of the primary cosmic-ray particles that leads to higher radiation exposure at the poles compared to the equator. Table 1 shows an overview of the NMs used in this study: Jungfraujoch (JUNG) is the standard reference for incoming radiation correction in CRNS research, Athens (ATHN) exhibits high vertical cutoff rigidity in Europe, Kiel (KIEL) is the closest NM to the study site, Oulu (OULU) exhibits the lowest cutoff rigidity in Europe, South pole (SOPO) the lowest globally, while Daejeon (DJON) and Doi Inthanon (PSNM) may serve as promising candidates to test the correction performance with NMs at very high cutoff rigidities and in very large distance to the study site.

2.2 Cosmic-ray neutron sensing (CRNS)

Detectors with a reduced amount of shielding are more sensitive to low-energy neutrons and, thus, to the local environment on the ground. A technology with reduced shielding is called cosmic-ray neutron sensing (CRNS) and is based on the response of low-energy neutrons to nearby environmental water content (Zreda et al., 2008). The main energies used in hydrological CRNS applications are the epithermal neutrons (with energies between 0.5 eV and 10^5 eV), and thermal neutrons (energies below 0.5 eV), as they show the strongest variation with water content (Köhli et al., 2015). In dry soil, the epithermal neutrons produced

Table 1. Overview of the Neutron Monitors (NM) and the buoy detector site used in this study, including their coordinates and geomagnetic cutoff rigidity, R_c, from two different sources (values for 2010 from `https://www.nmdb.eu` and for 2014 from `https://crnslab.org/util/rigidity.php`).

Neutron Monitor	Acronym	Country	R_c (2010)	R_c (2014)	Altitude	Latitude	Longitude
Doi Inthanon	PSNM	Thailand	16.80 GV	16.72 GV	2565 m	18.59°	98.49°
Daejeon	DJON	South Korea	11.22 GV	10.75 GV	200 m	36.24°	127.22°
Athens	ATHN	Greece	8.53 GV	8.27 GV	260 m	37.97°	23.78°
Jungfraujoch	JUNG	Switzerland	4.50 GV	4.54 GV	3570 m	46.55°	7.98°
Buoy	Buoy	Germany	2.99 GV	2.93 GV	78 m	51.58377°	12.41423°
Kiel	KIEL	Germany	2.36 GV	2.31 GV	54 m	54.34°	10.12°
Oulu	OULU	Finland	0.80 GV	0.63 GV	15 m	65.05°	25.47°
South Pole	SOPO	Antarctica	0.10 GV	0.06 GV	2820 m	-90°	0°

by the penetration of high-energy particles may leave the ground almost unhindered. In wet soil, on the other hand, the higher concentration of hydrogen efficiently moderates the neutrons on their way, leading to less epithermal neutron counts above the surface. While epithermal neutron variations are mainly dependent on the hydrogen abundance, thermal neutron radiation shows an additional dependency on chemical components and is still a subject of research. Thermal neutrons can be detected with standard neutron detectors, such as proportional counters. Epithermal neutrons can be detected with an additional layer of high-density polyethylene around these bare detector tubes (Zreda et al., 2012; Schrön et al., 2018).

The wetness of the ground is usually expressed as the soil moisture θ in units of g/g. Conversion functions exist to describe its relationship to epithermal neutrons, $N(\theta)$. The traditional function has been introduced by Desilets et al. (2010):

$$N^{\mathrm{Des}}(\theta) \propto \frac{0.0808}{\theta + 0.115} + 0.372. \tag{1}$$

It is independent on hydrogen in air, for instance, which could be addressed by a separate correction factor on the neutrons (see section below). A recent study by Köhli et al. (2021) introduced a universal transfer solution (UTS) for soil moisture conversion which is inseparable from the air humidity, h in g/m^3, of the environment:

$$N^{\mathrm{UTS}}(\theta, h) \propto \left(\frac{p_1 + p_2\,\theta}{p_1 + \theta} \cdot \left(p_3 + p_4\,h + p_5\,h^2\right) + e^{-p_6\,\theta}\,\left(p_7 + p_8\,h\right)\right), \tag{2}$$

where p_i represents a range of parameter sets out of many possible candidates offered by Table A1 in Köhli et al.. They either depend on different simulation approaches or employ different energy response functions (see also Köhli et al., 2018). The parameter set "MCNP drf" was derived from MCNP (Goorley et al., 2012) simulations, which include interaction processes of neutrons, protons, muons, and other particles. It also integrates the actual energy response function of the CRNS detector (drf). In contrast, the parameter set "MCNP THL" uses the MCNP model with a less accurate energy threshold window. Parameter sets "URANOS drf" and "URANOS THL" express similar detector models, while URANOS has been used instead of MCNP to simulate the neutron response to soil and water, which includes only neutron particle interactions and some effective and less accurate representation of other particles (see Köhli et al., 2023, for details).

Both approaches, Desilets et al. (2010) and Köhli et al. (2021), have in common that they provide a relative value for neutron count rates that can be scaled with a factor N_0, usually referred to as a calibration parameter. It is different for each approach and parameter set but essentially mimics the detector-specific count rate at a very dry state of the soil.

From calculations using typical ranges of θ and h it follows that the N_0 values for the UTS function are larger than N_0 for the Desilets approach by factors of 1.61, 2.09, 1.58, and 2.03 for the parameter sets "MCNP drf", "MCNP THL", "URANOS drf", and "URANOS THL", respectively.

To date, there is no published evidence of a preferred parameter set for CRNS data processing with the UTS approach. Standard evaluation procedures would require a high number of auxiliary measurements of soil moisture in the sensor footprint and different depths, in addition to consideration of spatial heterogeneity and other disturbing factors typically present at most field sites. However, an experiment with $\theta =$ const. could facilitate an empirical determination of $N(h)$ to shine a light on a suitable parameter set that describes this part of the model realistically.

A water body is expected to produce a minimal number of neutrons, which, unlike for soils, does not change as a result of rainfall events (i.e., $\theta =$ const.). Hence, it is expected that neutrons measured above a lake are only dependent on atmospheric conditions or solar activity. In the pure-water environment, we follow the limes approach by Schrön et al. (2023), $\theta \to \infty$, with which Eq. (1) reduces to:

$$\lim_{\theta\to\infty} N^{\mathrm{Des}}(\theta) = 0.372\,, \tag{3}$$

while Eq. (2) reduces to:

$$\lim_{\theta\to\infty} N^{\mathrm{UTS}}(\theta, h) = p_2\,(p_3 + p_4\,h + p_5\,h^2)\,. \tag{4}$$

The latter varies from 0.15 to 0.28 depending on air humidity and on the chosen parameter set (Table A1 in Köhli et al., 2021).

2.3 Atmospheric and geomagnetic corrections

Previous studies have introduced correction functions for the measured neutrons to remove the effect of air pressure P, air humidity h, and incoming radiation I. Conventionally, these functions are usually treated as factors on the neutron counts (except for Eq. (2)):

$$\begin{aligned}
\text{humidity-corrected} \quad N_h &= N(\theta)\cdot C_h\,, \\
\text{pressure-corrected} \quad N_P &= N(\theta)\cdot C_P\,, \\
\text{incoming-corrected} \quad N_I &= N(\theta)\cdot C_I\,, \\
\text{fully-corrected} \quad N_{hPI} &= N(\theta)\cdot C_h\cdot C_P\cdot C_I\,.
\end{aligned} \tag{5}$$

Air humidity can be corrected by two different approaches. The established approach by Rosolem et al. (2013) uses a separate correction factor based on the air humidity h (in g/m^3):

$$C_h = 1 + \alpha\,(h - h_{\mathrm{ref}})\,. \tag{6}$$

The parameter α accounts for water vapor in the near or total atmosphere. It was determined by Rosolem et al. (2013) using neutron transport simulations. However, systematic experimental validation has not been reported, yet. The other approach refers to Eq. (2), which intrinsically accounts for air humidity in a non-separable way. In this case, $N_h \equiv N(\theta, h)$ or $C_h = 1$.

Air pressure can be corrected using an established exponential function:

$$C_P = e^{\beta(P-P_{\mathrm{ref}})}\,. \tag{7}$$

The attenuation coefficient β equals the inverse attenuation length, L^{-1}, and has been used for decades to process atmospheric correction of cosmic rays. It can be determined using different analytical relations (Clem et al., 1997; Dunai, 2000; Desilets et al., 2006), by minimizing the correlation between incoming radiation and air pressure (Sapundjiev et al., 2014), or by comparing neutron time series with a reference station, where β is known (Paschalis et al., 2013). These various approaches show that β might be a complex variable that depends on several factors, such as latitude, altitude, type and energy of incident particles (Clem & Dorman, 2000; Dorman, 2004, and references therein), on variations during the solar cycle and during solar flare events (Dorman, 2004; Kobelev et al., 2011), and on properties and yield function of the detector device (Bütikofer, 1999).

We make use of an established calculation of L following Dunai (2000) and Desilets and Zreda (2001):

$$\beta^{-1} = L(i) = y + \frac{a}{\left(1 + e^{(x-i)/b}\right)^c} , \tag{8}$$

where i is the Earth's magnetic field inclination and the empirical parameters are $a = 19.85$, $b = -5.43$, $x = 62.05$, $y = 129.55$. The inclination at the buoy's location can be determined from National Centers for Environmental Information (2015) and was $i = 66.9°$. This leads to theoretical prediction of $L = 129.7\,\mathrm{g/cm^2}$ or $\beta = 0.0077\,\mathrm{mbar}$. An alternative tool that is often used by the CRNS community, is the website `http://crnslab.org/util/rigidity.php`, which predicts $L = 137.0\,\mathrm{g/cm^2}$ or $\beta = 0.0073\,\mathrm{mbar}$ for the buoy location. However, both tools are also based on calculations derived for high-energy particles and a specific temporal state of the magnetosphere, while the neutron attenuation has never been explicitly identified for the lower-energetic CRNS detectors. Given the uncertainty in determining the correct value for the attenuation coefficient, in this study, we use an average value of $L = 133.0\,\mathrm{g/cm^2}$.

The approach for correcting incoming radiation has been first formulated by Zreda et al. (2012) and generalized by Schrön et al. (2016):

$$C_I = \left(1 - \gamma\,(1 - I/I_{\mathrm{ref}})\right)^{-1} . \tag{9}$$

It uses reference data I from the neutron monitor database that measures only the incoming, high-energy component of the cosmic radiation at a few selected locations on Earth. The parameter γ depicts the amplitude scaling of signal variations depending on geomagnetic location. The conventional approach has been assuming $\gamma = 1$, but it failed to remove the incoming cosmic-ray variability, especially for large distances between CRNS and NM sites. The underlying challenge is the dependency of the incoming signal on the geomagnetic location, expressed by the cutoff rigidity, R_c in GV, of the geomagnetic field. For example, sites near the geomagnetic poles see different cosmic-ray particles than sites near the equator. So ideally, reference data for incoming radiation should be collected from an NM near the CRNS measurement site, i.e., at a similar cutoff rigidity.

Hawdon et al. (2014) presented a scaling concept to account for this geomagnetic effect using $\gamma = 1 - 0.075\,(R_\mathrm{c} - R_\mathrm{c}^{\mathrm{ref}})$, however, this approach has not been tested globally. A more recent approach by McJannet and Desilets (2023) uses so-called scaling factors that depend on R_c and on the atmospheric depth x for both the location of the site and of the neutron monitor used as a reference:

$$C_I = \tau^{-1} , \tag{10}$$

$$\tau(x, R_c) = \tau_{\mathrm{ref}}^{-1} \cdot \epsilon\,(-p_0\,x + p_1)\left(1 - \exp\left(-\,(p_2\,x + p_3)\,R_\mathrm{c}^{p_4\,x - p_5}\right)\right) , \tag{11}$$

with parameters p_i fitted on historical NM data. An empirical test of these approaches for the correction of incoming radiation is still missing.

Besides various correction functions, the neutron data presented in this study has been smoothed by temporal aggregation or moving average filters. These temporal smoothing approaches are useful to reduce noise in highly resolved time series in order to improve further comparative calculations, correlations, or visualizations. In the current processing scheme, the correction functions have been applied on the raw data first, followed by subsequent smoothing. Since there is also a debate about the correct order of these processing steps, we elaborated on this discussion in more detail in Appendix A.

2.4 The buoy deployment

To address the open questions on an empirical evaluation of atmospheric and geomagnetic correction approaches for the CRNS method, we decided to deploy a CRNS detector system on a lake. With a minimum amount of surrounding material, a detector system with a thermal and an epithermal neutron counter would mainly "see" the surrounding lake water. As the amount of surrounding water seen by the CRNS detector remained the same for floating device was not effected by precipitation or evapotranspiration, respectively, the total ground-related influence on the neutrons could be assumed constant. The remaining variations of neutrons should be induced by atmospheric conditions or solar activity only. An ideal set of correction functions would be able to reduce the neutron variations over time to zero ± stochastic errors.

For this experiment, we chose the lake *Seelhausener See*, which was located about 100 km southwest of Berlin, Germany at the border between the federal states Saxony and Saxony-Anhalt (Fig. 1a). The lake had formed in the abandoned opencast of a lignite mine (e.g. Geller et al., 2013). The lake is still not accessible for public use and thus offered the perfect place for exposing sensible technology in the environment. The surrounding is flat land with mainly natural vegetation.

In the preparation of this study, the URANOS model by Köhli et al. (2023) has been used to simulate the origin of the detected neutrons, following the signal contribution concept presented by Köhli et al. (2015) and Schrön et al. (2023). The environment has been modeled in a $700 \times 700\,\mathrm{m}^2$ domain (Fig. 1b) with a virtual detector above water, a given land structure with 10 % soil moisture, and air with $10\,\mathrm{g/m^3}$ humidity. We found that a distance of $\approx 300\,\mathrm{m}$ from the shore is appropriate to limit the influence of the land on the buoy detector to less than 2 %.

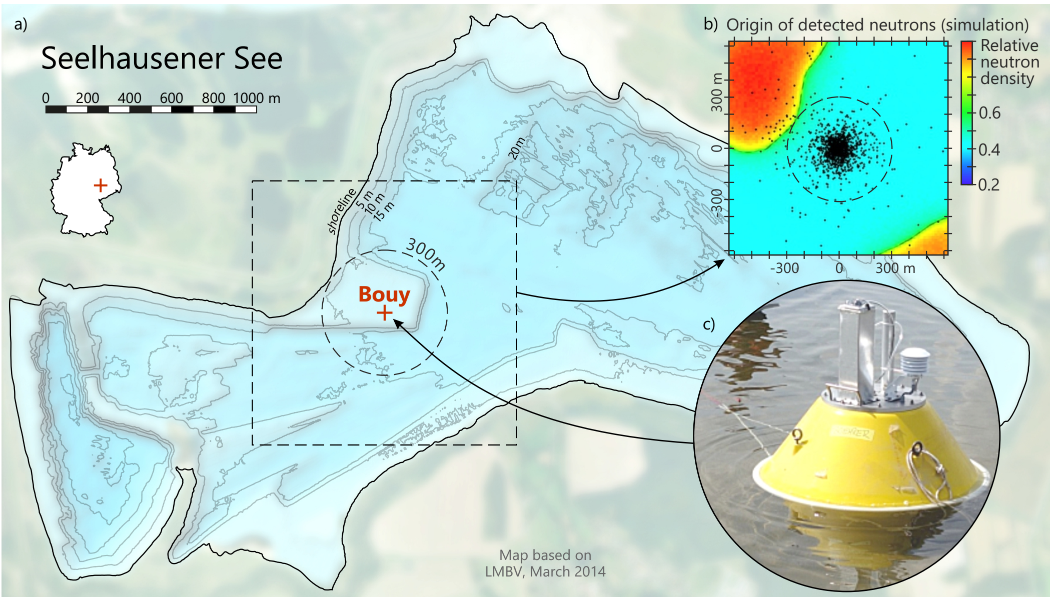

Figure 1. a) Location of the CRNS buoy detector at lake *Seelhausener See*. b) The distance of 300 m from the shoreline was chosen such that more than 98,% of detected neutrons had contact to water only (black dots, simulated with URANOS). c) Photograph of the buoy in operation. Map credits: adapted from LMBV, March 2014.

Instruments were placed inside a buoy of type `601 Profiler` from Idronaut S.r.l. and then tied between two anchors at the coordinates (51.58377°, 12.41423°). (Fig. 1c). Each rope was put under tension by mounting a trawl net ball (see Fig. 2). Other then usual anchoring techniques (e.g. Boehrer & Schultze, 2008), this arrangement kept the buoy in place within about 1 m and in the same orientation independently of rising or falling water levels over the entire study period.

The moderated and the bare tube was taken from a standard stationary CRNS system of type CRS1000 (Hydroinnova LLC, Albuquerque, US) that had previously been operated at the UFZ Leipzig (Schrön et al., 2018). The detectors were disassembled and integrated in a tailor-made aluminum lid, protruding upwards from the buoy (Fig. 2). The system was powered by eight batteries of type Yuasa NPL, 38 Ah, using lead-fleece technology to guarantee proper functioning under wobbling conditions. After installation on July 15th, 2014, the batteries had to be recharged by the end of September as the power supply lasted 2.5 months. Finally, the buoy was retracted under frosty conditions on December 2nd, 2014. An antenna regularly transmitted sensor data and GPS coordinates to an FTP server to allow scientists to remotely keep track of the battery status, and for the sake of protection against theft and tempest. The system further included external sensors for air temperature, relative air humidity, and air pressure to facilitate atmospheric corrections.

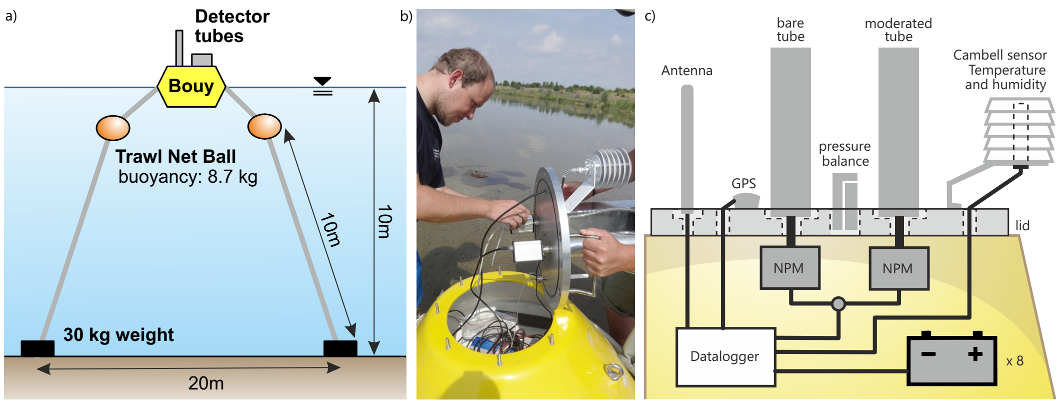

Figure 2. a) Setup of the buoy in the lake at around 10 m depth using trawl net balls and weights. b) Final checks with an open lid near the shore before the final launch into the water. c) Detector housing inside the tailor-made lid of the buoy, including GPS, antenna for data transmission, external sensors for air conditions, and a large battery array.

3 Results and Discussion

3.1 Buoy dataset

The measurement data of the buoy system is shown in Fig. 3. From July to December 2014, the air pressure varied by 30 mbar, while air temperature decreased from 20°C to 0°C and relative air humidity increased from 40 to 100 %. We have also calculated the absolute air humidity, h, following Rosolem et al. (2013). The epithermal neutron count rate has been 416 ± 41 cph, while thermal neutrons showed on average 240 ± 31 cph. According to counting statistics following Schrön et al. (2018), the expected stochastic error of the epithermal neutron count rate would be ± 20 cph (hourly) or ± 4 cph (daily), and of thermal neutrons ± 15 cph (hourly) or ± 3 cph (daily). In this context, the actually measured count rate already indicates a non-negligible influence of atmospheric and heliospheric factors. The time series has been gap-free with the exception of a short maintenance period in September 30th. Additionally, a Forbush decrease event has been captured on September 13th, which led to a significant drop of neutron count rates by ≈ 10 %.

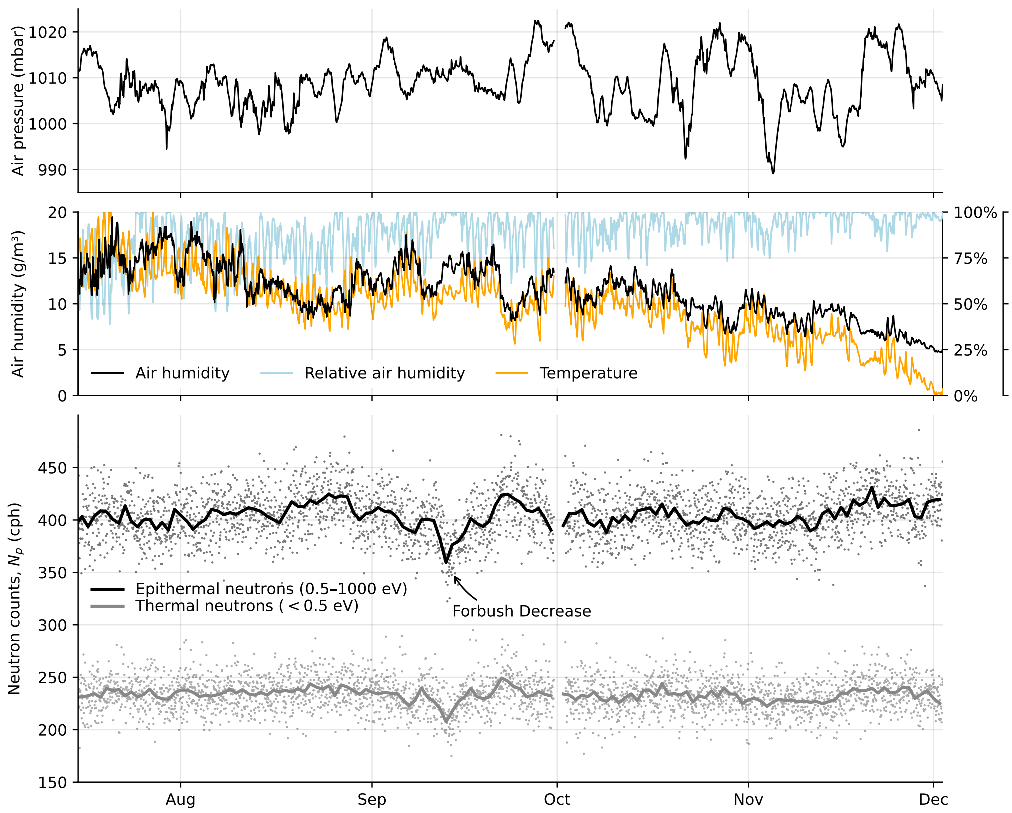

Figure 3. Data collected with the buoy instrument in 2014. Top: Air pressure. Middle: External air humidity and temperature. Bottom: pressure-corrected neutron counts of epithermal (0.5–1000 eV, black) and thermal energies (0–0.5 eV, grey). Dots depict hourly measurements, and solid lines depict the daily aggregation. A Forbush decrease event has been detected on September 13th. Maintenance work, including battery exchange, has been conducted on September 30th.

3.2 Challenging the neutrons-to-water relationship

Compared to typical over-land locations, the detector showed a significant drop of neutron counts over water by almost 50 % (compare Schrön et al., 2018, Fig. 3). Based on this observation, it was possible to test whether the existing concepts to describe the relationship between neutrons and water content, $N(\theta)$ (Eqs. (1), (2)), make the correct predictions following Eqs. (3) and (4).

The same detector type used in the buoy, CRS1000, has also been used on other locations, where $N_0^{\mathrm{Des}} \approx 1000\,\mathrm{cph}$ has been determined through calibration (see, e.g., Bogena et al., 2022). This corresponds to $N_0^{\mathrm{UTS}} = 1610\,\mathrm{cph}$, $2090\,\mathrm{cph}$, $1580\,\mathrm{cph}$, and $2030\,\mathrm{cph}$ for the UTS paremeter sets "MCNP drf", "MCNP THL", "URANOS drf", and "URANOS THL", respectively (section 2.2). Based on the assumption that these N_0 parameters are also applicable to the buoy detector, the expected count rate in a pure-water environment (Eqs. (3), (4)) would become 372 cph, 411 cph, 322 cph, 302 cph, 315 cph for the five approaches, respectively. Hence, the measured average count rate of 416 cph on the lake is in best agreement with the theoretical value of the "MCNP drf" parameter set from Köhli et al. (2021) for $\theta \to \infty$. The agreement is certainly within the uncertainty band of the data (see Fig. 3), while the remaining discrepancy could arise from a non-negligible effect of neutrons produced by the buoy material and the lead batteries themselves.

From this analysis, we can draw two conclusions. Firstly, the recently suggested parameter set for $N(\theta, h)$ derived from the full particle-physics model (MCNP) and the full detector response model (drf) fits best to the measured data and thus creates evidence for its potential superiority over the other parameter sets, including the approach from Desilets et al. (2010). Secondly, the buoy detector in this study seems to be a suitable representation of a pure-water scenario despite the substantial extent and material of the buoy itself and despite the finite distance to the shore.

3.3 Correlation of epithermal and thermal neutrons to external factors

The influences of (i) air pressure, (ii) air humidity, and (iii) incoming radiation on epithermal neutrons have been addressed in the literature, where various approaches exist to correct for these effects (section 2.3). Corrections for thermal neutrons have not been investigated so far, usually following the assumption that the same functions apply for them, too. For both neutron energies, however, empirical validation remains difficult, since neutron measurements above soils are always governed by the spatial and temporal variability of soil moisture, as well as by the site-specific heterogeneity (Schrön et al., 2023). In contrast, it is expected that neutron observations on a lake would not show terrestrial variability, thereby allowing for an evaluation of non-terrestrial correction approaches.

Fig. 4 shows the correlation between the daily relative neutron intensity and atmospheric variables. In each panel, neutron counts have been corrected for two variables and correlated to the corresponding third variable (compare section 2.3). Variations in air pressure exert the strongest influence on epithermal neutrons ($R^2 = 0.91$), followed by variations in incoming radiation ($R^2 = 0.67$), represented by data from the JUNG NM, and absolute air humidity ($R^2 = 0.61$). Thermal neutrons follow the same rank order.

For air pressure, the correction parameter $\beta = 0.0077\,\mathrm{mb}^{-1}$ seems to be an adequate choice for both thermal and epithermal neutrons. It matches exactly (within the uncertainty bounds) with the theoretical value of 0.0077 predicted by Dunai (2000). However, it differs slightly from the value of 0.0073 suggested by Desilets et al. (2006) and the corresponding and typically used calculation tool `http://crnslab.org/util/rigidity.php`. Note that β can change in time and space, such that the value determined in this experiment is not globally transferable. Further research should investigate the performance of the two methods with experimental data at other locations.

The regression coefficient for absolute air humidity, $0.0054\,\mathrm{m}^3/\mathrm{g}$, exactly matches the linear correction factor α derived by Rosolem et al. (2013), confirming the robustness of this approach. Unlike for epithermal neutrons, the correction procedure required for thermal neutrons has remained under debate. For instance, Andreasen et al. (2017) and Rasche et al. (2021) did not correct thermal neutrons for variations in air humidity, arguing that

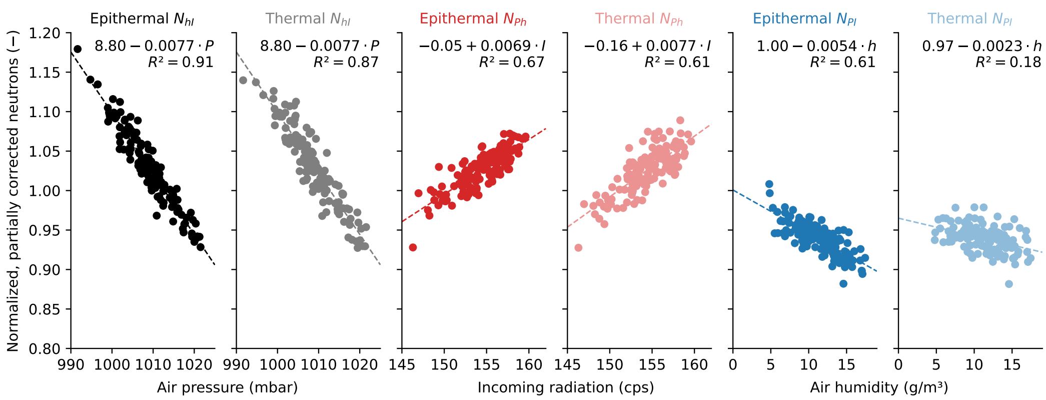

Figure 4. Partially corrected daily epithermal and thermal neutron observations normalized by their mean, correlated with three meteorological variables. Left two panels: neutrons corrected for air humidity and incoming radiation versus air pressure. Middle two panels: neutrons corrected for air humidity and air pressure versus incoming radiation. Right two panels: neutrons corrected for air pressure and incoming radiation versus air humidity. Each panel also shows the parameters of a linear model fit (dashed line).

the traditional correction functions have been derived for epithermal neutrons only. From dedicated simulations, Rasche et al. (2023) found a new value for thermal neutron correction, $\alpha = 0.0021\,\mathrm{m}^3/\mathrm{g}$. In contrast, based on empirical findings, Jakobi et al. (2018, 2022) correct thermal neutron intensities for air pressure and absolute humidity but not for variations in incoming radiation. They claimed that their empirical findings suggested better performance against biomass estimations.

The buoy-detector observations shed light on the required correction procedures for thermal neutrons as the effect of other hydrogen pools (e.g., biomass and soil moisture) on the empirical relationship can be excluded. Fig. 4 indicates that thermal neutrons are similarly dependent on variations in air pressure and incoming radiation compared to epithermal neutrons. The largest difference between epithermal and thermal neutrons by applying the same correction occurs in respect to variations in absolute air humidity. We found that the linear regression slope, 0.0023, is less than half of that of epithermal neutrons and very close to the value recently found by Rasche et al. (2023). The difference of thermal to epithermal neutron response to air humidity is likely linked to the generally higher production rate of thermal neutrons by epithermal neutron moderation than the thermal neutron absorption rate which leads to a weaker response of thermal neutrons to variations in environmental hydrogen (Weimar et al., 2020).

Consequently, the observations in this study indicate that epithermal and thermal neutron intensities need to be corrected for all three atmospheric variables. With respect to existing correction approaches, it is evident that the correction factor for air humidity should be different for epithermal and thermal neutrons, using $\alpha = 0.0054\,\mathrm{m}^3/\mathrm{g}$ (Rosolem et al., 2013) and $\alpha = 0.0021\,\mathrm{m}^3/\mathrm{g}$ (Rasche et al., 2023), respectively.

3.4 Apparent correlation of thermal neutrons to water temperature

The observation that the air humidity correction parameters for epithermal and thermal neutrons are different may have significant impact on the growing number of studies related to thermal neutron monitoring. Some previous studies applied the same correction approach from epithermals also to the thermal neutrons without accounting for this difference (Jakobi et al., 2018, 2022; Bogena et al., 2020). This may introduce a risk of overcorrection and apparent correlation to other variables. In the case of the buoy experiment, the conventional air humidity correction would cause an apparent correlation of thermal neutrons to lake water temperature. In fact, the observed corrected count rate of thermal neutrons in Fig. 5a showed a significantly higher correlation to the lake temperature ($R^2 = 0.26$) compared to corrected epithermal neutrons ($R^2 = 0.01$). We will explain below that this connection appears logical at first glance, but it is a fallacy on closer inspection.

By definition, the energy range of thermal neutrons corresponds to the mean kinetic energy of atoms in the environment, and thus their temperature. The theoretical foundation for this phenomenon is the temperature dependency of neutron cross sections (Glasstone & Sesonske, 1981). The cross section σ represents the probability of an interaction with an atomic nucleus. Interaction is less likely for larger relative velocities between target and particle v, i.e., $\sigma \propto 1/v$. In equilibrium, velocity and temperature are related by the Maxwell-Boltzmann distribution, where the (mean) particle energy is given by $E \propto mv^2 \propto kT$. Hence, σ ultimately depends on the temperature T of the scattering target: $\sigma(T) \propto \sqrt{1/T}$. Since water has a much higher density than humid air, the temperature of the lake might be more relevant than the air temperature.

While the higher temperature increases the thermal neutron density in air and water, it reduces the detection probability of the helium-3 counting gas in the same way (Krüger et al., 2008). The total observable influence on the thermal neutron count rate is a combination of two effects as air and lake temperatures decrease towards the winter: (i) increasing cross sections of nuclei in air and water, which removes more neutrons on their way to the detector and leads to a decreasing thermal neutron density in the system, and (ii) at the same time, increasing cross sections of nuclei in the Helium-3 gas, enabling higher detection efficiency which leads to higher count rates. Both processes scale with $\sqrt{1/T}$ in different directions. Since lake water temperature and detector temperature show the same dynamics (Appendix B), the two effects should almost annihilate each other. Fig. 5b shows the calculated temperature effect of the lake on the thermal neutron production (blue) and the thermal neutron detection (orange). The combined effects (black) almost cancel each other out and leave a nearly constant influence on the thermal neutron count rate.

Hence, the remaining correlation of thermal neutrons to lake temperature results from the wrong correction coefficient of $\alpha = 0.0054\,\mathrm{m^3/g}$. The observation data in Fig. 4 demonstrate that the thermal neutrons response to air humidity is much smaller compared to epithermal neutrons. Using the recently published correction factor, $\alpha = 0.0021\,\mathrm{m^3/g}$ (Rasche et al., 2023), which is very close the empirical observation from the buoy, the new correlation becomes $R^2 = 0.01$ for thermal neutrons and thereby confirms the insignificance of the temperature effect.

The example demonstrates the risk of overcorrection and false conclusions from data when the physical process understanding is incomplete. On the other hand, we cannot exclude remaining features in the data that could indicate systematic influences on the neutron count rate. For example, dew formation or ice on the buoy lid could be responsible for additional neutron moderation in autumn and winter, while extreme variations of shore moisture could impact the count rate in the summer. After a finalized analysis of the known external influences, we have further investigated the remaining correlations in section 3.7.

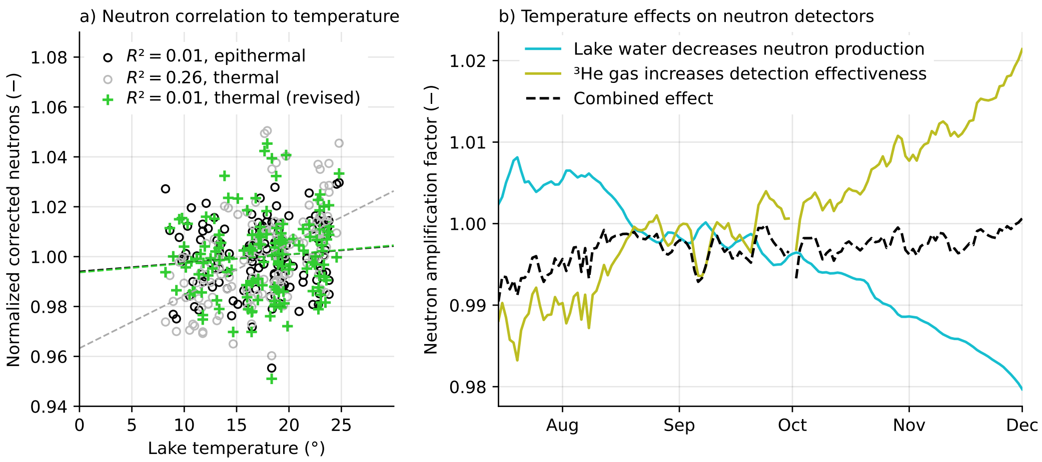

Figure 5. The effect of temperature on the measured buoy neutrons. a) Correlation of epithermal (black) and thermal neutrons (grey) to the lake temperature after conventional atmospheric corrections. This introduced an overcorrection for thermal neutrons. A revised air humidity correction approach simulated by Rasche et al. (2023) and confirmed by this study removed this remaining correlation. (b) Processes relevant for neutron production and absorption based on temperature over time. The reduced production of colder water essentially cancels out the enhanced detection efficiency of the detector gas.

3.5 Challenging the air humidity correction for epithermal neutrons

As discussed before, air humidity can have a significant effect on the neutron count rate due to varying density and amount of hydrogen atoms in the atmosphere. Rosolem et al. (2013) and Köhli et al. (2021) derived mathematical relationships from neutron transport simulations, but they are difficult to validate experimentally due to the high amount of other influencing environmental variables. With the exclusion of terrestrial factors, such as soil moisture and biomass, the use of lake-side measurements can be again an advantageous solution here.

To investigate which correction approach performs best at the buoy site, we correct the epithermal neutrons with air pressure and incoming radiation (N_{Pi}). If the remaining variability is only related to air humidity changes, the P, i-corrected neutrons should equal the inverse correction factor C_h^{-1}. In this ideal case, this difference is expected to become zero. To quantify the performance of each air humidity correction approach, we calculate the root-mean square error (RMSE) between N_{Pi} and C_h^{-1} over the whole measurement period.

Table 2 shows the result of this calculation. The hitherto approach from Rosolem et al. (2013) exhibits the lowest RMSE, again confirming a good performance for air humidity correction, see also section 3.3. However, the UTS approach with the parameter set "MCNP drf" is comparable in performance with an insignificantly larger error, while other parameter sets show weaker performance. This confirms the results from section 3.2 and the robustness of the full particle-physics and detector models. The fact that the approach from Rosolem et al. provides slightly better results than the UTS may be linked to the fact that the UTS was not tailored to describe the neutron response to changing air humidity alone. UTS has been optimized to solve the neutron response to the complex combination of soil moisture and air humidity, which could introduce lesser accuracy for air humidity variations alone.

Table 2. Root mean square error (RMSE) between the observed corrected epithermal intensity for air pressure and incoming radiation, N_{Pi}, and the inverse air humidity correction C_h^{-1} for the approaches from Rosolem et al. (2013) and UTS (see section 2.3). The analysis has also been performed for three different approaches of incoming radiation to test its robustness.

Incoming correction for N_{Pi}	Rosolem et al.	MCNP drf	MCNP THL	URANOS drf	URANOS THL
Zreda et al. (2012)	**5.39**	5.50	6.18	6.42	6.94
Hawdon et al. (2014)	**5.40**	5.48	6.09	6.31	6.82
McJannet and Desilets (2023)	**5.38**	5.48	6.13	6.37	6.88

3.6 Challenging the incoming cosmic-ray correction

Buoy-detector observations of neutrons in the epithermal and thermal energy range above a water surface and over a period of several months also allows for a comparison of the different correction approaches available for correcting neutron observations for variations in incoming radiation. The three available correction approaches described in the methods section were tested with seven different neutron monitors shown in Tab. 1 and compared with a thermal and epithermal neutron observations corrected for variations in air pressure and absolute air humidity (N_{Ph}), as this correction level should represent variations from changes in incoming radiation, only. In order to reduce the statistical noise in the data from the buoy detector, a 25-hour moving average was applied after applying the corrections. The epithermal and thermal N_{Ph} was then compared to the inverted correction factors for incoming radiation based on Zreda et al. (2012), Hawdon et al. (2014) and McJannet and Desilets (2023) (see section 2.3).

Table 3 shows the results from the analysis performed for selected neutron monitor stations. The Kling-Gupta Efficiency (KGE) was chosen as the goodness-of-fit measure in order to equally account for variation, correlation, and bias. The analysis reveals that the performance is generally lower for thermal neutrons compared to epithermal neutrons. This can be linked to the higher statistical uncertainty in the thermal neutron data due to the lower count rates. Likewise, a higher difference in cutoff rigidity between the locations of the neutron monitor and the study site leads to a lower KGE for both neutron energies. However, the Jungfraujoch neutron monitor still reveals the highest KGE, although its cutoff rigidity and altitude are higher than at the study site (compare Tab. 1).

Furthermore, it can be seen that the approaches from Hawdon et al. (2014) and McJannet and Desilets (2023) improve the KGE for the comparison with neutron monitors with higher cutoff rigidity than the study site compared to the approach after Zreda et al. (2012). In contrast, for neutron monitors with a lower cutoff rigidity, this improvement disappears and the approach according to Zreda et al. (2012) reveals a higher KGE with the data from the buoy detector. This effect is evident for both epithermal and thermal neutrons. The recent approach from McJannet and Desilets (2023) outperforms the approach by Hawdon et al. (2014), while both only lead to improvements for higher cutoff rigidities compared to the standard approach after Zreda et al. (2012). On average and over all neutron monitors investigated, the approach after McJannet and Desilets (2023) performs best in scaling neutron monitor signals to the location of the buoy detector, followed by the approach after Hawdon et al. (2014) and Zreda et al. (2012).

All three approaches provided robust results using data from the JUNG NM, with a slightly superior performance of Hawdon et al. (2014) at the study site. Additionally, the correct selection of a reference monitor seems to be more influential than then correction

Table 3. Performance measured by the Kling-Gupta Efficiency (KGE) of different correction approaches to rescale incoming neutron intensities from different neutron monitor stations compared with the observed and P, h-corrected epithermal (E) and thermal (T) neutron counts of the buoy. See also Tab. 1 for the corresponding cutoff rigidities and altitudes.

	C_I approach	PSNM	DJON	ATHN	JUNG	KIEL	OULU	SOPO	Average
E	Zreda et al. (2012)	0.269	0.34	0.465	0.737	0.678	0.667	**0.765**	0.560
E	Hawdon et al. (2014)	0.560	0.543	0.640	**0.790**	0.651	0.566	0.692	0.634
E	McJannet and Desilets (2023)	0.639	0.703	**0.761**	0.760	0.647	0.613	0.619	0.677
T	Zreda et al. (2012)	0.220	0.280	0.408	**0.635**	0.594	0.587	0.714	0.491
T	Hawdon et al. (2014)	0.481	0.460	0.567	**0.689**	0.569	0.493	0.614	0.553
T	McJannet and Desilets (2023)	0.627	0.624	**0.699**	0.657	0.565	0.537	0.545	0.608

method. The results generally indicate the advanced correction approaches from Hawdon et al. (2014) and particularly McJannet and Desilets (2023) improve the performance only for higher cutoff rigidities (i.e., regions near the equator). These findings may be also linked to the complex behavior of incoming radiation with different effects occurring at different cutoff rigidities, altitudes, latitudes, and longitudes (López-Comazzi & Blanco, 2020, 2022). The time series of epithermal and thermal neutrons are shown in Fig. 6 together with the time series of the JUNG, PSNM, and SOPO neutron monitors. Especially during the Forbush decrease in September 2014, a dampening of the neutron signal of the PSNM neutron monitor compared to the JUNG neutron monitor can be seen, which is linked to the higher R_c of PSNM. In addition, a temporal shift between PSNM and JUNG indicates differences between neutron monitor intensities due to different longitudinal locations. Lastly, the epithermal and thermal intensities decrease stronger than JUNG and PSNM, but similar to SOPO. This is an unexpected behavior, as the cutoff rigidity of SOPO is much lower than at the buoy location. The coincidence could indicate that low-energy neutron counters generally respond stronger to geomagnetic changes than high-energy NMs. Particularly with regards to the Forbush decrease, the observed discrepancy could also be linked to a change of the primary cosmic-ray energy spectrum during solar events (Bütikofer, 2018), which may lead to stronger changes of secondary low-energy cosmic-ray neutrons.

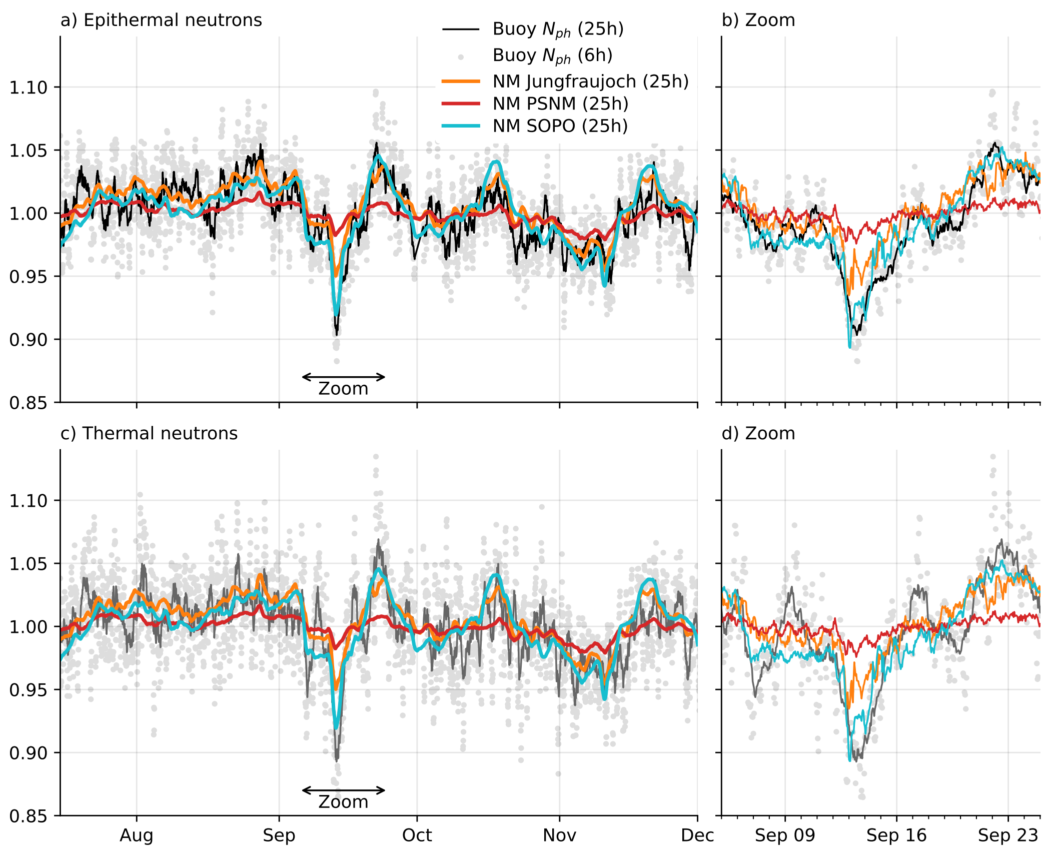

Figure 6. Normalized pressure- and humidity-corrected neutron count rates of the buoy detector compared with neutron monitor data. a) Epithermal buoy neutrons with a moving average window of 6 hours (grey dots) and 25 hours (black line). The latter filter was also applied to the NM data from JUNG in Switzerland (orange), PSNM in Thailand (red), and SOPO near the South Pole (blue). b) Zoom-in to the Forbush decrease event. c-d) Same as a-b for thermal buoy neutrons.

Depending on the moderator material and material thickness, proportional neutron detectors show varying sensitivity to neutrons of different energies (Garny et al., 2009; Köhli et al., 2018). A difference in the response of a bare thermal neutron detector and a neutron monitor has been shown by Nuntiyakul et al. (2018). Furthermore, Hubert et al. (2019) found a different response to solar events for neutrons of different energies. For the correction of neutron intensities for incoming radiation in the scope of CRNS, it, therefore, may not be sufficient to scale the neutron monitor response to different cutoff rigidities and atmospheric shielding depths only (Hawdon et al., 2014; McJannet & Desilets, 2023), but also to account for the different response of low-energy neutron detectors and neutron monitors.

The question about the choice of the most suitable neutron monitor for CRNS correction is equivalent to the question of which monitor better represents the local changes of cosmic-ray neutrons at the CRNS site. Sometimes, the answer is not obvious considering just geographical location parameters. For example, compared to the location of the buoy experiment, the KIEL monitor has more similar distance, altitude, and cutoff rigidity than JUNG. However, the neutron dynamics of the buoy can be better explained by JUNG, while KIEL behaves differently during and beyond the Forbush decrease event. These findings indicate the need for further research on the role of primary incoming radiation for low-energy cosmic-ray neutron sensing.

3.7 Residual correlations

The proper correction of all influencing factors on the neutrons should result in a time series, where residual deviations from the mean represent Poissonian noise. To test this hypothesis, a correlation analysis of N_{Phi} was conducted using a selection of atmospheric variables. In addition, different aggregation levels have been applied to further test the either random or systematic character of the relationships. The Spearman's rank correlation coefficient is shown in Tab. 4. It indicates that the influence of air pressure, incoming radiation, and absolute humidity is removed by the previously discussed correction procedures. However, a significant correlation between the N_{Phi} and relative air humidity remained for all aggregation levels and for both neutron energies.

High values of relative air humidity may indicate the formation of dew and, thus, a thin film of water on the buoy-detector, which reduces the observed neutron intensity of the epithermal and thermal detector due to higher neutron absorption. For example, Sentelhas et al. (2008) use a threshold of ≥ 90 percent relative humidity to distinguish periods with leaf wetness. Applying this threshold to the neutron observations reveals that epithermal and thermal N_{Phi} are, on average, 0.44 and 0.56 percent lower in periods with dew, respectively. This indicates that some influencing atmospheric variables are not yet considered in the standard correction procedures and illustrates the need for further research.

Furthermore, the statistical accuracy increases strongly with increasing integration times. Already at the 6-hour aggregation level, the Poisson standard deviation of the uncorrected neutron observations becomes lower than 2 percent. However, neutron transport simulation revealed that approx. 2 percent of epithermal neutrons reach the buoy-detector from the shore, indicating that with higher statistical accuracy, terrestrial variables such as soil moisture variations could influence the neutron observations of the buoy detector. This indicates some limitations of the measurement design in this study and illustrates potential improvements for future lake-side neutron measurements.

Table 4. Spearman's rank correlation coefficient between the corrected intensity (N_{Phi}) of epithermal (E) and thermal (T) neutrons aggregated to different temporal resolutions. Asterisk indicates statistical significance with $p < 0.05$.

	Variable	aggregation: 1 hour	6 hour	12 hour	24 hour
E	Air pressure	0.04	0.07	0.07	0.1
E	NM (Jungfraujoch)	0.003	0.02	−0.006	0.01
E	Abs. air humidity	−0.02	−0.04	−0.05	−0.09
E	Air temperature	0.003	0.02	0.01	0.0009
E	Rel. air humidity	−0.07*	−0.2*	−0.2*	−0.3*
E	Water temperature	0.01	0.03	0.03	0.008
E	Moist air density	0.006	−0.000004	0.01	0.03
E	Precipitation	0.0005	−0.09	−0.10	−0.20
T	Air pressure	0.03	0.08	0.06	0.03
T	NM (Jungfraujoch)	−0.006	−0.02	−0.04	−0.08
T	Abs. air humidity	−0.04*	−0.08	−0.10	−0.20*
T	Air temperature	−0.0007	−0.01	−0.07	−0.1
T	Rel. air humidity	−0.07*	−0.1*	−0.2*	−0.2*
T	Water temperature	−0.002	0.02	0.03	0.08
T	Moist air density	0.009	0.03	0.08	0.1
T	Precipitation	0.01	−0.006	−0.08	−0.10

3.8 Potential for the buoy as a reference for CRNS probes

Typical CRNS stations are located on natural ground to monitor soil moisture dynamics or agricultural fields, grass lands, or even snow dynamics in the alps. The conventional correction approach uses incoming radiation from neutron monitors (e.g., Jungfraujoch) to remove unwanted effects from solar activity, such as Forbush decreases.

We used data from a nearby terrestrial CRNS site at the UFZ Leipzig (25 km distance), where six identical CRNS stations were co-located on a $20 \times 20\,\mathrm{m}^2$ grassland patch. The sum of their signals mimics a larger CRNS station with up to 6000 cph ($\approx 1.4\,\%$ uncertainty).

Figure 7 shows the epithermal neutron data from this aggregated sensor corrected for air pressure and air humidity (dashed line). The solid line shows the data conventionally corrected for incoming neutrons with the NM Jungfraujoch. It is evident that the correction generally improves the obvious response to rain events, but the correction of the Forbush decrease in September 13 was not strong enough. The orange line shows the same correction approach with the epithermal neutron data measured at the same time by the buoy. The data was filtered by a 3-day moving average to reduce the buoy's noise level. The correction using the local buoy data better removes the Forbush decrease from the corrected CRNS neutron counts (September 13) and is also able to strengthen the response to some rain events (e.g., August 24 and September 17).

The results demonstrate that the concept of buoy detector can be used as an alternative to neutron monitors to correct for the incoming radiation. However, measurements on the buoy are limited by the low count rate due to the surrounding water and small detectors, such that there is a risk of introducing additional noise to the CRNS station data by this correction approach.

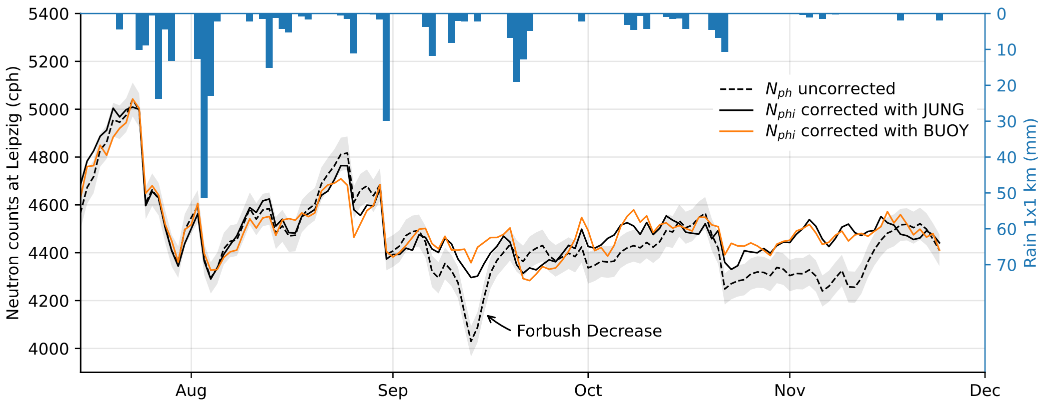

Figure 7. Epithermal neutrons aggregated from six collocated CRNS stations at the UFZ Leipzig, 25 km away (Schrön et al., 2018, data from). Neutron counts were corrected for air pressure and air humidity (dashed black) and corrected for incoming radiation using NM Jungfraujoch (solid black) and the buoy data (solid orange). Daily precipitation is indicated from Radolan measurements.

4 Conclusion

This study presents the concept of a thermal and an epithermal neutron detector in a buoy on a lake. The arrangement depicts an innovative opportunity to monitor the response of low-energy cosmic-ray neutrons to atmospheric conditions and to space weather without the influence of the ground, soil moisture, or any other nearby terrestrial heterogeneity that can influence the neutron counts. The experiment conducted on a lake in East Germany covered an almost gap-free period of five months from July 15th to December 2nd, 2014, including temperatures from 30 to 0°C, and - by chance - a major solar event (Forbush decrease). The unique data set facilitates empirical research on challenging conventional theories and traditional correction functions for atmospheric, geomagnetic, and heliospheric variations. The experiment revealed the following insights:

1. The epithermal neutron count rate over water dropped by more than 50 % compared to values over typical soil. The measured count rate was not in agreement with the theoretical value predicted by the previous $N(\theta)$ model (Desilets et al., 2010). In contrast, the value was almost exactly predicted by the UTS approach (Köhli et al., 2021) using the parameter set "MCNP drf". This finding might indicate a potential superiority of UTS for the conversion from neutrons to soil moisture also for other CRNS applications.
2. The buoy data showed strong correlation to air pressure, which was similar for both, epithermal and thermal neutrons. The thereby empirically determined neutron attenuation length was in very good agreement with the theoretical prediction by Dunai (2000), while it was 5 % lower than the conventional calculation for this region. This indicates that further research is needed to better adapt traditional calculation methods on the special requirements of low-energy neutron detectors.
3. The different approaches for air humidity correction have been challenged by their ability to remove undesired variations of the buoy signal. The conventional approach by Rosolem et al. (2013) performed best and its parameter $\alpha = 0.0054$ has been confirmed for epithermal neutrons. Almost similar performance was achieved by the UTS approach using the parameter set "MCNP drf", while all other parameter sets were not able to fully remove air humidity variations.
4. Conventional thermal neutron corrections for air humidity, however, led to a significant overcorrection. A potential influence of lake water temperature on the thermal neutrons has been excluded by analysis of the nuclear interaction cross sections. A different correction parameter for thermal neutrons has been identified, which confirmed independent results from Rasche et al. (2023).
5. The response to incoming cosmic radiation is almost similar for both, epithermal and thermal neutrons, in contrast to assumptions by some previous studies. We challenged three existing correction approaches by comparing the buoy data with data from various neutron monitors and found robust performance for NM Jungfraujoch and the approach from Zreda et al. (2012). The more sophisticated approaches by Hawdon et al. (2014) and McJannet and Desilets (2023) showed particularly good skills in rescaling data from NMs with higher cut-off rigidities than the measurement site.
6. The remarkable Forbush decrease (FD) observed in Sept 2014 was more pronounced in the buoy data than in data from the NMs, particularly for thermal neutrons. In addition to the findings from the pressure correction above, this is another indication that the scaling of incoming radiation from NMs to CRNS is not well enough understood, probably due to the sensitivity to different particle energies.
7. After all corrections were applied, the remaining variations of the buoy signal have been investigated. For both, thermal and epithermal neutrons, a significant correlation to relative air humidity became evident, which could be an indication for yet unnoticed sensitivity to dew.

In a final test, we used the buoy data as a reference signal for the incoming radiation correction of a nearby CRNS site. Here, a slightly better correction capability was evident, particularly during the FD event. This experiment demonstrated that a buoy could act as a suitable local alternative for a neutron monitor, especially since it measures similar energy levels as the CRNS, it is much cheaper than an NM, and it could be installed more closer to CRNS sites, thereby avoiding any geomagnetic or location-specific biases. However, buoys are limited in size, such that their data is highly uncertain due to the low count rates. Daily temporal resolution was the minimum for our system to be applicable as a reference monitor. To overcome this weakness, future studies could deploy buoy detectors on high-altitude lakes or glaciers, which would equally well resemble a pure-water environment for the neutrons with much higher count rates (e.g., Gugerli et al., 2019, 2022).

We encourage the usage of the presented data set for further research on new theories or correction functions. One more example is the debate of whether to apply temporal smoothing algorithms before or after atmospheric corrections. With the buoy data, we were able to show that correction prior to smoothing is crucial for maintaining correlation to the incoming radiation data, for instance (see sect. Appendix A).

Appendix A The order of smoothing and correction procedures matters

The buoy experiment provides a perfect test for meteorological correction functions. For example, it has been discussed in the community whether smoothing prior (Heidbüchel et al., 2016) or after correcting neutron data (Franz et al., 2020; Davies et al., 2022) is recommended. With the buoy data, this hypotheses can be tested without influence of ground-based variations.

In general, temporal smoothing of a time series is a linear operation f, since

$$f: \quad x(t) = \sum_{t-\tau}^{t+\tau} w \cdot x(t') / \sum_{t-\tau}^{t+\tau} w \,,$$

where 2τ is the window size over which the data is averaged, and w is a weighting factor (e.g., 1 for a uniform average, or $e^{-\tau}$ for exponential filters). In contrast, some correction functions can be non-linear, e.g., the correction for air pressure or for incoming radiation. For the combination of linear f and non-linear functions g, the following rule generally holds:

$$f(g(x)) \neq g(f(x)) \,.$$

For this reason, the order of processing operations generally matters. In the case of neutron count variations, corrections should be applied on the raw data, and only the final product should then be averaged (smoothed). Otherwise, it is not guaranteed that a measurement $N(t)$ is corrected for the air pressure $P(t)$ at the same time t, for instance. Fig. A1 shows that the correlation between the buoy experimental epithermal neutron intensity corrected for variations in atmospheric pressure and absolute humidity and the inverted primary influx correction from Zreda et al. (2012) generally increases with increasing moving average window size when the correction procedures are applied *before* averaging the raw data. In contrast, a correction *after* averaging the raw data leads to (i) a lower maximum correlation and (ii) a decrease of the correlation at window sizes larger than 25 hours. This is in line with recent findings by Davies et al. (2022), who found a general improvement of the CRNS-derived soil moisture when the correction procedure is applied prior filtering

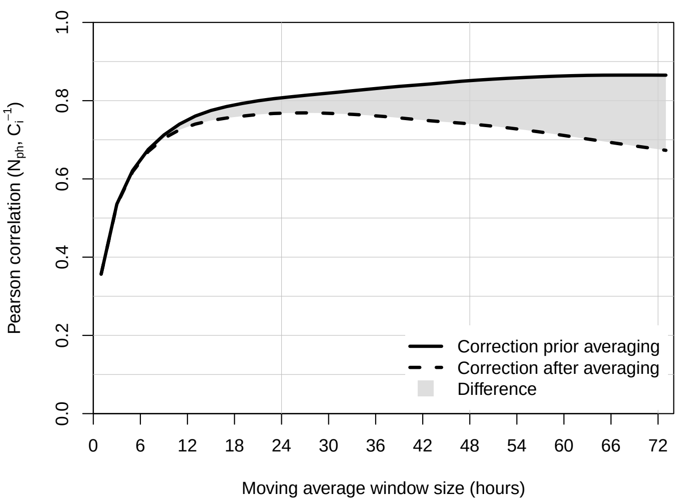

Figure A1. Pearson correlation coefficient between the epithermal N_{ph} vs. inverted influx correction after (Zreda et al., 2012) using the JUNG neutron monitor, when the correction is applied prior or after smoothing with a moving average of the neutron intensity time series. In general, for filtering approaches based on a moving window, the window size needs to be odd in order to create a centered filter to avoid a temporal shift in the filtered time series. For example, a centered 24-hour moving average equals a 25-hour moving average.

Appendix B Determination of the lake water temperature

At the study location, lake *Seelhausener See*, direct measurements of the water temperature were not available. However, it is possible to use measurements of a nearby lake as a proxy.

Surface temperatures in lakes are mainly determined by the local weather. Hence lakes located close to each other at the same geographic altitude show similar temperatures. This was verified in a comparison of surface temperatures of mine pit lakes in the Central German and Lusatian Mining District, in which also *Seelhausener See* is located. Boehrer et al. (2014) found that the lake temperatures measured in 0.5 m depth were nearly identical. Only in cases of rapidly rising temperatures (e.g., in spring time), a difference of up to 2°C was detected between very small and larger lakes. Numerical models that are calibrated specifically for the conditions of a single lake often reach about the same accuracy (e.g. Weber et al., 2017), while models that are not specifically calibrated (e.g. occasional local temperature measurements) will show greater deviations. Alternative methods, such as satellite imaging and thermometry, only provide sporadic measurements and do not reach a similar accuracy without additional support from numerical models (Zhang et al., 2020).

Lake *Rassnitzer See* is situated in 31 km distance south west of the study area and was previously called ”Mine Pit Lake Merseburg-Ost 1b” (Heidenreich et al., 1999). The lakes *Seelhausener See* and *Rassnitzer See* exhibit similar morphology, similar size, and are exposed to similar air temperatures (Böhrer et al., 1998). Since it can be assumed that temperatures will hardly differ by more than 1°C, the surface temperatures (i.e., at 0.5 m depth) from *Rassnitzer See* can be used as an accurate approximation for temperatures in *Seelhausener See* at the same depth. This assumption has been supported by the fact that the observed air temperatures were very similar at both lakes throughout the investigation period (shown in Fig. B1).

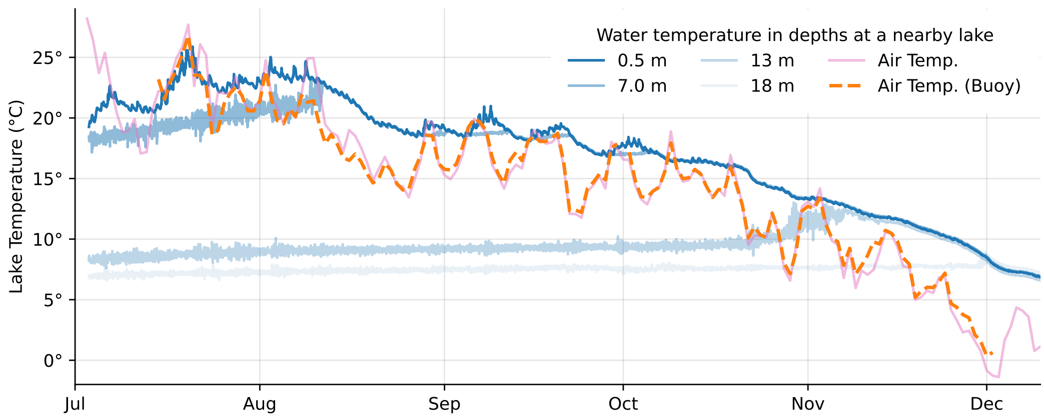

Figure B1. Water temperatures measured by an anchored weather station with attached thermistor chain in *Rassnitzer See* from July 2014 to January 2015 in several depths (blue shading). Air temperature has been measured at both lakes, *Rassnitzer See* (pink solid) and *Seelhausener See* (orange dashed).

Acknowledgments

The data used in this manuscript has been processed with Corny (`https://git.ufz.de/CRNS/cornish_pasdy`) and is available in the supplements. The research was inspired and partly supported by the Deutsche Forschungsgemeinschaft (grant no. 357874777; research unit FOR 2694, Cosmic Sense II) and the Bundesministerium für Bildung und Forschung (grant no. 02WIL1522; German–Israeli Cooperation in Water Technology Research). S. Kögler greatly supported the development of the buoy detector lid, took care about the electro-technical setup, and organized the boat trips to the lake site. Special thanks goes to Prof. Peter Dietrich, who supported the idea, vision, and implementation of the endeavour and who always facilitated curiosity-driven experiments. We further thank K. Rahn for supporting technical implementation of the buoy. Permission to access the lake was kindly granted by D. Onnasch and P. Morszeck (LMBV). Particular thanks to B. Dannenberg for support and instructions at the lake site. We thank TERENO (Terrestrial Environmental Observatories), funded by the Helmholtz-Gemeinschaft for the financing and maintenance of CRNS stations used in this study. We acknowledge the NMDB database (www.nmdb.eu) founded under the European Union's FP7 programme (contract no. 213 007), and the PIs of individual neutron monitors.

References

Abunin, A., Kobelev, P., Abunina, M., Preobragenskiy, M., Smirnov, D., & Lukovnikova, A. (2016, March). A wind effect of neutron component of cosmic rays at Antarctic station "Mirny". *Solar-Terrestrial Physics (Solnechno-zemnaya fizika)*, *2*(1), 71-75. doi: 10.12737/13505

Andreasen, M., Jensen, K. H., Desilets, D., Zreda, M., Bogena, H. R., & Looms, M. C. (2017). Cosmic-ray neutron transport at a forest field site: the sensitivity to various environmental conditions with focus on biomass and canopy interception. *Hydrology and Earth System Sciences*, *21*(4), 1875–1894. doi: 10.5194/hess-21-1875-2017

Aplin, K., Harrison, R., & Bennett, A. (2005). Effect of the troposphere on surface neutron counter measurements. *Advances in Space Research*, *35*(8), 1484 - 1491. doi: 10.1016/j.asr.2005.02.055

Baatz, R., Bogena, H., Hendricks-Franssen, H.-J., Huisman, J., Qu, W., Montzka, C., & Vereecken, H. (2014). Calibration of a catchment scale cosmic-ray probe network: A comparison of three parameterization methods. *Journal of Hydrology*, *516*, 231–244. doi: 10.1016/j.jhydrol.2014.02.026

Belov, A., Baisultanova, L., Eroshenko, E., Mavromichalaki, H., Yanke, V., Pchelkin, V., ... Mariatos, G. (2005). Magnetospheric effects in cosmic rays during the unique magnetic storm on November 2003. *Journal of Geophysical Research: Space Physics*, *110*(A9). doi: 10.1029/2005JA011067

Boehrer, B., Kiwel, U., Rahn, K., & Schultze, M. (2014). Chemocline erosion and its conservation by freshwater introduction to meromictic salt lakes. *Limnologica*, *44*, 81—89. doi: 10.1016/j.limno.2013.08.003

Boehrer, B., & Schultze, M. (2008). Stratification of lakes. *Reviews of Geophysics*, *46*(2).

Bogena, H. R., Herrmann, F., Jakobi, J., Brogi, C., Ilias, A., Huisman, J. A., ... Pisinaras, V. (2020). Monitoring of Snowpack Dynamics With Cosmic-Ray Neutron Probes: A Comparison of Four Conversion Methods. *Frontiers in Water*, *2*. Retrieved 2023-12-19, from `https://www.frontiersin.org/articles/10.3389/frwa.2020.00019`

Bogena, H. R., Schrön, M., Jakobi, J., Ney, P., Zacharias, S., Andreasen, M., ... Vereecken, H. (2022). COSMOS-Europe: a European network of cosmic-ray neutron soil moisture sensors. *Earth Syst. Sci. Data*, *14*(3), 1125–1151. doi: 10.5194/essd-14-1125-2022

Böhrer, B., Heidenreich, H., Schimmele, M., & Schultze, M. (1998). Numerical prognosis for salinity profiles of future lakes in the opencast mine merseburg-ost. *International Journal of Salt Lake Research*, *7*(3), 235–260. doi: 10.1007/BF02441877

Bütikofer, R. (1999). Pressure correction of GLE measurements in turbulent winds. In *International cosmic ray conference* (Vol. 6, p. 395).

Bütikofer, R. (2018). Ground-based measurements of energetic particles by neutron monitors. In O. E. Malandraki & N. B. Crosby (Eds.), *Solar particle radiation storms forecasting and analysis: The hesperia horizon 2020 project and beyond* (pp. 95–111). Cham: Springer International Publishing. doi: 10.1007/978-3-319-60051-2_6

Clem, J. M., Bieber, J. W., Evenson, P., Hall, D., Humble, J. E., & Duldig, M. (1997). Contribution of obliquely incident particles to neutron monitor counting rate. *Journal of Geophysical Research: Space Physics*, *102*(A12), 26919–26926. doi: 10.1029/97JA02366

Clem, J. M., & Dorman, L. I. (2000). Neutron monitor response functions. *Space Science Reviews*, *93*(1), 335–359. doi: 10.1023/A:1026508915269

Davies, P., Baatz, R., Bogena, H. R., Quansah, E., & Amekudzi, L. K. (2022). Optimal temporal filtering of the cosmic-ray neutron signal to reduce soil moisture uncertainty. *Sensors*, *22*(23). doi: 10.3390/s22239143

Desilets, D., & Zreda, M. (2001). On scaling cosmogenic nuclide production rates for altitude and latitude using cosmic-ray measurements. *Earth and Planetary Science Letters*, *193*(1–2), 213–225. doi: 10.1016/S0012-821X(01)00477-0

Desilets, D., & Zreda, M. (2013). Footprint diameter for a cosmic-ray soil moisture probe: Theory and Monte Carlo simulations. *Water Resources Research*, *49*(6), 3566–3575. doi: 10.1002/wrcr.20187

Desilets, D., Zreda, M., & Ferré, T. (2010). Nature's neutron probe: Land surface hydrology at an elusive scale with cosmic rays. *Water Resources Research*, *46*(11). doi: 10.1029/2009WR008726

Desilets, D., Zreda, M., & Prabu, T. (2006). Extended scaling factors for in situ cosmogenic nuclides: New measurements at low latitude. *Earth and Planetary Science Letters*, *246*(3-4), 265–276. doi: 10.1016/j.epsl.2006.03.051

Döpper, V., Jagdhuber, T., Holtgrave, A.-K., Heistermann, M., Francke, T., Kleinschmit, B., & Förster, M. (2022). Following the cosmic-ray-neutron-sensing-based soil moisture under grassland and forest: Exploring the potential of optical and SAR remote sensing. *Science of Remote Sensing*, *5*, 100056. doi: 10.1016/j.srs.2022.100056

Dorman, L. I. (2004). *Cosmic rays in the earth's atmosphere and underground*. Springer Netherlands. doi: 10.1007/978-1-4020-2113-8

Dunai, T. J. (2000). Scaling factors for production rates of in situ produced cosmogenic nuclides: a critical reevaluation. *Earth and Planetary Science Letters*, *176*(1), 157–169.

Fersch, B., Francke, T., Heistermann, M., Schrön, M., Döpper, V., Jakobi, J., ... Oswald, S. E. (2020). A dense network of cosmic-ray neutron sensors for soil moisture observation in a highly instrumented pre-Alpine headwater catchment in Germany. *Earth System Science Data*, *12*(3), 2289–2309. doi: 10.5194/essd-12-2289-2020

Franz, T. E., Wahbi, A., Zhang, J., Vreugdenhil, M., Heng, L., Dercon, G., ... Wagner, W. (2020). Practical data products from cosmic-ray neutron sensing for hydrological applications. *Frontiers in Water*, *2*. doi: 10.3389/frwa.2020.00009

Franz, T. E., Zreda, M., Ferré, T. P. A., & Rosolem, R. (2013). An assessment of the effect of horizontal soil moisture heterogeneity on the area-average measurement of cosmic-ray neutrons. *Water Resources Research*, *49*(10), 6450–6458. doi: 10.1002/wrcr.20530

Garny, S., Mares, V., & Rühm, W. (2009). Response functions of a bonner sphere spectrometer calculated with geant4. *Nuclear Instruments and Methods in Physics Research Section A: Accelerators, Spectrometers, Detectors and Associated Equipment*, *604*(3), 612–617. doi: 10.1016/j.nima.2009.02.044

Geller, W., Schultze, M., Kleinmann, B., & Wolkersdorfer, C. (2013). *Acidic pit lakes: The legacy of coal and metal surface mines*. Springer Berlin Heidelberg. doi: 10.1007/978-3-642-29384-9

Glasstone, S., & Sesonske, A. (1981). *Nuclear reactor engineering*. Krieger Publishing Company, Malabar, Florida.

Goorley, T., James, M., Booth, T., Brown, F., Bull, J., Cox, L., ... Zukaitis, T. (2012). Initial MCNP6 release overview. *Nuclear Technology*, *180*(3), 298–315. doi: 10.13182/

NT11-135
Gugerli, R., Desilets, D., & Salzmann, N. (2022). Brief communication: Application of a muonic cosmic ray snow gauge to monitor the snow water equivalent on alpine glaciers. *The Cryosphere*, *16*(3), 799–806.
Gugerli, R., Salzmann, N., Huss, M., & Desilets, D. (2019). Continuous and autonomous snow water equivalent measurements by a cosmic ray sensor on an alpine glacier. *The Cryosphere*, *13*(12), 3413–3434. doi: 10.5194/tc-13-3413-2019
Hands, A. D. P., Baird, F., Ryden, K. A., Dyer, C. S., Lei, F., Evans, J. G., ... Henley, E. M. (2021). Detecting Ground Level Enhancements Using Soil Moisture Sensor Networks. *Space Weather*, *19*(8), e2021SW002800. doi: 10.1029/2021SW002800
Hawdon, A., McJannet, D., & Wallace, J. (2014). Calibration and correction procedures for cosmic-ray neutron soil moisture probes located across Australia. *Water Resources Research*, *50*(6), 5029–5043. doi: 10.1002/2013WR015138
Heidbüchel, I., Güntner, A., & Blume, T. (2016). Use of cosmic-ray neutron sensors for soil moisture monitoring in forests. *Hydrology and Earth System Sciences*, *20*(3), 1269–1288. doi: 10.5194/hess-20-1269-2016
Heidenreich, H., Boehrer, B., Kater, R., & Hennig, G. (1999). Gekoppelte Modellierung geohydraulischer und limnophysikalischer Vorgänge in Tagebaurestseen und ihrer Umgebung. *Grundwasser*, *4*(2), 49—54. doi: 10.1007/s767-1999-8604-4
Herbst, K., Kopp, A., & Heber, B. (2013). Influence of the terrestrial magnetic field geometry on the cutoff rigidity of cosmic ray particles. In *Annales geophysicae* (Vol. 31, pp. 1637–1643). doi: 10.5194/angeo-31-1637-2013
Hess, W. N., Canfield, E. H., & Lingenfelter, R. E. (1961). Cosmic-ray neutron demography. *Journal of Geophysical Research (1896-1977)*, *66*(3), 665–677. doi: 10.1029/JZ066i003p00665
Hubert, G., Pazianotto, M. T., Federico, C. A., & Ricaud, P. (2019). Analysis of the forbush decreases and ground-level enhancement on september 2017 using neutron spectrometers operated in antarctic and midlatitude stations. *Journal of Geophysical Research: Space Physics*, *124*(1), 661–673. doi: 10.1029/2018JA025834
Iwema, J., Rosolem, R., Rahman, M., Blyth, E., & Wagener, T. (2017). Land surface model performance using cosmic-ray and point-scale soil moisture measurements for calibration. *Hydrology and Earth System Sciences*, *21*(6), 2843–2861. doi: 10.5194/hess-21-2843-2017
Iwema, J., Schrön, M., Koltermann Da Silva, J., Schweiser De Paiva Lopes, R., & Rosolem, R. (2021, November). Accuracy and precision of the cosmic-ray neutron sensor for soil moisture estimation at humid environments. *Hydrological Processes*, *35*(11). doi: 10.1002/hyp.14419
Jakobi, J., Huisman, J. A., Fuchs, H., Vereecken, H., & Bogena, H. R. (2022). Potential of thermal neutrons to correct cosmic-ray neutron soil moisture content measurements for dynamic biomass effects. *Water Resources Research*, *58*(8), e2022WR031972. doi: 10.1029/2022WR031972
Jakobi, J., Huisman, J. A., Vereecken, H., Diekkrüger, B., & Bogena, H. R. (2018). Cosmic ray neutron sensing for simultaneous soil water content and biomass quantification in drought conditions. *Water Resources Research*, *54*(10), 7383–7402. doi: 10.1029/2018WR022692
Kobelev, P., Belov, A., Mavromichalaki, E., Gerontidou, M., & Yanke, V. (2011). Variations of barometric coefficients of the neutron component in the 22-23 cycles of solar activity. *CD Proc. 32nd ICRC, id0654, Beijing*.
Kodama, M. (1980). Continuous monitoring of snow water equivalent using cosmic ray neutrons. *Cold Regions Science and Technology*, *3*(4), 295–303. doi: 10.1016/0165-232x(80)90036-1
Kodama, M., Kawasaki, S., & Wada, M. (1975). A cosmic-ray snow gauge. *The International Journal of Applied Radiation and Isotopes*, *26*(12), 774–775.
Kodama, M., Kudo, S., & Kosuge, T. (1985). Application of atmospheric neutrons to soil moisture measurement. *Soil Science*, *140*(4), 237–242.

Köhli, M., Schrön, M., & Schmidt, U. (2018). Response functions for detectors in cosmic ray neutron sensing. *Nuclear Instruments and Methods in Physics Research Section A: Accelerators, Spectrometers, Detectors and Associated Equipment*, *902*, 184–189. doi: 10.1016/j.nima.2018.06.052

Köhli, M., Schrön, M., Zacharias, S., & Schmidt, U. (2023). URANOS v1.0 – the Ultra Rapid Adaptable Neutron-Only Simulation for Environmental Research. *Geoscientific Model Development*, *16*(2), 449–477. doi: 10.5194/gmd-16-449-2023

Köhli, M., Schrön, M., Zreda, M., Schmidt, U., Dietrich, P., & Zacharias, S. (2015). Footprint characteristics revised for field-scale soil moisture monitoring with cosmic-ray neutrons. *Water Resources Research*, *51*(7), 5772–5790. doi: 10.1002/2015wr017169

Köhli, M., Weimar, J., Schrön, M., Baatz, R., & Schmidt, U. (2021). Soil moisture and air humidity dependence of the above-ground cosmic-ray neutron intensity. *Frontiers in Water*, *2*. doi: 10.3389/frwa.2020.544847

Korotkov, V. K., Berkova, M. D., Belov, A. V., Eroshenko, E. A., Kobelev, P. G., & Yanke, V. G. (2011). Effect of snow in cosmic ray variations and methods for taking it into consideration. *Geomagnetism and Aeronomy*, *51*(2), 247–253. doi: 10.1134/S0016793211020095

Krüger, H., & Moraal, H. (2010). A calibration neutron monitor: Statistical accuracy and environmental sensitivity. *Advances in Space Research*, *46*(11), 1394–1399. doi: 10.1016/j.asr.2010.07.008

Krüger, H., Moraal, H., Bieber, J. W., Clem, J. M., Evenson, P. A., Pyle, K. R., … Humble, J. E. (2008). A calibration neutron monitor: Energy response and instrumental temperature sensitivity. *Journal of Geophysical Research: Space Physics*, *113*(A8). (A08101) doi: 10.1029/2008JA013229

Kudela, K. (2012). Variability of Low Energy Cosmic Rays Near Earth. In *Exploring the Solar Wind.* IntechOpen. doi: 10.5772/37482

Laken, B., Kniveton, D., & Wolfendale, A. (2011). Forbush decreases, solar irradiance variations, and anomalous cloud changes. *Journal of Geophysical Research: Atmospheres*, *116*(D9). doi: 10.1029/2010JD014900

Lingri, D., Mavromichalaki, H., Belov, A., Abunina, M., Eroshenko, E., & Abunin, A. (2019, June). An Extended Study of the Precursory Signs of Forbush Decreases: New Findings over the Years 2008-2016. *Solar Physics*, *294*(6), 70. doi: 10.1007/s11207-019-1461-3

López-Comazzi, A., & Blanco, J. J. (2020). Short-term periodicities observed in neutron monitor counting rates. *Solar Physics*, *295*(6). doi: 10.1007/s11207-020-01649-5

López-Comazzi, A., & Blanco, J. J. (2022). Short- and mid-term periodicities observed in neutron monitor counting rates throughout solar cycles 20–24. *The Astrophysical Journal*, *927*(2), 155. doi: 10.3847/1538-4357/ac4e19

Mavromichalaki, H., Papaioannou, A., Plainaki, C., Sarlanis, C., Souvatzoglou, G., Gerontidou, M., … others (2011). Applications and usage of the real-time neutron monitor database. *Advances in Space Research*, *47*(12), 2210–2222. doi: 10.1016/j.asr.2010.02.019

McJannet, D. L., & Desilets, D. (2023). Incoming Neutron Flux Corrections for Cosmic-Ray Soil and Snow Sensors Using the Global Neutron Monitor Network. *Water Resources Research*, *59*(4), e2022WR033889. doi: 10.1029/2022WR033889

McJannet, D. L., Franz, T. E., Hawdon, A., Boadle, D., Baker, B., Almeida, A., … Desilets, D. (2014). Field testing of the universal calibration function for determination of soil moisture with cosmic-ray neutrons. *Water Resources Research*, *50*(6), 5235–5248. doi: 10.1002/2014WR015513

Mishev, A. L., Kocharov, L. G., & Usoskin, I. G. (2014). Analysis of the ground level enhancement on 17 May 2012 using data from the global neutron monitor network. *Journal of Geophysical Research: Space Physics*, *119*(2), 670–679. doi: 10.1002/2013JA019253

Montzka, C., Bogena, H. R., Zreda, M., Monerris, A., Morrison, R., Muddu, S., & Vereecken, H. (2017). Validation of spaceborne and modelled surface soil moisture products with

cosmic-ray neutron probes. *Remote sensing*, *9*(2), 103.
National Centers for Environmental Information. (2015). *Magnetic field calculators.* Retrieved 2023-12-17, from `https://www.ngdc.noaa.gov/geomag/calculators/magcalc.shtml#igrfwmm`
Nuntiyakul, W., Sáiz, A., Ruffolo, D., Mangeard, P.-S., Evenson, P., Bieber, J. W., ... Humble, J. E. (2018). Bare neutron counter and neutron monitor response to cosmic rays during a 1995 latitude survey. *Journal of Geophysical Research: Space Physics*, *123*(9), 7181–7195. doi: 10.1029/2017JA025135
Oh, S., Bieber, J. W., Evenson, P., Clem, J., Yi, Y., & Kim, Y. (2013). Record neutron monitor counting rates from galactic cosmic rays. *J. Geophys. Res. Space Physics*, *118*, 5431-5436. doi: 10.1002/jgra.50544
Paschalis, P., Mavromichalaki, H., Yanke, V., Belov, A., Eroshenko, E., Gerontidou, M., & Koutroumpi, I. (2013). Online application for the barometric coefficient calculation of the nmdb stations. *New Astronomy*, *19*, 10–18.
Patil, A., Fersch, B., Hendricks-Franssen, H.-J., & Kunstmann, H. (2021). Assimilation of Cosmogenic Neutron Counts for Improved Soil Moisture Prediction in a Distributed Land Surface Model. *Frontiers in Water*, *3*. doi: 10.3389/frwa.2021.729592
Rasche, D., Köhli, M., Schrön, M., Blume, T., & Güntner, A. (2021). Towards disentangling heterogeneous soil moisture patterns in cosmic-ray neutron sensor footprints. *Hydrology and Earth System Sciences*, *25*(12), 6547–6566. doi: 10.5194/hess-25-6547-2021
Rasche, D., Weimar, J., Schrön, M., Köhli, M., Morgner, M., Güntner, A., & Blume, T. (2023). A change in perspective: downhole cosmic-ray neutron sensing for the estimation of soil moisture. *Hydrology and Earth System Sciences*, *27*(16), 3059–3082. doi: 10.5194/hess-27-3059-2023
Rockenbach, M., Dal Lago, A., Schuch, N. J., Munakata, K., Kuwabara, T., Oliveira, A., ... others (2014). Global muon detector network used for space weather applications. *Space Science Reviews*, *182*, 1–18. doi: 10.1007/s11214-014-0048-4
Rosolem, R., Shuttleworth, W. J., Zreda, M., Franz, T. E., Zeng, X., & Kurc, S. a. (2013, October). The Effect of Atmospheric Water Vapor on Neutron Count in the Cosmic-Ray Soil Moisture Observing System. *Journal of Hydrometeorology*, *14*(5), 1659–1671. doi: 10.1175/JHM-D-12-0120.1
Ruffolo, D., Sáiz, A., Mangeard, P.-S., Kamyan, N., Muangha, P., Nutaro, T., ... Munakata, K. (2016). Monitoring short-term cosmic-ray spectral variations using neutron monitor time-delay measurements. *The Astrophysical Journal*, *817*(1), 38. doi: 10.3847/0004-637x/817/1/38
Sapundjiev, D., Nemry, M., Stankov, S., & Jodogne, J.-C. (2014). Data reduction and correction algorithm for digital real-time processing of cosmic ray measurements: NM64 monitoring at Dourbes. *Advances in Space Research*, *53*(1), 71–76. doi: 10.1016/j.asr.2013.09.037
Schmidt, T., Schrön, M., Li, Z., Francke, T., Zacharias, S., Hildebrandt, A., & Peng, J. (2024). Comprehensive quality assessment of satellite- and model-based soil moisture products against the COSMOS network in Germany. *Remote Sensing of Environment*, *301*, 113930. doi: 10.1016/j.rse.2023.113930
Schrön, M. (2017). *Cosmic-ray neutron sensing and its applications to soil and land surface hydrology* (phdthesis, University of Potsdam). Retrieved 2023-05-10, from `https://publishup.uni-potsdam.de/frontdoor/index/index/docId/39543` (Thesis)
Schrön, M., Köhli, M., & Zacharias, S. (2023). Signal contribution of distant areas to cosmic-ray neutron sensors – implications for footprint and sensitivity. *Hydrol. Earth Syst. Sci.*, *27*(3), 723–738. doi: 10.5194/hess-27-723-2023
Schrön, M., Zacharias, S., Köhli, M., Weimar, J., & Dietrich, P. (2016, August). Monitoring environmental water with ground albedo neutrons from cosmic rays. In *Proceedings of the 34th international cosmic ray conference — pos(icrc2015).* Sissa Medialab. doi: 10.22323/1.236.0231
Schrön, M., Zacharias, S., Womack, G., Köhli, M., Desilets, D., Oswald, S. E., ... Dietrich, P. (2018). Intercomparison of cosmic-ray neutron sensors and water balance mon-

itoring in an urban environment. *Geoscientific Instrumentation, Methods and Data Systems*, *7*(1), 83–99. doi: 10.5194/gi-7-83-2018

Sentelhas, P. C., Dalla Marta, A., & Orlandini, S. (2008). Suitability of relative humidity as an estimator of leaf wetness duration. *Agricultural and Forest Meteorology*, *148*(3), 392–400. doi: 10.1016/j.agrformet.2007.09.011

Simpson, J. A. (1983). Elemental and isotopic composition of the galactic cosmic rays. *Annual Review of Nuclear and Particle Science*, *33*(1), 323-382. doi: 10.1146/annurev.ns.33.120183.001543

Stevanato, L., Baroni, G., Oswald, S. E., Lunardon, M., Mares, V., Marinello, F., ... Rühm, W. (2022). An Alternative Incoming Correction for Cosmic-Ray Neutron Sensing Observations Using Local Muon Measurement. *Geophysical Research Letters*, *49*(6). doi: 10.1029/2021gl095383

Tian, Z., Li, Z., Liu, G., Li, B., & Ren, T. (2016). Soil water content determination with cosmic-ray neutron sensor: Correcting aboveground hydrogen effects with thermal/fast neutron ratio. *Journal of Hydrology*, *540*, 923–933. doi: 10.1016/j.jhydrol.2016.07.004

Usoskin, I. G., Bazilevskaya, G. A., & Kovaltsov, G. A. (2011). Solar modulation parameter for cosmic rays since 1936 reconstructed from ground-based neutron monitors and ionization chambers. *Journal of Geophysical Research: Space Physics*, *116*(A2). doi: 10.1029/2010JA016105

Väisänen, P., Usoskin, I., & Mursula, K. (2021). Seven decades of neutron monitors (1951–2019): Overview and evaluation of data sources. *Journal of Geophysical Research: Space Physics*, *126*(5), e2020JA028941. doi: 10.1029/2020JA028941

Weber, M., Rinke, K., Hipsey, M., & Boehrer, B. (2017). Optimizing withdrawal from drinking water reservoirs to reduce downstream temperature pollution and reservoir hypoxia. *Journal of Environmental Management*, *197*, 96—105. doi: 10.1016/j.jenvman.2017.03.020

Weimar, J. (2022). *Advances in Cosmic-Ray Neutron Sensing by Monte Carlo simulations and neutron detector development* (phdthesis, Heidelberg University). Retrieved 2023-01-17, from `https://archiv.ub.uni-heidelberg.de/volltextserver/32046/` (Thesis)

Weimar, J., Köhli, M., Budach, C., & Schmidt, U. (2020). Large-scale boron-lined neutron detection systems as a 3he alternative for cosmic ray neutron sensing. *Frontiers in Water*, *2*. doi: 10.3389/frwa.2020.00016

Zhang, X., Wang, K., Frassl, M. A., & Boehrer, B. (2020). Reconstructing six decades of surface temperatures at a shallow lake. *Water*, *12*(2), 405. doi: 10.3390/w12020405

Zreda, M., Desilets, D., Ferré, T. P. A., & Scott, R. L. (2008). Measuring soil moisture content non-invasively at intermediate spatial scale using cosmic-ray neutrons. *Geophysical Research Letters*, *35*(21). doi: 10.1029/2008GL035655

Zreda, M., Shuttleworth, W. J., Zeng, X., Zweck, C., Desilets, D., Franz, T. E., & Rosolem, R. (2012). COSMOS: The COsmic-ray Soil Moisture Observing System. *Hydrology and Earth System Sciences*, *16*(11), 4079–4099. doi: 10.5194/hess-16-4079-2012

Buoy-based detection of low-energy cosmic-ray neutrons to monitor the influence of atmospheric, geomagnetic, and heliospheric effects

Martin Schrön[1,*], Daniel Rasche[2,*], Jannis Weimar[3], Markus Köhli[3], Konstantin Herbst[4], Bertram Boehrer[5], Lasse Hertle[1], Simon Kögler[1], Steffen Zacharias[1]

[1]Helmholtz-Centre for Environmental Research - UFZ, Department for Monitoring and Exploration Technologies, Leipzig, Germany
[2]GFZ German Research Centre for Geosciences, Section Hydrology, Potsdam, Germany
[3]Physikalisches Institut, Heidelberg University, Im Neuenheimer Feld 226, 69120 Heidelberg, Germany
[4]Institute for Experimental and Applied Physics, University of Kiel, Kiel, Germany
[5]Helmholtz-Centre for Environmental Research - UFZ, Department for Limnology, Leipzig, Germany
[*]These authors contributed equally to this study

Key Points:

- Neutron detectors on a buoy were deployed in the center of a lake for five months.
- Thermal and epithermal signals correlated with air pressure, air humidity, and secondary cosmic rays from neutron monitors.
- Data was used to challenge traditional correction approaches and to serve as an alternative neutron monitor.

Corresponding author: Martin Schrön, `martin.schroen@ufz.de`

Abstract

Cosmic radiation on Earth responds to heliospheric, geomagnetic, atmospheric, and lithospheric changes. In order to use its signal for soil hydrological monitoring, the signal of thermal and epithermal neutron detectors needs to be corrected for external influencing factors. However, theories about the neutron response to soil water, air pressure, air humidity, and incoming cosmic radiation are still under debate. To challenge these theories, we isolated the neutron response from almost any terrestrial changes by operating a bare and a moderated neutron detector in a buoy on a lake in Germany from July 15 to December 02, 2014. We found that the count rate over water has been better predicted by a theory from Köhli et al. (2021) compared to the traditional approach from Desilets et al. (2010). We further found strong linear correlation parameters to air pressure ($\beta = 0.0077\,\mathrm{mb}^{-1}$) and air humidity ($\alpha = 0.0054\,\mathrm{m}^3/\mathrm{g}$) for epithermal neutrons, while thermal neutrons responded with $\alpha = 0.0023\,\mathrm{m}^3/\mathrm{g}$. Both approaches, from Rosolem et al. (2013) and from Köhli et al. (2021), were similarly able to remove correlations of epithermal neutrons to air humidity. Correction for incoming radiation proved to be necessary for both thermal and epithermal neutrons, for which we tested different neutron monitor stations and correction methods. Here, the approach from Zreda et al. (2012) worked best with the Jungfraujoch monitor in Switzerland, while the approach from McJannet and Desilets (2023) was able to adequately rescale data from more remote neutron monitors. However, no approach was able to sufficiently remove the signal from a major Forbush decrease event on September 13th, to which thermal and epithermal neutrons showed a comparatively strong response. The buoy detector experiment provided a unique dataset for empirical testing of traditional and new theories on CRNS. It could serve as a local alternative to reference data from remote neutron monitors.

Plain Language Summary

Earth's cosmic radiation near the ground is influenced by solar activity and atmospheric conditions but is also crucial for monitoring soil moisture and snow. To better understand how cosmic-ray neutron measurements should be corrected for meteorological effects, we operated a detector for low-energy neutrons in a buoy on a lake in Germany for five months in 2014. Since the water content in the surroundings is constant, we were able to isolate the signal from almost any ground-related disturbances. With this instrument, we challenged traditional and recent theories on the neutron response to water, air humidity, and to reference data from high-energy neutron monitors around the world. We found that in some cases, recent theories showed superior performance over traditional approaches. We also found a stronger response of the neutrons detected by the buoy to a major solar event than was observed by traditional neutron monitors. The concept of a neutron detector on a lake could be useful as a reference station for similar land-side detectors and help provide more reliable soil moisture products.

1 Introduction

The natural background radiation on Earth is mainly produced by the omnipresent and continuous exposure to galactic cosmic rays, which are modulated by solar activity, filtered by the geomagnetic field, and moderated by the Earth's atmosphere (Hess et al., 1961; Dorman, 2004; Usoskin et al., 2011). Since 1951, neutron monitors have been in operation at various places around the globe to continuously monitor high-energy cosmogenic neutrons as a proxy for space weather (Väisänen et al., 2021). About half a century ago, Kodama et al. (1975) revealed the potential of the lower energetic component of cosmic-ray neutrons for estimating water content in snow. Two decades after Kodama (1980) and Kodama et al. (1985) presented more experimental findings also related to soil moisture, Dorman (2004) proposed the broader use of this concept for hydrological applications. Yet, Zreda et al. (2008) were the first to introduce the methodological framework of Cosmic-Ray Neutron Sensing (CRNS) and to demonstrate its potential for large-scale monitoring of soil moisture. Soon after, Desilets et al. (2010) proposed an empirical but turned-out-to-be robust relationship to convert neutrons to soil moisture, followed by Zreda et al. (2012) presenting the concept and establishment of a continental CRNS network. To date, CRNS is a growing non-invasive and low-maintenance technique providing continuous hectare-scale root-zone soil moisture to inform and validate products of hydrological models (Baatz et al., 2014; Iwema et al., 2017; Patil et al., 2021) and remote sensing (Montzka et al., 2017; Döpper et al., 2022; Schmidt et al., 2024).

The ambient epithermal neutron radiation above the ground is of key interest for CRNS, as this energy band shows the highest sensitivity to hydrogen in soils (Desilets et al., 2010; Zreda et al., 2012; Köhli et al., 2015). Some CRNS probes additionally measure thermal neutrons as a potential proxy for soil chemistry, snow, biomass, or spatial heterogeneity (Tian et al., 2016; Jakobi et al., 2022; Rasche et al., 2021). In order to isolate the response of neutrons to the ground from external influences, CRNS data processing heavily relies on accurate corrections for changes in atmospheric shielding depth (i.e., air pressure), atmospheric hydrogen content (i.e., air humidity), and incoming cosmic rays (i.e., high-energy hadron flux). For epithermal neutrons, such corrections have been proposed based on literature about high-energy cosmic rays (Desilets et al., 2006; Zreda et al., 2012) or on dedicated simulations (Rosolem et al., 2013). However, no commonly accepted correction approaches exist for thermal neutrons, while the transferability of the epithermal correction functions is under debate (Andreasen et al., 2017; Jakobi et al., 2018, 2022; Rasche et al., 2021).

There is an ongoing debate about many aspects of CRNS theory and the traditional correction approaches since correlations to external signals were sometimes not removed sufficiently, and unexplained variations in the data remained. For example, Köhli et al. (2021) used new simulation approaches to explain neutron variations specifically in semi-arid regions, where limitations of the widely established approaches from Desilets et al. (2010) and Rosolem et al. (2013) became evident. However, the simulations from Köhli et al. (2021) were also insufficient to conclude on a final choice out of many offered correction models. Moreover, many authors have found inconsistencies in using the neutron monitor "Jungfraujoch" in Switzerland as a reference for the incoming cosmic-ray flux at different periods and locations on Earth (e.g. Hawdon et al., 2014; Schrön, 2017; Hands et al., 2021). The main reason is the dependence of the cosmic-ray flux on the geomagnetic field, which changes continuously in space and time (Belov et al., 2005; Kudela, 2012; Herbst et al., 2013). To account for that, authors suggested different correction approaches to rescale data from a neutron monitor site to a CRNS location (Hawdon et al., 2014; McJannet & Desilets, 2023), while their performance is yet to be tested. Nevertheless, more issues complicate the use of the neutron monitor network as a reference for CRNS stations across the world: the instruments measure different neutron energies than CRNS, they are sometimes prone to weather effects, the few neutron monitors have only scarce coverage on Earth, the data exhibits varying consistency and quality, and a single institute is responsible for the data provision and processing (Bütikofer, 1999; Aplin et al., 2005; Korotkov et al., 2011; Oh et al., 2013; Abunin et al., 2016; Ruffolo et al., 2016; Väisänen et al., 2021). Consequently, the future availability of incoming cosmic-ray reference data may not be guaranteed, which explains the current search for alternative concepts (e.g. Schrön et al., 2016; Fersch et al., 2020; Gugerli et al., 2022; Stevanato et al., 2022).

An empirical and objective evaluation of traditional and new theories on the neutron response to the ground, to the atmosphere, and to the magnetosphere, is a challenging endeavour. Any ground-based CRNS measurement inherently depends on the spatial and temporal variability of nearby hydrogen pools, such as soil moisture, biomass, ponding water, etc. (Iwema et al., 2021; Schrön et al., 2023). However, such variability can be considered negligible above lakes or other water bodies, were even rain events would not introduce a significant addition of water. Neutron measurements on a lake with a detector that has a comparable energy sensitivity to CRNS could provide a unique data set to investigate the local and "actual" influence of non-terrestrial variability on thermal and epithermal neutrons. In terrestrial CRNS applications, many of the external, ground-related influencing factors are often unknown and thus challenging to model, leading to uncertainties in the interpretation of the CRNS signal. A buoy detector on a lake, however, has a clear pure-water boundary condition and would allow for a more direct comparison of the observations with simulations of the sensor response. Moreover, a lake-base buoy CRNS detector might be even suitable as a reference monitor for the incoming cosmic-ray flux.

The advantage of water bodies beneath a neutron detector has been first reported by Krüger and Moraal (2010), who performed intercalibration measurements of high-energy neutron monitors all over the world by placing a miniature detector over a small nearby pool. CRNS detectors, however, are sensitive to the surrounding environment up to radii of 300 meters (Desilets & Zreda, 2013; Köhli et al., 2015). Hence, Franz et al. (2013) suggested short measurements on a lake to calibrate the pure-water limit of the sensor response, which was conducted using rafts for a few days by McJannet et al. (2014), Andreasen et al. (2017) and Rasche et al. (2023). The first long-term experiment of CRNS detectors on a lake was proposed and conducted in 2014 and later reported by Schrön et al. (2016) and Schrön (2017). The idea was further extended by Weimar (2022) with static and mobile measurements. The present study performs a first detailed analysis of the data set from 2014 and uses it to challenge traditional correction functions and recent CRNS theories.

The first hypothesis of this study is that state-of-the-art theories about the neutron-to-water relationship can predict the drop in neutron count rates from land to water. Here, we will challenge the widely established method from Desilets et al. (2010) and the more recent findings from Köhli et al. (2021). With any ground-related changes of water content removed, we further hypothesize that the hitherto established and partly debated correction functions for air pressure (Desilets et al., 2006; Zreda et al., 2012), air humidity (Rosolem et al., 2013; Köhli et al., 2021), and incoming cosmic radiation (Zreda et al., 2012; Hawdon et al., 2014; McJannet & Desilets, 2023) can adequately remove all remaining temporal variations during the study period. The performance of these approaches will also be tested for thermal neutrons, for which no study has yet confirmed their applicability. Finally, we propose using the buoy detector as an alternative for neutron monitors as a reference for incoming radiation, and test this hypothesis at a nearby CRNS research site.

2 Methods

2.1 Detection of cosmic radiation on Earth

Cosmic radiation mainly consists of protons and heavier ions, permanently penetrating the Earth's magnetic field and interacting with the Earth's atmosphere (Simpson, 1983). Their collision with nitrogen, carbon, or oxygen atoms in the air produces high-energy particle showers, which consist of neutrons, protons, muons, and other particles. Neutrons and protons can be detected by high-energy neutron monitors (NM) on Earth (Mavromichalaki et al., 2011; Väisänen et al., 2021). The muon component is regularly monitored by the global muon detector network (Rockenbach et al., 2014). Both their signals are a measure of the incoming cosmic radiation on Earth's surface and, as such, highly correlated to space weather and solar activity. Besides typical periodicities, such as the 22-year solar cycle, also irregular short-term events may change the incoming cosmic-ray flux significantly. Examples of these striking solar events are Forbush decreases (FD) or Ground-Level Enhancement (GLE). They are temporary reductions or enhancements of the cosmic ray flux observed on Earth, caused by the passage of a solar flare or coronal mass ejection (Laken et al., 2011; Mishev et al., 2014; Lingri et al., 2019; Hands et al., 2021).

As the cosmic-ray particles interact with the atmosphere, their signal on the ground additionally carries information on atmospheric conditions, such as air pressure, air humidity, and atmospheric temperature. For research on space weather, it is important to correct for such atmospheric factors, while research on the response of cosmic rays to the ground surface requires both atmospheric and heliospheric influences to be corrected for. To investigate these corrections empirically with ground-based sensors, however, it is necessary to exclude any ground-related influencing factors.

The interaction of high-energy cosmic rays with the ground usually produces lower energetic neutrons, which are, in turn, sensitive to environmental factors such as water content (Zreda et al., 2012). NMs make use of thick high-density polyethylene shields and lead producers to do both, reduce the influence of those low-energy neutrons that have already interacted with the ground, and tailor the sensitivity to direct high-energy cosmic radiation. Data from NMs available from the global Neutron Monitor database (`https://www.nmdb.eu`) is already corrected for atmospheric pressure and acts as a reference of incoming cosmic radiation on Earth for many adjacent research fields (Mavromichalaki et al., 2011). The distribution of NM stations across the globe aims at covering a range of geomagnetic locations, since the intensity and variability of cosmic rays are a function of the so-called vertical cutoff rigidity of the geomagnetic field, (R_c). This quantity relates to the alignment of the magnetic field lines, which acts as an energy filter of the primary cosmic-ray particles that leads to higher radiation exposure at the poles compared to the equator. Table 1 shows an overview of the NMs used in this study: Jungfraujoch (JUNG) is the standard reference for incoming radiation correction in CRNS research, Athens (ATHN) exhibits high vertical cutoff rigidity in Europe, Kiel (KIEL) is the closest NM to the study site, Oulu (OULU) exhibits the lowest cutoff rigidity in Europe, South pole (SOPO) the lowest globally, while Daejeon (DJON) and Doi Inthanon (PSNM) may serve as promising candidates to test the correction performance with NMs at very high cutoff rigidities and in very large distance to the study site.

2.2 Cosmic-ray neutron sensing (CRNS)

Detectors with a reduced amount of shielding are more sensitive to low-energy neutrons and, thus, to the local environment on the ground. A technology with reduced shielding is called cosmic-ray neutron sensing (CRNS) and is based on the response of low-energy neutrons to nearby environmental water content (Zreda et al., 2008). The main energies used in hydrological CRNS applications are the epithermal neutrons (with energies between 0.5 eV and 10^5 eV), and thermal neutrons (energies below 0.5 eV), as they show the strongest variation with water content (Köhli et al., 2015). In dry soil, the epithermal neutrons produced

Table 1. Overview of the Neutron Monitors (NM) and the buoy detector site used in this study, including their coordinates and geomagnetic cutoff rigidity, R_c, from two different sources (values for 2010 from `https://www.nmdb.eu` and for 2014 from `https://crnslab.org/util/rigidity.php`).

Neutron Monitor	Acronym	Country	R_c (2010)	R_c (2014)	Altitude	Latitude	Longitude
Doi Inthanon	PSNM	Thailand	16.80 GV	16.72 GV	2565 m	18.59°	98.49°
Daejeon	DJON	South Korea	11.22 GV	10.75 GV	200 m	36.24°	127.22°
Athens	ATHN	Greece	8.53 GV	8.27 GV	260 m	37.97°	23.78°
Jungfraujoch	JUNG	Switzerland	4.50 GV	4.54 GV	3570 m	46.55°	7.98°
Buoy	Buoy	Germany	2.99 GV	2.93 GV	78 m	51.58377°	12.41423°
Kiel	KIEL	Germany	2.36 GV	2.31 GV	54 m	54.34°	10.12°
Oulu	OULU	Finland	0.80 GV	0.63 GV	15 m	65.05°	25.47°
South Pole	SOPO	Antarctica	0.10 GV	0.06 GV	2820 m	-90°	0°

by the penetration of high-energy particles may leave the ground almost unhindered. In wet soil, on the other hand, the higher concentration of hydrogen efficiently moderates the neutrons on their way, leading to less epithermal neutron counts above the surface. While epithermal neutron variations are mainly dependent on the hydrogen abundance, thermal neutron radiation shows an additional dependency on chemical components and is still a subject of research. Thermal neutrons can be detected with standard neutron detectors, such as proportional counters. Epithermal neutrons can be detected with an additional layer of high-density polyethylene around these bare detector tubes (Zreda et al., 2012; Schrön et al., 2018).

The wetness of the ground is usually expressed as the soil moisture θ in units of g/g. Conversion functions exist to describe its relationship to epithermal neutrons, $N(\theta)$. The traditional function has been introduced by Desilets et al. (2010):

$$N^{\mathrm{Des}}(\theta) \propto \frac{0.0808}{\theta + 0.115} + 0.372. \quad (1)$$

It is independent on hydrogen in air, for instance, which could be addressed by a separate correction factor on the neutrons (see section below). A recent study by Köhli et al. (2021) introduced a universal transfer solution (UTS) for soil moisture conversion which is inseparable from the air humidity, h in g/m^3, of the environment:

$$N^{\mathrm{UTS}}(\theta, h) \propto \Big(\frac{p_1 + p_2\,\theta}{p_1 + \theta} \cdot \big(p_3 + p_4\,h + p_5\,h^2\big) + e^{-p_6\,\theta}\,\left(p_7 + p_8\,h\right)\Big), \quad (2)$$

where p_i represents a range of parameter sets out of many possible candidates offered by Table A1 in Köhli et al.. They either depend on different simulation approaches or employ different energy response functions (see also Köhli et al., 2018). The parameter set "MCNP drf" was derived from MCNP (Goorley et al., 2012) simulations, which include interaction processes of neutrons, protons, muons, and other particles. It also integrates the actual energy response function of the CRNS detector (drf). In contrast, the parameter set "MCNP THL" uses the MCNP model with a less accurate energy threshold window. Parameter sets "URANOS drf" and "URANOS THL" express similar detector models, while URANOS has been used instead of MCNP to simulate the neutron response to soil and water, which includes only neutron particle interactions and some effective and less accurate representation of other particles (see Köhli et al., 2023, for details).

Both approaches, Desilets et al. (2010) and Köhli et al. (2021), have in common that they provide a relative value for neutron count rates that can be scaled with a factor N_0, usually referred to as a calibration parameter. It is different for each approach and parameter set but essentially mimics the detector-specific count rate at a very dry state of the soil.

From calculations using typical ranges of θ and h it follows that the N_0 values for the UTS function are larger than N_0 for the Desilets approach by factors of 1.61, 2.09, 1.58, and 2.03 for the parameter sets "MCNP drf", "MCNP THL", "URANOS drf", and "URANOS THL", respectively.

To date, there is no published evidence of a preferred parameter set for CRNS data processing with the UTS approach. Standard evaluation procedures would require a high number of auxiliary measurements of soil moisture in the sensor footprint and different depths, in addition to consideration of spatial heterogeneity and other disturbing factors typically present at most field sites. However, an experiment with $\theta =$ const. could facilitate an empirical determination of $N(h)$ to shine a light on a suitable parameter set that describes this part of the model realistically.

A water body is expected to produce a minimal number of neutrons, which, unlike for soils, does not change as a result of rainfall events (i.e., $\theta =$ const.). Hence, it is expected that neutrons measured above a lake are only dependent on atmospheric conditions or solar activity. In the pure-water environment, we follow the limes approach by Schrön et al. (2023), $\theta \to \infty$, with which Eq. (1) reduces to:

$$\lim_{\theta\to\infty} N^{\mathrm{Des}}(\theta) = 0.372\,, \tag{3}$$

while Eq. (2) reduces to:

$$\lim_{\theta\to\infty} N^{\mathrm{UTS}}(\theta, h) = p_2\,(p_3 + p_4\,h + p_5\,h^2)\,. \tag{4}$$

The latter varies from 0.15 to 0.28 depending on air humidity and on the chosen parameter set (Table A1 in Köhli et al., 2021).

2.3 Atmospheric and geomagnetic corrections

Previous studies have introduced correction functions for the measured neutrons to remove the effect of air pressure P, air humidity h, and incoming radiation I. Conventionally, these functions are usually treated as factors on the neutron counts (except for Eq. (2)):

$$\begin{aligned} \text{humidity-corrected} \quad N_h &= N(\theta)\cdot C_h\,, \\ \text{pressure-corrected} \quad N_P &= N(\theta)\cdot C_P\,, \\ \text{incoming-corrected} \quad N_I &= N(\theta)\cdot C_I\,, \\ \text{fully-corrected} \quad N_{hPI} &= N(\theta)\cdot C_h\cdot C_P\cdot C_I\,. \end{aligned} \tag{5}$$

Air humidity can be corrected by two different approaches. The established approach by Rosolem et al. (2013) uses a separate correction factor based on the air humidity h (in g/m^3):

$$C_h = 1 + \alpha\,(h - h_{\mathrm{ref}})\,. \tag{6}$$

The parameter α accounts for water vapor in the near or total atmosphere. It was determined by Rosolem et al. (2013) using neutron transport simulations. However, systematic experimental validation has not been reported, yet. The other approach refers to Eq. (2), which intrinsically accounts for air humidity in a non-separable way. In this case, $N_h \equiv N(\theta, h)$ or $C_h = 1$.

Air pressure can be corrected using an established exponential function:

$$C_P = e^{\beta(P - P_{\mathrm{ref}})}\,. \tag{7}$$

The attenuation coefficient β equals the inverse attenuation length, L^{-1}, and has been used for decades to process atmospheric correction of cosmic rays. It can be determined using different analytical relations (Clem et al., 1997; Dunai, 2000; Desilets et al., 2006), by minimizing the correlation between incoming radiation and air pressure (Sapundjiev et al., 2014), or by comparing neutron time series with a reference station, where β is known (Paschalis et al., 2013). These various approaches show that β might be a complex variable that depends on several factors, such as latitude, altitude, type and energy of incident particles (Clem & Dorman, 2000; Dorman, 2004, and references therein), on variations during the solar cycle and during solar flare events (Dorman, 2004; Kobelev et al., 2011), and on properties and yield function of the detector device (Bütikofer, 1999).

We make use of an established calculation of L following Dunai (2000) and Desilets and Zreda (2001):

$$\beta^{-1} = L(i) = y + \frac{a}{\left(1 + e^{(x-i)/b}\right)^c}\,, \tag{8}$$

where i is the Earth's magnetic field inclination and the empirical parameters are $a = 19.85$, $b = -5.43$, $x = 62.05$, $y = 129.55$. The inclination at the buoy's location can be determined from National Centers for Environmental Information (2015) and was $i = 66.9°$. This leads to theoretical prediction of $L = 129.7\,\mathrm{g/cm^2}$ or $\beta = 0.0077\,\mathrm{mbar}$. An alternative tool that is often used by the CRNS community, is the website `http://crnslab.org/util/rigidity.php`, which predicts $L = 137.0\,\mathrm{g/cm^2}$ or $\beta = 0.0073\,\mathrm{mbar}$ for the buoy location. However, both tools are also based on calculations derived for high-energy particles and a specific temporal state of the magnetosphere, while the neutron attenuation has never been explicitly identified for the lower-energetic CRNS detectors. Given the uncertainty in determining the correct value for the attenuation coefficient, in this study, we use an average value of $L = 133.0\,\mathrm{g/cm^2}$.

The approach for correcting incoming radiation has been first formulated by Zreda et al. (2012) and generalized by Schrön et al. (2016):

$$C_I = \left(1 - \gamma\,(1 - I/I_{\mathrm{ref}})\right)^{-1}\,. \tag{9}$$

It uses reference data I from the neutron monitor database that measures only the incoming, high-energy component of the cosmic radiation at a few selected locations on Earth. The parameter γ depicts the amplitude scaling of signal variations depending on geomagnetic location. The conventional approach has been assuming $\gamma = 1$, but it failed to remove the incoming cosmic-ray variability, especially for large distances between CRNS and NM sites. The underlying challenge is the dependency of the incoming signal on the geomagnetic location, expressed by the cutoff rigidity, R_c in GV, of the geomagnetic field. For example, sites near the geomagnetic poles see different cosmic-ray particles than sites near the equator. So ideally, reference data for incoming radiation should be collected from an NM near the CRNS measurement site, i.e., at a similar cutoff rigidity.

Hawdon et al. (2014) presented a scaling concept to account for this geomagnetic effect using $\gamma = 1 - 0.075\,(R_\mathrm{c} - R_\mathrm{c}^{\mathrm{ref}})$, however, this approach has not been tested globally. A more recent approach by McJannet and Desilets (2023) uses so-called scaling factors that depend on R_c and on the atmospheric depth x for both the location of the site and of the neutron monitor used as a reference:

$$C_I = \tau^{-1}\,, \tag{10}$$

$$\tau(x, R_c) = \tau_{\mathrm{ref}}^{-1} \cdot \epsilon\,(-p_0\,x + p_1)\left(1 - \exp\left(-\,(p_2\,x + p_3)\,R_\mathrm{c}^{p_4\,x - p_5}\right)\right)\,, \tag{11}$$

with parameters p_i fitted on historical NM data. An empirical test of these approaches for the correction of incoming radiation is still missing.

Besides various correction functions, the neutron data presented in this study has been smoothed by temporal aggregation or moving average filters. These temporal smoothing approaches are useful to reduce noise in highly resolved time series in order to improve further comparative calculations, correlations, or visualizations. In the current processing scheme, the correction functions have been applied on the raw data first, followed by subsequent smoothing. Since there is also a debate about the correct order of these processing steps, we elaborated on this discussion in more detail in Appendix A.

2.4 The buoy deployment

To address the open questions on an empirical evaluation of atmospheric and geomagnetic correction approaches for the CRNS method, we decided to deploy a CRNS detector system on a lake. With a minimum amount of surrounding material, a detector system with a thermal and an epithermal neutron counter would mainly "see" the surrounding lake water. As the amount of surrounding water seen by the CRNS detector remained the same for floating device was not effected by precipitation or evapotranspiration, respectively, the total ground-related influence on the neutrons could be assumed constant. The remaining variations of neutrons should be induced by atmospheric conditions or solar activity only. An ideal set of correction functions would be able to reduce the neutron variations over time to zero ± stochastic errors.

For this experiment, we chose the lake *Seelhausener See*, which was located about 100 km southwest of Berlin, Germany at the border between the federal states Saxony and Saxony-Anhalt (Fig. 1a). The lake had formed in the abandoned opencast of a lignite mine (e.g. Geller et al., 2013). The lake is still not accessible for public use and thus offered the perfect place for exposing sensible technology in the environment. The surrounding is flat land with mainly natural vegetation.

In the preparation of this study, the URANOS model by Köhli et al. (2023) has been used to simulate the origin of the detected neutrons, following the signal contribution concept presented by Köhli et al. (2015) and Schrön et al. (2023). The environment has been modeled in a $700\times700\,\mathrm{m}^2$ domain (Fig. 1b) with a virtual detector above water, a given land structure with 10 % soil moisture, and air with 10 g/m³ humidity. We found that a distance of ≈ 300 m from the shore is appropriate to limit the influence of the land on the buoy detector to less than 2 %.

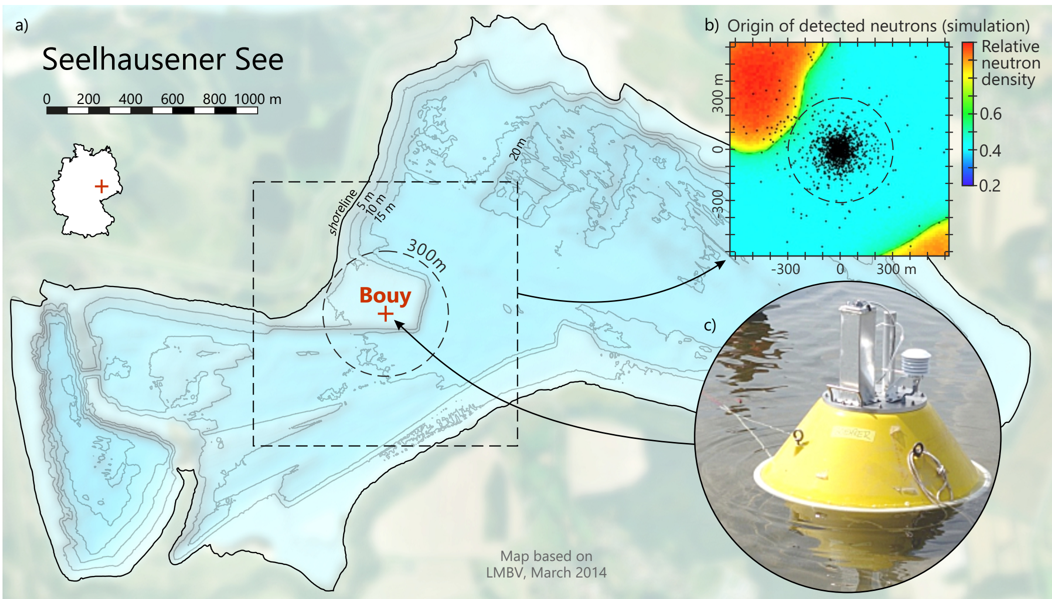

Figure 1. a) Location of the CRNS buoy detector at lake *Seelhausener See*. b) The distance of 300 m from the shoreline was chosen such that more than 98,% of detected neutrons had contact to water only (black dots, simulated with URANOS). c) Photograph of the buoy in operation. Map credits: adapted from LMBV, March 2014.

Instruments were placed inside a buoy of type `601 Profiler` from Idronaut S.r.l. and then tied between two anchors at the coordinates (51.58377°, 12.41423°). (Fig. 1c). Each rope was put under tension by mounting a trawl net ball (see Fig. 2). Other then usual anchoring techniques (e.g. Boehrer & Schultze, 2008), this arrangement kept the buoy in place within about 1 m and in the same orientation independently of rising or falling water levels over the entire study period.

The moderated and the bare tube was taken from a standard stationary CRNS system of type CRS1000 (Hydroinnova LLC, Albuquerque, US) that had previously been operated at the UFZ Leipzig (Schrön et al., 2018). The detectors were disassembled and integrated in a tailor-made aluminum lid, protruding upwards from the buoy (Fig. 2). The system was powered by eight batteries of type Yuasa NPL, 38 Ah, using lead-fleece technology to guarantee proper functioning under wobbling conditions. After installation on July 15th, 2014, the batteries had to be recharged by the end of September as the power supply lasted 2.5 months. Finally, the buoy was retracted under frosty conditions on December 2nd, 2014. An antenna regularly transmitted sensor data and GPS coordinates to an FTP server to allow scientists to remotely keep track of the battery status, and for the sake of protection against theft and tempest. The system further included external sensors for air temperature, relative air humidity, and air pressure to facilitate atmospheric corrections.

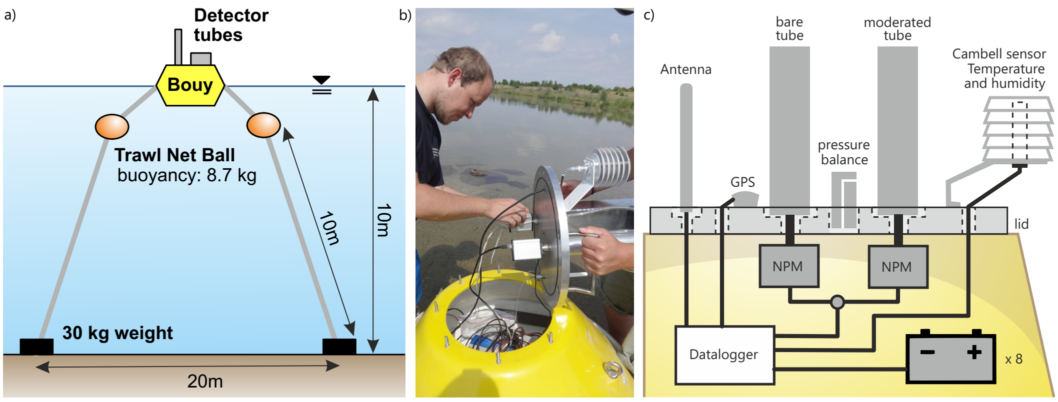

Figure 2. a) Setup of the buoy in the lake at around 10 m depth using trawl net balls and weights. b) Final checks with an open lid near the shore before the final launch into the water. c) Detector housing inside the tailor-made lid of the buoy, including GPS, antenna for data transmission, external sensors for air conditions, and a large battery array.

3 Results and Discussion

3.1 Buoy dataset

The measurement data of the buoy system is shown in Fig. 3. From July to December 2014, the air pressure varied by 30 mbar, while air temperature decreased from 20°C to 0°C and relative air humidity increased from 40 to 100 %. We have also calculated the absolute air humidity, h, following Rosolem et al. (2013). The epithermal neutron count rate has been 416 ± 41 cph, while thermal neutrons showed on average 240 ± 31 cph. According to counting statistics following Schrön et al. (2018), the expected stochastic error of the epithermal neutron count rate would be ±20 cph (hourly) or ±4 cph (daily), and of thermal neutrons ±15 cph (hourly) or ±3 cph (daily). In this context, the actually measured count rate already indicates a non-negligible influence of atmospheric and heliospheric factors. The time series has been gap-free with the exception of a short maintenance period in September 30th. Additionally, a Forbush decrease event has been captured on September 13th, which led to a significant drop of neutron count rates by ≈ 10 %.

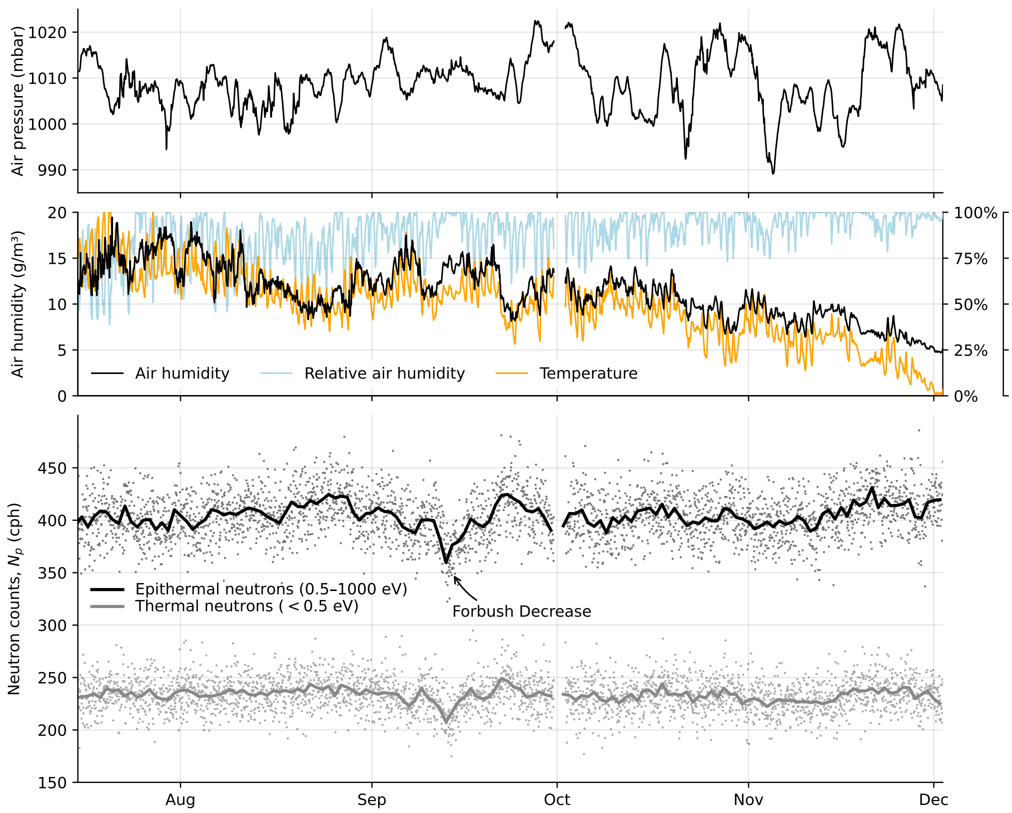

Figure 3. Data collected with the buoy instrument in 2014. Top: Air pressure. Middle: External air humidity and temperature. Bottom: pressure-corrected neutron counts of epithermal (0.5–1000 eV, black) and thermal energies (0–0.5 eV, grey). Dots depict hourly measurements, and solid lines depict the daily aggregation. A Forbush decrease event has been detected on September 13th. Maintenance work, including battery exchange, has been conducted on September 30th.

3.2 Challenging the neutrons-to-water relationship

Compared to typical over-land locations, the detector showed a significant drop of neutron counts over water by almost 50 % (compare Schrön et al., 2018, Fig. 3). Based on this observation, it was possible to test whether the existing concepts to describe the relationship between neutrons and water content, $N(\theta)$ (Eqs. (1), (2)), make the correct predictions following Eqs. (3) and (4).

The same detector type used in the buoy, CRS1000, has also been used on other locations, where $N_0^{\mathrm{Des}} \approx 1000\,\mathrm{cph}$ has been determined through calibration (see, e.g., Bogena et al., 2022). This corresponds to $N_0^{\mathrm{UTS}} = 1610\,\mathrm{cph}$, 2090 cph, 1580 cph, and 2030 cph for the UTS paremeter sets "MCNP drf", "MCNP THL", "URANOS drf", and "URANOS THL", respectively (section 2.2). Based on the assumption that these N_0 parameters are also applicable to the buoy detector, the expected count rate in a pure-water environment (Eqs. (3), (4)) would become 372 cph, 411 cph, 322 cph, 302 cph, 315 cph for the five approaches, respectively. Hence, the measured average count rate of 416 cph on the lake is in best agreement with the theoretical value of the "MCNP drf" parameter set from Köhli et al. (2021) for $\theta \to \infty$. The agreement is certainly within the uncertainty band of the data (see Fig. 3), while the remaining discrepancy could arise from a non-negligible effect of neutrons produced by the buoy material and the lead batteries themselves.

From this analysis, we can draw two conclusions. Firstly, the recently suggested parameter set for $N(\theta, h)$ derived from the full particle-physics model (MCNP) and the full detector response model (drf) fits best to the measured data and thus creates evidence for its potential superiority over the other parameter sets, including the approach from Desilets et al. (2010). Secondly, the buoy detector in this study seems to be a suitable representation of a pure-water scenario despite the substantial extent and material of the buoy itself and despite the finite distance to the shore.

3.3 Correlation of epithermal and thermal neutrons to external factors

The influences of (i) air pressure, (ii) air humidity, and (iii) incoming radiation on epithermal neutrons have been addressed in the literature, where various approaches exist to correct for these effects (section 2.3). Corrections for thermal neutrons have not been investigated so far, usually following the assumption that the same functions apply for them, too. For both neutron energies, however, empirical validation remains difficult, since neutron measurements above soils are always governed by the spatial and temporal variability of soil moisture, as well as by the site-specific heterogeneity (Schrön et al., 2023). In contrast, it is expected that neutron observations on a lake would not show terrestrial variability, thereby allowing for an evaluation of non-terrestrial correction approaches.

Fig. 4 shows the correlation between the daily relative neutron intensity and atmospheric variables. In each panel, neutron counts have been corrected for two variables and correlated to the corresponding third variable (compare section 2.3). Variations in air pressure exert the strongest influence on epithermal neutrons ($R^2 = 0.91$), followed by variations in incoming radiation ($R^2 = 0.67$), represented by data from the JUNG NM, and absolute air humidity ($R^2 = 0.61$). Thermal neutrons follow the same rank order.

For air pressure, the correction parameter $\beta = 0.0077\,\mathrm{mb}^{-1}$ seems to be an adequate choice for both thermal and epithermal neutrons. It matches exactly (within the uncertainty bounds) with the theoretical value of 0.0077 predicted by Dunai (2000). However, it differs slightly from the value of 0.0073 suggested by Desilets et al. (2006) and the corresponding and typically used calculation tool `http://crnslab.org/util/rigidity.php`. Note that β can change in time and space, such that the value determined in this experiment is not globally transferable. Further research should investigate the performance of the two methods with experimental data at other locations.

The regression coefficient for absolute air humidity, $0.0054\,\mathrm{m}^3/\mathrm{g}$, exactly matches the linear correction factor α derived by Rosolem et al. (2013), confirming the robustness of this approach. Unlike for epithermal neutrons, the correction procedure required for thermal neutrons has remained under debate. For instance, Andreasen et al. (2017) and Rasche et al. (2021) did not correct thermal neutrons for variations in air humidity, arguing that

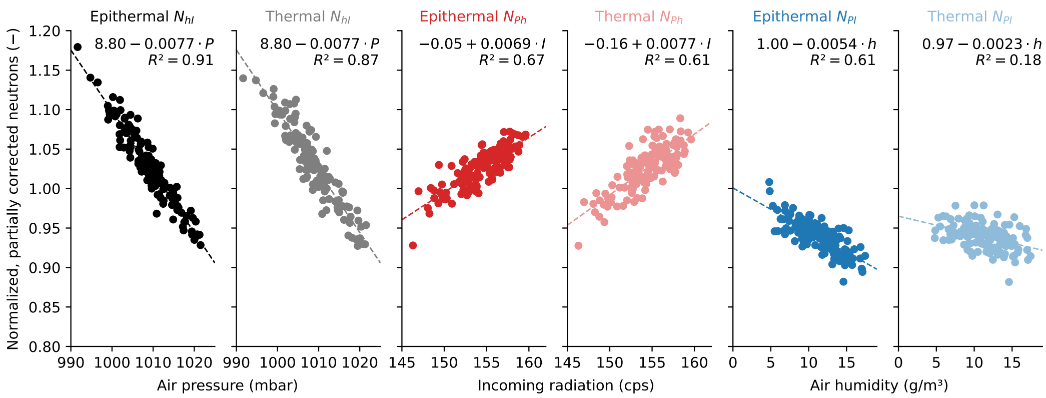

Figure 4. Partially corrected daily epithermal and thermal neutron observations normalized by their mean, correlated with three meteorological variables. Left two panels: neutrons corrected for air humidity and incoming radiation versus air pressure. Middle two panels: neutrons corrected for air humidity and air pressure versus incoming radiation. Right two panels: neutrons corrected for air pressure and incoming radiation versus air humidity. Each panel also shows the parameters of a linear model fit (dashed line).

the traditional correction functions have been derived for epithermal neutrons only. From dedicated simulations, Rasche et al. (2023) found a new value for thermal neutron correction, $\alpha = 0.0021\,\mathrm{m}^3/\mathrm{g}$. In contrast, based on empirical findings, Jakobi et al. (2018, 2022) correct thermal neutron intensities for air pressure and absolute humidity but not for variations in incoming radiation. They claimed that their empirical findings suggested better performance against biomass estimations.

The buoy-detector observations shed light on the required correction procedures for thermal neutrons as the effect of other hydrogen pools (e.g., biomass and soil moisture) on the empirical relationship can be excluded. Fig. 4 indicates that thermal neutrons are similarly dependent on variations in air pressure and incoming radiation compared to epithermal neutrons. The largest difference between epithermal and thermal neutrons by applying the same correction occurs in respect to variations in absolute air humidity. We found that the linear regression slope, 0.0023, is less than half of that of epithermal neutrons and very close to the value recently found by Rasche et al. (2023). The difference of thermal to epithermal neutron response to air humidity is likely linked to the generally higher production rate of thermal neutrons by epithermal neutron moderation than the thermal neutron absorption rate which leads to a weaker response of thermal neutrons to variations in environmental hydrogen (Weimar et al., 2020).

Consequently, the observations in this study indicate that epithermal and thermal neutron intensities need to be corrected for all three atmospheric variables. With respect to existing correction approaches, it is evident that the correction factor for air humidity should be different for epithermal and thermal neutrons, using $\alpha = 0.0054\,\mathrm{m}^3/\mathrm{g}$ (Rosolem et al., 2013) and $\alpha = 0.0021\,\mathrm{m}^3/\mathrm{g}$ (Rasche et al., 2023), respectively.

3.4 Apparent correlation of thermal neutrons to water temperature

The observation that the air humidity correction parameters for epithermal and thermal neutrons are different may have significant impact on the growing number of studies related to thermal neutron monitoring. Some previous studies applied the same correction approach from epithermals also to the thermal neutrons without accounting for this difference (Jakobi et al., 2018, 2022; Bogena et al., 2020). This may introduce a risk of overcorrection and apparent correlation to other variables. In the case of the buoy experiment, the conventional air humidity correction would cause an apparent correlation of thermal neutrons to lake water temperature. In fact, the observed corrected count rate of thermal neutrons in Fig. 5a showed a significantly higher correlation to the lake temperature ($R^2 = 0.26$) compared to corrected epithermal neutrons ($R^2 = 0.01$). We will explain below that this connection appears logical at first glance, but it is a fallacy on closer inspection.

By definition, the energy range of thermal neutrons corresponds to the mean kinetic energy of atoms in the environment, and thus their temperature. The theoretical foundation for this phenomenon is the temperature dependency of neutron cross sections (Glasstone & Sesonske, 1981). The cross section σ represents the probability of an interaction with an atomic nucleus. Interaction is less likely for larger relative velocities between target and particle v, i.e., $\sigma \propto 1/v$. In equilibrium, velocity and temperature are related by the Maxwell-Boltzmann distribution, where the (mean) particle energy is given by $E \propto mv^2 \propto kT$. Hence, σ ultimately depends on the temperature T of the scattering target: $\sigma(T) \propto \sqrt{1/T}$. Since water has a much higher density than humid air, the temperature of the lake might be more relevant than the air temperature.

While the higher temperature increases the thermal neutron density in air and water, it reduces the detection probability of the helium-3 counting gas in the same way (Krüger et al., 2008). The total observable influence on the thermal neutron count rate is a combination of two effects as air and lake temperatures decrease towards the winter: (i) increasing cross sections of nuclei in air and water, which removes more neutrons on their way to the detector and leads to a decreasing thermal neutron density in the system, and (ii) at the same time, increasing cross sections of nuclei in the Helium-3 gas, enabling higher detection efficiency which leads to higher count rates. Both processes scale with $\sqrt{1/T}$ in different directions. Since lake water temperature and detector temperature show the same dynamics (Appendix B), the two effects should almost annihilate each other. Fig. 5b shows the calculated temperature effect of the lake on the thermal neutron production (blue) and the thermal neutron detection (orange). The combined effects (black) almost cancel each other out and leave a nearly constant influence on the thermal neutron count rate.

Hence, the remaining correlation of thermal neutrons to lake temperature results from the wrong correction coefficient of $\alpha = 0.0054\,\mathrm{m^3/g}$. The observation data in Fig. 4 demonstrate that the thermal neutrons response to air humidity is much smaller compared to epithermal neutrons. Using the recently published correction factor, $\alpha = 0.0021\,\mathrm{m^3/g}$ (Rasche et al., 2023), which is very close the empirical observation from the buoy, the new correlation becomes $R^2 = 0.01$ for thermal neutrons and thereby confirms the insignificance of the temperature effect.

The example demonstrates the risk of overcorrection and false conclusions from data when the physical process understanding is incomplete. On the other hand, we cannot exclude remaining features in the data that could indicate systematic influences on the neutron count rate. For example, dew formation or ice on the buoy lid could be responsible for additional neutron moderation in autumn and winter, while extreme variations of shore moisture could impact the count rate in the summer. After a finalized analysis of the known external influences, we have further investigated the remaining correlations in section 3.7.

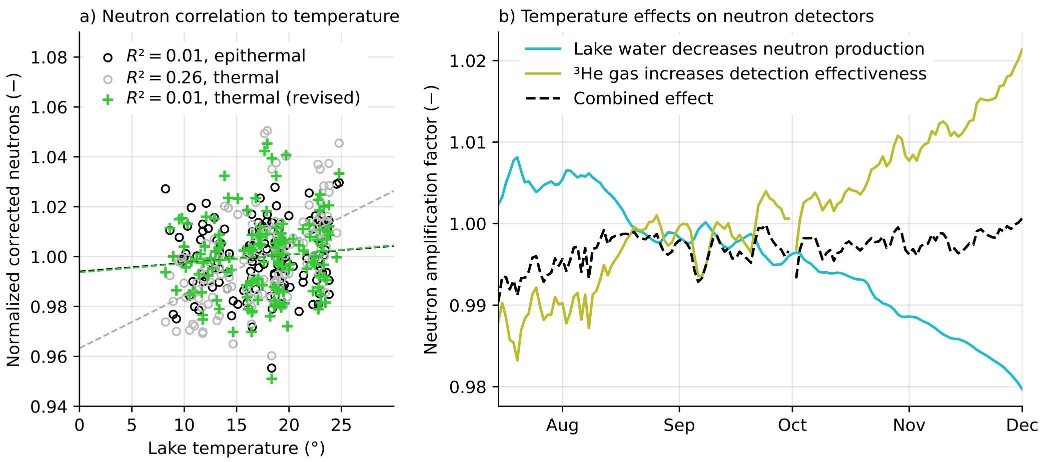

Figure 5. The effect of temperature on the measured buoy neutrons. a) Correlation of epithermal (black) and thermal neutrons (grey) to the lake temperature after conventional atmospheric corrections. This introduced an overcorrection for thermal neutrons. A revised air humidity correction approach simulated by Rasche et al. (2023) and confirmed by this study removed this remaining correlation. (b) Processes relevant for neutron production and absorption based on temperature over time. The reduced production of colder water essentially cancels out the enhanced detection efficiency of the detector gas.

3.5 Challenging the air humidity correction for epithermal neutrons

As discussed before, air humidity can have a significant effect on the neutron count rate due to varying density and amount of hydrogen atoms in the atmosphere. Rosolem et al. (2013) and Köhli et al. (2021) derived mathematical relationships from neutron transport simulations, but they are difficult to validate experimentally due to the high amount of other influencing environmental variables. With the exclusion of terrestrial factors, such as soil moisture and biomass, the use of lake-side measurements can be again an advantageous solution here.

To investigate which correction approach performs best at the buoy site, we correct the epithermal neutrons with air pressure and incoming radiation (N_{Pi}). If the remaining variability is only related to air humidity changes, the P, i-corrected neutrons should equal the inverse correction factor C_h^{-1}. In this ideal case, this difference is expected to become zero. To quantify the performance of each air humidity correction approach, we calculate the root-mean square error (RMSE) between N_{Pi} and C_h^{-1} over the whole measurement period.

Table 2 shows the result of this calculation. The hitherto approach from Rosolem et al. (2013) exhibits the lowest RMSE, again confirming a good performance for air humidity correction, see also section 3.3. However, the UTS approach with the parameter set "MCNP drf" is comparable in performance with an insignificantly larger error, while other parameter sets show weaker performance. This confirms the results from section 3.2 and the robustness of the full particle-physics and detector models. The fact that the approach from Rosolem et al. provides slightly better results than the UTS may be linked to the fact that the UTS was not tailored to describe the neutron response to changing air humidity alone. UTS has been optimized to solve the neutron response to the complex combination of soil moisture and air humidity, which could introduce lesser accuracy for air humidity variations alone.

Table 2. Root mean square error (RMSE) between the observed corrected epithermal intensity for air pressure and incoming radiation, N_{Pi}, and the inverse air humidity correction C_h^{-1} for the approaches from Rosolem et al. (2013) and UTS (see section 2.3). The analysis has also been performed for three different approaches of incoming radiation to test its robustness.

Incoming correction for N_{Pi}	Rosolem et al.	MCNP drf	MCNP THL	URANOS drf	URANOS THL
Zreda et al. (2012)	**5.39**	5.50	6.18	6.42	6.94
Hawdon et al. (2014)	**5.40**	5.48	6.09	6.31	6.82
McJannet and Desilets (2023)	**5.38**	5.48	6.13	6.37	6.88

3.6 Challenging the incoming cosmic-ray correction

Buoy-detector observations of neutrons in the epithermal and thermal energy range above a water surface and over a period of several months also allows for a comparison of the different correction approaches available for correcting neutron observations for variations in incoming radiation. The three available correction approaches described in the methods section were tested with seven different neutron monitors shown in Tab. 1 and compared with a thermal and epithermal neutron observations corrected for variations in air pressure and absolute air humidity (N_{Ph}), as this correction level should represent variations from changes in incoming radiation, only. In order to reduce the statistical noise in the data from the buoy detector, a 25-hour moving average was applied after applying the corrections. The epithermal and thermal N_{Ph} was then compared to the inverted correction factors for incoming radiation based on Zreda et al. (2012), Hawdon et al. (2014) and McJannet and Desilets (2023) (see section 2.3).

Table 3 shows the results from the analysis performed for selected neutron monitor stations. The Kling-Gupta Efficiency (KGE) was chosen as the goodness-of-fit measure in order to equally account for variation, correlation, and bias. The analysis reveals that the performance is generally lower for thermal neutrons compared to epithermal neutrons. This can be linked to the higher statistical uncertainty in the thermal neutron data due to the lower count rates. Likewise, a higher difference in cutoff rigidity between the locations of the neutron monitor and the study site leads to a lower KGE for both neutron energies. However, the Jungfraujoch neutron monitor still reveals the highest KGE, although its cutoff rigidity and altitude are higher than at the study site (compare Tab. 1).

Furthermore, it can be seen that the approaches from Hawdon et al. (2014) and McJannet and Desilets (2023) improve the KGE for the comparison with neutron monitors with higher cutoff rigidity than the study site compared to the approach after Zreda et al. (2012). In contrast, for neutron monitors with a lower cutoff rigidity, this improvement disappears and the approach according to Zreda et al. (2012) reveals a higher KGE with the data from the buoy detector. This effect is evident for both epithermal and thermal neutrons. The recent approach from McJannet and Desilets (2023) outperforms the approach by Hawdon et al. (2014), while both only lead to improvements for higher cutoff rigidities compared to the standard approach after Zreda et al. (2012). On average and over all neutron monitors investigated, the approach after McJannet and Desilets (2023) performs best in scaling neutron monitor signals to the location of the buoy detector, followed by the approach after Hawdon et al. (2014) and Zreda et al. (2012).

All three approaches provided robust results using data from the JUNG NM, with a slightly superior performance of Hawdon et al. (2014) at the study site. Additionally, the correct selection of a reference monitor seems to be more influential than then correction

Table 3. Performance measured by the Kling-Gupta Efficiency (KGE) of different correction approaches to rescale incoming neutron intensities from different neutron monitor stations compared with the observed and P, h-corrected epithermal (E) and thermal (T) neutron counts of the buoy. See also Tab. 1 for the corresponding cutoff rigidities and altitudes.

	C_I approach	PSNM	DJON	ATHN	JUNG	KIEL	OULU	SOPO	Average
E	Zreda et al. (2012)	0.269	0.34	0.465	0.737	0.678	0.667	**0.765**	0.560
E	Hawdon et al. (2014)	0.560	0.543	0.640	**0.790**	0.651	0.566	0.692	0.634
E	McJannet and Desilets (2023)	0.639	0.703	**0.761**	0.760	0.647	0.613	0.619	0.677
T	Zreda et al. (2012)	0.220	0.280	0.408	**0.635**	0.594	0.587	0.714	0.491
T	Hawdon et al. (2014)	0.481	0.460	0.567	**0.689**	0.569	0.493	0.614	0.553
T	McJannet and Desilets (2023)	0.627	0.624	**0.699**	0.657	0.565	0.537	0.545	0.608

method. The results generally indicate the advanced correction approaches from Hawdon et al. (2014) and particularly McJannet and Desilets (2023) improve the performance only for higher cutoff rigidities (i.e., regions near the equator). These findings may be also linked to the complex behavior of incoming radiation with different effects occurring at different cutoff rigidities, altitudes, latitudes, and longitudes (López-Comazzi & Blanco, 2020, 2022). The time series of epithermal and thermal neutrons are shown in Fig. 6 together with the time series of the JUNG, PSNM, and SOPO neutron monitors. Especially during the Forbush decrease in September 2014, a dampening of the neutron signal of the PSNM neutron monitor compared to the JUNG neutron monitor can be seen, which is linked to the higher R_c of PSNM. In addition, a temporal shift between PSNM and JUNG indicates differences between neutron monitor intensities due to different longitudinal locations. Lastly, the epithermal and thermal intensities decrease stronger than JUNG and PSNM, but similar to SOPO. This is an unexpected behavior, as the cutoff rigidity of SOPO is much lower than at the buoy location. The coincidence could indicate that low-energy neutron counters generally respond stronger to geomagnetic changes than high-energy NMs. Particularly with regards to the Forbush decrease, the observed discrepancy could also be linked to a change of the primary cosmic-ray energy spectrum during solar events (Bütikofer, 2018), which may lead to stronger changes of secondary low-energy cosmic-ray neutrons.

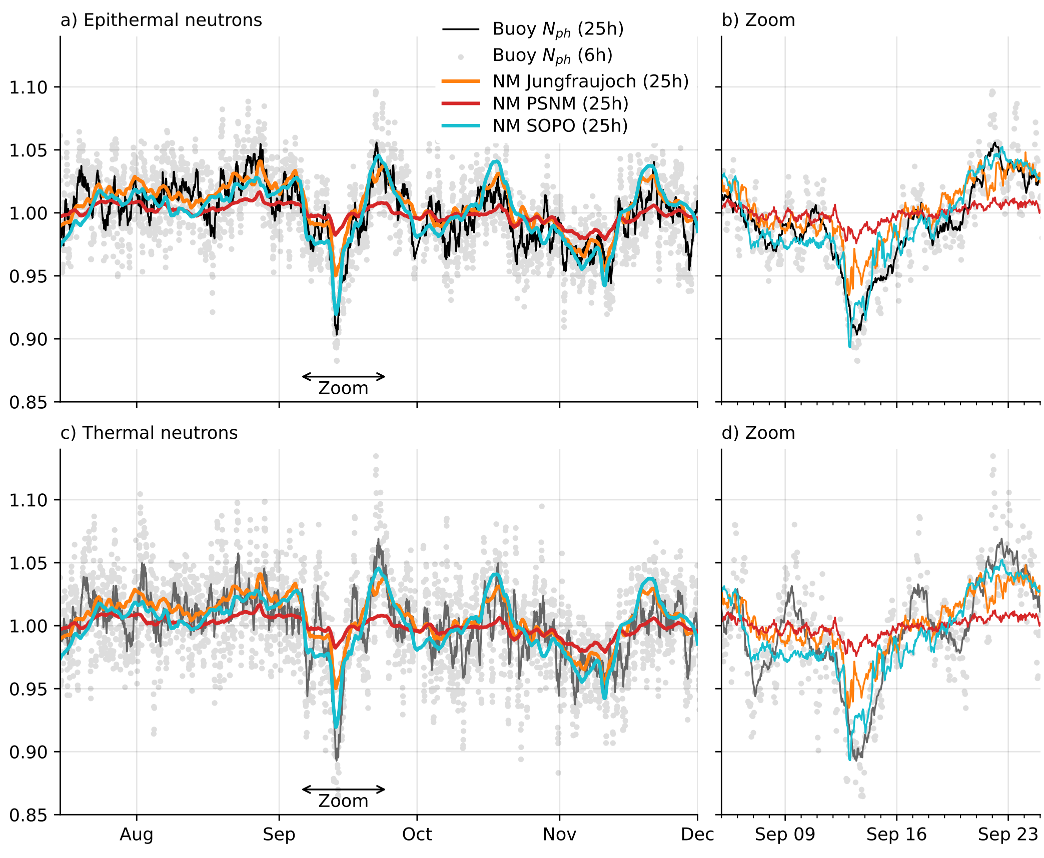

Figure 6. Normalized pressure- and humidity-corrected neutron count rates of the buoy detector compared with neutron monitor data. a) Epithermal buoy neutrons with a moving average window of 6 hours (grey dots) and 25 hours (black line). The latter filter was also applied to the NM data from JUNG in Switzerland (orange), PSNM in Thailand (red), and SOPO near the South Pole (blue). b) Zoom-in to the Forbush decrease event. c-d) Same as a-b for thermal buoy neutrons.

Depending on the moderator material and material thickness, proportional neutron detectors show varying sensitivity to neutrons of different energies (Garny et al., 2009; Köhli et al., 2018). A difference in the response of a bare thermal neutron detector and a neutron monitor has been shown by Nuntiyakul et al. (2018). Furthermore, Hubert et al. (2019) found a different response to solar events for neutrons of different energies. For the correction of neutron intensities for incoming radiation in the scope of CRNS, it, therefore, may not be sufficient to scale the neutron monitor response to different cutoff rigidities and atmospheric shielding depths only (Hawdon et al., 2014; McJannet & Desilets, 2023), but also to account for the different response of low-energy neutron detectors and neutron monitors.

The question about the choice of the most suitable neutron monitor for CRNS correction is equivalent to the question of which monitor better represents the local changes of cosmic-ray neutrons at the CRNS site. Sometimes, the answer is not obvious considering just geographical location parameters. For example, compared to the location of the buoy experiment, the KIEL monitor has more similar distance, altitude, and cutoff rigidity than JUNG. However, the neutron dynamics of the buoy can be better explained by JUNG, while KIEL behaves differently during and beyond the Forbush decrease event. These findings indicate the need for further research on the role of primary incoming radiation for low-energy cosmic-ray neutron sensing.

3.7 Residual correlations

The proper correction of all influencing factors on the neutrons should result in a time series, where residual deviations from the mean represent Poissonian noise. To test this hypothesis, a correlation analysis of N_{Phi} was conducted using a selection of atmospheric variables. In addition, different aggregation levels have been applied to further test the either random or systematic character of the relationships. The Spearman's rank correlation coefficient is shown in Tab. 4. It indicates that the influence of air pressure, incoming radiation, and absolute humidity is removed by the previously discussed correction procedures. However, a significant correlation between the N_{Phi} and relative air humidity remained for all aggregation levels and for both neutron energies.

High values of relative air humidity may indicate the formation of dew and, thus, a thin film of water on the buoy-detector, which reduces the observed neutron intensity of the epithermal and thermal detector due to higher neutron absorption. For example, Sentelhas et al. (2008) use a threshold of ≥ 90 percent relative humidity to distinguish periods with leaf wetness. Applying this threshold to the neutron observations reveals that epithermal and thermal N_{Phi} are, on average, 0.44 and 0.56 percent lower in periods with dew, respectively. This indicates that some influencing atmospheric variables are not yet considered in the standard correction procedures and illustrates the need for further research.

Furthermore, the statistical accuracy increases strongly with increasing integration times. Already at the 6-hour aggregation level, the Poisson standard deviation of the uncorrected neutron observations becomes lower than 2 percent. However, neutron transport simulation revealed that approx. 2 percent of epithermal neutrons reach the buoy-detector from the shore, indicating that with higher statistical accuracy, terrestrial variables such as soil moisture variations could influence the neutron observations of the buoy detector. This indicates some limitations of the measurement design in this study and illustrates potential improvements for future lake-side neutron measurements.

Table 4. Spearman's rank correlation coefficient between the corrected intensity (N_{Phi}) of epithermal (E) and thermal (T) neutrons aggregated to different temporal resolutions. Asterisk indicates statistical significance with $p < 0.05$.

	Variable	aggregation: 1 hour	6 hour	12 hour	24 hour
E	Air pressure	0.04	0.07	0.07	0.1
E	NM (Jungfraujoch)	0.003	0.02	−0.006	0.01
E	Abs. air humidity	−0.02	−0.04	−0.05	−0.09
E	Air temperature	0.003	0.02	0.01	0.0009
E	Rel. air humidity	−0.07*	−0.2*	−0.2*	−0.3*
E	Water temperature	0.01	0.03	0.03	0.008
E	Moist air density	0.006	−0.000004	0.01	0.03
E	Precipitation	0.0005	−0.09	−0.10	−0.20
T	Air pressure	0.03	0.08	0.06	0.03
T	NM (Jungfraujoch)	−0.006	−0.02	−0.04	−0.08
T	Abs. air humidity	−0.04*	−0.08	−0.10	−0.20*
T	Air temperature	−0.0007	−0.01	−0.07	−0.1
T	Rel. air humidity	−0.07*	−0.1*	−0.2*	−0.2*
T	Water temperature	−0.002	0.02	0.03	0.08
T	Moist air density	0.009	0.03	0.08	0.1
T	Precipitation	0.01	−0.006	−0.08	−0.10

3.8 Potential for the buoy as a reference for CRNS probes

Typical CRNS stations are located on natural ground to monitor soil moisture dynamics or agricultural fields, grass lands, or even snow dynamics in the alps. The conventional correction approach uses incoming radiation from neutron monitors (e.g., Jungfraujoch) to remove unwanted effects from solar activity, such as Forbush decreases.

We used data from a nearby terrestrial CRNS site at the UFZ Leipzig (25 km distance), where six identical CRNS stations were co-located on a $20 \times 20\,\mathrm{m}^2$ grassland patch. The sum of their signals mimics a larger CRNS station with up to 6000 cph ($\approx 1.4\,\%$ uncertainty).

Figure 7 shows the epithermal neutron data from this aggregated sensor corrected for air pressure and air humidity (dashed line). The solid line shows the data conventionally corrected for incoming neutrons with the NM Jungfraujoch. It is evident that the correction generally improves the obvious response to rain events, but the correction of the Forbush decrease in September 13 was not strong enough. The orange line shows the same correction approach with the epithermal neutron data measured at the same time by the buoy. The data was filtered by a 3-day moving average to reduce the buoy's noise level. The correction using the local buoy data better removes the Forbush decrease from the corrected CRNS neutron counts (September 13) and is also able to strengthen the response to some rain events (e.g., August 24 and September 17).

The results demonstrate that the concept of buoy detector can be used as an alternative to neutron monitors to correct for the incoming radiation. However, measurements on the buoy are limited by the low count rate due to the surrounding water and small detectors, such that there is a risk of introducing additional noise to the CRNS station data by this correction approach.

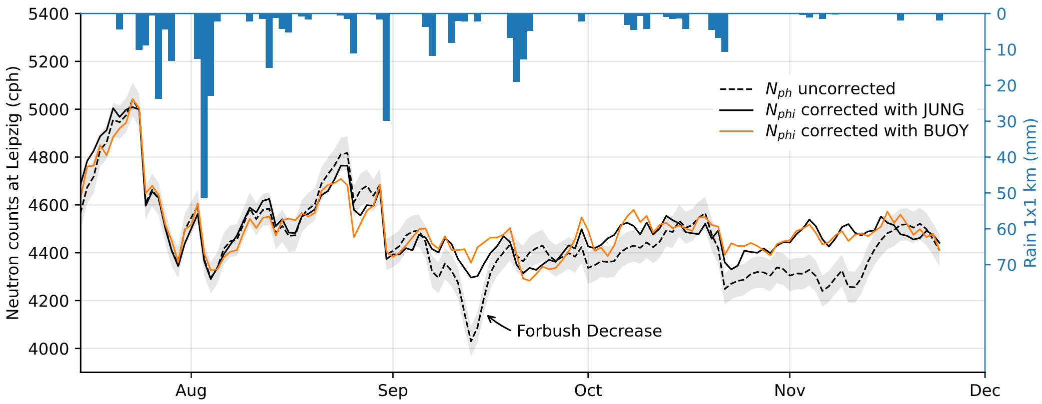

Figure 7. Epithermal neutrons aggregated from six collocated CRNS stations at the UFZ Leipzig, 25 km away (Schrön et al., 2018, data from). Neutron counts were corrected for air pressure and air humidity (dashed black) and corrected for incoming radiation using NM Jungfraujoch (solid black) and the buoy data (solid orange). Daily precipitation is indicated from Radolan measurements.

4 Conclusion

This study presents the concept of a thermal and an epithermal neutron detector in a buoy on a lake. The arrangement depicts an innovative opportunity to monitor the response of low-energy cosmic-ray neutrons to atmospheric conditions and to space weather without the influence of the ground, soil moisture, or any other nearby terrestrial heterogeneity that can influence the neutron counts. The experiment conducted on a lake in East Germany covered an almost gap-free period of five months from July 15th to December 2nd, 2014, including temperatures from 30 to 0°C, and - by chance - a major solar event (Forbush decrease). The unique data set facilitates empirical research on challenging conventional theories and traditional correction functions for atmospheric, geomagnetic, and heliospheric variations. The experiment revealed the following insights:

1. The epithermal neutron count rate over water dropped by more than 50 % compared to values over typical soil. The measured count rate was not in agreement with the theoretical value predicted by the previous $N(\theta)$ model (Desilets et al., 2010). In contrast, the value was almost exactly predicted by the UTS approach (Köhli et al., 2021) using the parameter set "MCNP drf". This finding might indicate a potential superiority of UTS for the conversion from neutrons to soil moisture also for other CRNS applications.
2. The buoy data showed strong correlation to air pressure, which was similar for both, epithermal and thermal neutrons. The thereby empirically determined neutron attenuation length was in very good agreement with the theoretical prediction by Dunai (2000), while it was 5 % lower than the conventional calculation for this region. This indicates that further research is needed to better adapt traditional calculation methods on the special requirements of low-energy neutron detectors.
3. The different approaches for air humidity correction have been challenged by their ability to remove undesired variations of the buoy signal. The conventional approach by Rosolem et al. (2013) performed best and its parameter $\alpha = 0.0054$ has been confirmed for epithermal neutrons. Almost similar performance was achieved by the UTS approach using the parameter set "MCNP drf", while all other parameter sets were not able to fully remove air humidity variations.
4. Conventional thermal neutron corrections for air humidity, however, led to a significant overcorrection. A potential influence of lake water temperature on the thermal neutrons has been excluded by analysis of the nuclear interaction cross sections. A different correction parameter for thermal neutrons has been identified, which confirmed independent results from Rasche et al. (2023).
5. The response to incoming cosmic radiation is almost similar for both, epithermal and thermal neutrons, in contrast to assumptions by some previous studies. We challenged three existing correction approaches by comparing the buoy data with data from various neutron monitors and found robust performance for NM Jungfraujoch and the approach from Zreda et al. (2012). The more sophisticated approaches by Hawdon et al. (2014) and McJannet and Desilets (2023) showed particularly good skills in rescaling data from NMs with higher cut-off rigidities than the measurement site.
6. The remarkable Forbush decrease (FD) observed in Sept 2014 was more pronounced in the buoy data than in data from the NMs, particularly for thermal neutrons. In addition to the findings from the pressure correction above, this is another indication that the scaling of incoming radiation from NMs to CRNS is not well enough understood, probably due to the sensitivity to different particle energies.
7. After all corrections were applied, the remaining variations of the buoy signal have been investigated. For both, thermal and epithermal neutrons, a significant correlation to relative air humidity became evident, which could be an indication for yet unnoticed sensitivity to dew.

In a final test, we used the buoy data as a reference signal for the incoming radiation correction of a nearby CRNS site. Here, a slightly better correction capability was evident, particularly during the FD event. This experiment demonstrated that a buoy could act as a suitable local alternative for a neutron monitor, especially since it measures similar energy levels as the CRNS, it is much cheaper than an NM, and it could be installed more closer to CRNS sites, thereby avoiding any geomagnetic or location-specific biases. However, buoys are limited in size, such that their data is highly uncertain due to the low count rates. Daily temporal resolution was the minimum for our system to be applicable as a reference monitor. To overcome this weakness, future studies could deploy buoy detectors on high-altitude lakes or glaciers, which would equally well resemble a pure-water environment for the neutrons with much higher count rates (e.g., Gugerli et al., 2019, 2022).

We encourage the usage of the presented data set for further research on new theories or correction functions. One more example is the debate of whether to apply temporal smoothing algorithms before or after atmospheric corrections. With the buoy data, we were able to show that correction prior to smoothing is crucial for maintaining correlation to the incoming radiation data, for instance (see sect. Appendix A).

Appendix A The order of smoothing and correction procedures matters

The buoy experiment provides a perfect test for meteorological correction functions. For example, it has been discussed in the community whether smoothing prior (Heidbüchel et al., 2016) or after correcting neutron data (Franz et al., 2020; Davies et al., 2022) is recommended. With the buoy data, this hypotheses can be tested without influence of ground-based variations.

In general, temporal smoothing of a time series is a linear operation f, since

$$f: \quad x(t) = \sum_{t-\tau}^{t+\tau} w \cdot x(t') / \sum_{t-\tau}^{t+\tau} w \,,$$

where 2τ is the window size over which the data is averaged, and w is a weighting factor (e.g., 1 for a uniform average, or $e^{-\tau}$ for exponential filters). In contrast, some correction functions can be non-linear, e.g., the correction for air pressure or for incoming radiation. For the combination of linear f and non-linear functions g, the following rule generally holds:

$$f(g(x)) \neq g(f(x)) \,.$$

For this reason, the order of processing operations generally matters. In the case of neutron count variations, corrections should be applied on the raw data, and only the final product should then be averaged (smoothed). Otherwise, it is not guaranteed that a measurement $N(t)$ is corrected for the air pressure $P(t)$ at the same time t, for instance. Fig. A1 shows that the correlation between the buoy experimental epithermal neutron intensity corrected for variations in atmospheric pressure and absolute humidity and the inverted primary influx correction from Zreda et al. (2012) generally increases with increasing moving average window size when the correction procedures are applied *before* averaging the raw data. In contrast, a correction *after* averaging the raw data leads to (i) a lower maximum correlation and (ii) a decrease of the correlation at window sizes larger than 25 hours. This is in line with recent findings by Davies et al. (2022), who found a general improvement of the CRNS-derived soil moisture when the correction procedure is applied prior filtering

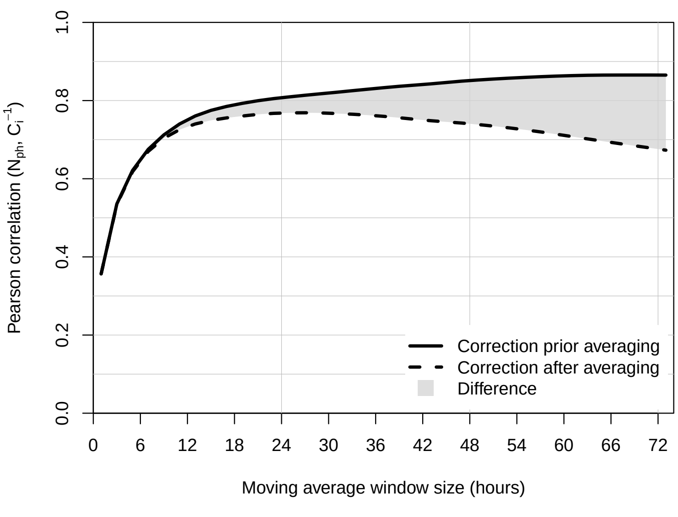

Figure A1. Pearson correlation coefficient between the epithermal N_{ph} vs. inverted influx correction after (Zreda et al., 2012) using the JUNG neutron monitor, when the correction is applied prior or after smoothing with a moving average of the neutron intensity time series. In general, for filtering approaches based on a moving window, the window size needs to be odd in order to create a centered filter to avoid a temporal shift in the filtered time series. For example, a centered 24-hour moving average equals a 25-hour moving average.

Appendix B Determination of the lake water temperature

At the study location, lake *Seelhausener See*, direct measurements of the water temperature were not available. However, it is possible to use measurements of a nearby lake as a proxy.

Surface temperatures in lakes are mainly determined by the local weather. Hence lakes located close to each other at the same geographic altitude show similar temperatures. This was verified in a comparison of surface temperatures of mine pit lakes in the Central German and Lusatian Mining District, in which also *Seelhausener See* is located. Boehrer et al. (2014) found that the lake temperatures measured in 0.5 m depth were nearly identical. Only in cases of rapidly rising temperatures (e.g., in spring time), a difference of up to 2°C was detected between very small and larger lakes. Numerical models that are calibrated specifically for the conditions of a single lake often reach about the same accuracy (e.g. Weber et al., 2017), while models that are not specifically calibrated (e.g. occasional local temperature measurements) will show greater deviations. Alternative methods, such as satellite imaging and thermometry, only provide sporadic measurements and do not reach a similar accuracy without additional support from numerical models (Zhang et al., 2020).

Lake *Rassnitzer See* is situated in 31 km distance south west of the study area and was previously called "Mine Pit Lake Merseburg-Ost 1b" (Heidenreich et al., 1999). The lakes *Seelhausener See* and *Rassnitzer See* exhibit similar morphology, similar size, and are exposed to similar air temperatures (Böhrer et al., 1998). Since it can be assumed that temperatures will hardly differ by more than 1°C, the surface temperatures (i.e., at 0.5 m depth) from *Rassnitzer See* can be used as an accurate approximation for temperatures in *Seelhausener See* at the same depth. This assumption has been supported by the fact that the observed air temperatures were very similar at both lakes throughout the investigation period (shown in Fig. B1).

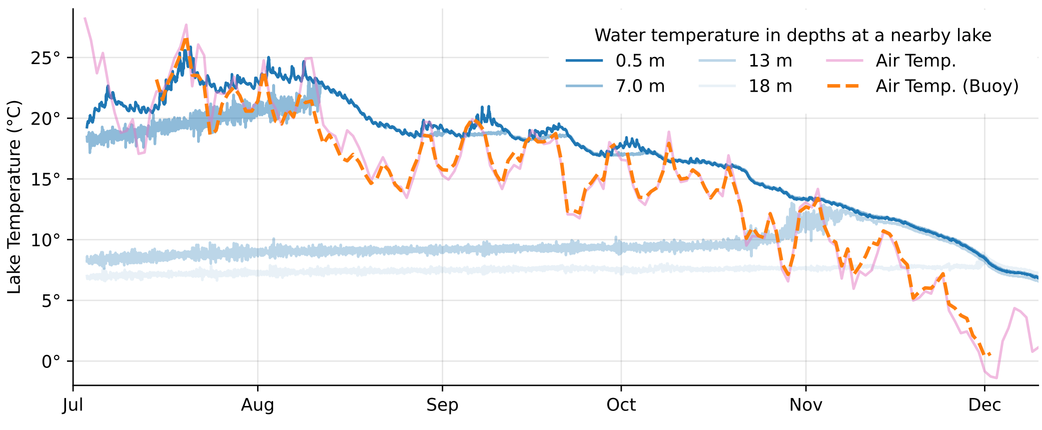

Figure B1. Water temperatures measured by an anchored weather station with attached thermistor chain in *Rassnitzer See* from July 2014 to January 2015 in several depths (blue shading). Air temperature has been measured at both lakes, *Rassnitzer See* (pink solid) and *Seelhausener See* (orange dashed).

Acknowledgments

The data used in this manuscript has been processed with Corny (`https://git.ufz.de/CRNS/cornish_pasdy`) and is available in the supplements. The research was inspired and partly supported by the Deutsche Forschungsgemeinschaft (grant no. 357874777; research unit FOR 2694, Cosmic Sense II) and the Bundesministerium für Bildung und Forschung (grant no. 02WIL1522; German–Israeli Cooperation in Water Technology Research). S. Kögler greatly supported the development of the buoy detector lid, took care about the electro-technical setup, and organized the boat trips to the lake site. Special thanks goes to Prof. Peter Dietrich, who supported the idea, vision, and implementation of the endeavour and who always facilitated curiosity-driven experiments. We further thank K. Rahn for supporting technical implementation of the buoy. Permission to access the lake was kindly granted by D. Onnasch and P. Morszeck (LMBV). Particular thanks to B. Dannenberg for support and instructions at the lake site. We thank TERENO (Terrestrial Environmental Observatories), funded by the Helmholtz-Gemeinschaft for the financing and maintenance of CRNS stations used in this study. We acknowledge the NMDB database (www.nmdb.eu) founded under the European Union's FP7 programme (contract no. 213 007), and the PIs of individual neutron monitors.

References

Abunin, A., Kobelev, P., Abunina, M., Preobragenskiy, M., Smirnov, D., & Lukovnikova, A. (2016, March). A wind effect of neutron component of cosmic rays at Antarctic station "Mirny". *Solar-Terrestrial Physics (Solnechno-zemnaya fizika)*, *2*(1), 71-75. doi: 10.12737/13505

Andreasen, M., Jensen, K. H., Desilets, D., Zreda, M., Bogena, H. R., & Looms, M. C. (2017). Cosmic-ray neutron transport at a forest field site: the sensitivity to various environmental conditions with focus on biomass and canopy interception. *Hydrology and Earth System Sciences*, *21*(4), 1875–1894. doi: 10.5194/hess-21-1875-2017

Aplin, K., Harrison, R., & Bennett, A. (2005). Effect of the troposphere on surface neutron counter measurements. *Advances in Space Research*, *35*(8), 1484 - 1491. doi: 10.1016/j.asr.2005.02.055

Baatz, R., Bogena, H., Hendricks-Franssen, H.-J., Huisman, J., Qu, W., Montzka, C., & Vereecken, H. (2014). Calibration of a catchment scale cosmic-ray probe network: A comparison of three parameterization methods. *Journal of Hydrology*, *516*, 231–244. doi: 10.1016/j.jhydrol.2014.02.026

Belov, A., Baisultanova, L., Eroshenko, E., Mavromichalaki, H., Yanke, V., Pchelkin, V., ... Mariatos, G. (2005). Magnetospheric effects in cosmic rays during the unique magnetic storm on November 2003. *Journal of Geophysical Research: Space Physics*, *110*(A9). doi: 10.1029/2005JA011067

Boehrer, B., Kiwel, U., Rahn, K., & Schultze, M. (2014). Chemocline erosion and its conservation by freshwater introduction to meromictic salt lakes. *Limnologica*, *44*, 81—89. doi: 10.1016/j.limno.2013.08.003

Boehrer, B., & Schultze, M. (2008). Stratification of lakes. *Reviews of Geophysics*, *46*(2).

Bogena, H. R., Herrmann, F., Jakobi, J., Brogi, C., Ilias, A., Huisman, J. A., ... Pisinaras, V. (2020). Monitoring of Snowpack Dynamics With Cosmic-Ray Neutron Probes: A Comparison of Four Conversion Methods. *Frontiers in Water*, *2*. Retrieved 2023-12-19, from `https://www.frontiersin.org/articles/10.3389/frwa.2020.00019`

Bogena, H. R., Schrön, M., Jakobi, J., Ney, P., Zacharias, S., Andreasen, M., ... Vereecken, H. (2022). COSMOS-Europe: a European network of cosmic-ray neutron soil moisture sensors. *Earth Syst. Sci. Data*, *14*(3), 1125–1151. doi: 10.5194/essd-14-1125-2022

Böhrer, B., Heidenreich, H., Schimmele, M., & Schultze, M. (1998). Numerical prognosis for salinity profiles of future lakes in the opencast mine merseburg-ost. *International Journal of Salt Lake Research*, *7*(3), 235–260. doi: 10.1007/BF02441877

Bütikofer, R. (1999). Pressure correction of GLE measurements in turbulent winds. In *International cosmic ray conference* (Vol. 6, p. 395).

Bütikofer, R. (2018). Ground-based measurements of energetic particles by neutron monitors. In O. E. Malandraki & N. B. Crosby (Eds.), *Solar particle radiation storms forecasting and analysis: The hesperia horizon 2020 project and beyond* (pp. 95–111). Cham: Springer International Publishing. doi: 10.1007/978-3-319-60051-2_6

Clem, J. M., Bieber, J. W., Evenson, P., Hall, D., Humble, J. E., & Duldig, M. (1997). Contribution of obliquely incident particles to neutron monitor counting rate. *Journal of Geophysical Research: Space Physics*, *102*(A12), 26919–26926. doi: 10.1029/97JA02366

Clem, J. M., & Dorman, L. I. (2000). Neutron monitor response functions. *Space Science Reviews*, *93*(1), 335–359. doi: 10.1023/A:1026508915269

Davies, P., Baatz, R., Bogena, H. R., Quansah, E., & Amekudzi, L. K. (2022). Optimal temporal filtering of the cosmic-ray neutron signal to reduce soil moisture uncertainty. *Sensors*, *22*(23). doi: 10.3390/s22239143

Desilets, D., & Zreda, M. (2001). On scaling cosmogenic nuclide production rates for altitude and latitude using cosmic-ray measurements. *Earth and Planetary Science Letters*, *193*(1–2), 213–225. doi: 10.1016/S0012-821X(01)00477-0

Desilets, D., & Zreda, M. (2013). Footprint diameter for a cosmic-ray soil moisture probe: Theory and Monte Carlo simulations. *Water Resources Research*, *49*(6), 3566–3575. doi: 10.1002/wrcr.20187

Desilets, D., Zreda, M., & Ferré, T. (2010). Nature's neutron probe: Land surface hydrology at an elusive scale with cosmic rays. *Water Resources Research*, *46*(11). doi: 10.1029/2009WR008726

Desilets, D., Zreda, M., & Prabu, T. (2006). Extended scaling factors for in situ cosmogenic nuclides: New measurements at low latitude. *Earth and Planetary Science Letters*, *246*(3-4), 265–276. doi: 10.1016/j.epsl.2006.03.051

Döpper, V., Jagdhuber, T., Holtgrave, A.-K., Heistermann, M., Francke, T., Kleinschmit, B., & Förster, M. (2022). Following the cosmic-ray-neutron-sensing-based soil moisture under grassland and forest: Exploring the potential of optical and SAR remote sensing. *Science of Remote Sensing*, *5*, 100056. doi: 10.1016/j.srs.2022.100056

Dorman, L. I. (2004). *Cosmic rays in the earth's atmosphere and underground*. Springer Netherlands. doi: 10.1007/978-1-4020-2113-8

Dunai, T. J. (2000). Scaling factors for production rates of in situ produced cosmogenic nuclides: a critical reevaluation. *Earth and Planetary Science Letters*, *176*(1), 157–169.

Fersch, B., Francke, T., Heistermann, M., Schrön, M., Döpper, V., Jakobi, J., … Oswald, S. E. (2020). A dense network of cosmic-ray neutron sensors for soil moisture observation in a highly instrumented pre-Alpine headwater catchment in Germany. *Earth System Science Data*, *12*(3), 2289–2309. doi: 10.5194/essd-12-2289-2020

Franz, T. E., Wahbi, A., Zhang, J., Vreugdenhil, M., Heng, L., Dercon, G., … Wagner, W. (2020). Practical data products from cosmic-ray neutron sensing for hydrological applications. *Frontiers in Water*, *2*. doi: 10.3389/frwa.2020.00009

Franz, T. E., Zreda, M., Ferré, T. P. A., & Rosolem, R. (2013). An assessment of the effect of horizontal soil moisture heterogeneity on the area-average measurement of cosmic-ray neutrons. *Water Resources Research*, *49*(10), 6450–6458. doi: 10.1002/wrcr.20530

Garny, S., Mares, V., & Rühm, W. (2009). Response functions of a bonner sphere spectrometer calculated with geant4. *Nuclear Instruments and Methods in Physics Research Section A: Accelerators, Spectrometers, Detectors and Associated Equipment*, *604*(3), 612–617. doi: 10.1016/j.nima.2009.02.044

Geller, W., Schultze, M., Kleinmann, B., & Wolkersdorfer, C. (2013). *Acidic pit lakes: The legacy of coal and metal surface mines*. Springer Berlin Heidelberg. doi: 10.1007/978-3-642-29384-9

Glasstone, S., & Sesonske, A. (1981). *Nuclear reactor engineering*. Krieger Publishing Company, Malabar, Florida.

Goorley, T., James, M., Booth, T., Brown, F., Bull, J., Cox, L., … Zukaitis, T. (2012). Initial MCNP6 release overview. *Nuclear Technology*, *180*(3), 298–315. doi: 10.13182/

NT11-135

Gugerli, R., Desilets, D., & Salzmann, N. (2022). Brief communication: Application of a muonic cosmic ray snow gauge to monitor the snow water equivalent on alpine glaciers. *The Cryosphere*, *16*(3), 799–806.

Gugerli, R., Salzmann, N., Huss, M., & Desilets, D. (2019). Continuous and autonomous snow water equivalent measurements by a cosmic ray sensor on an alpine glacier. *The Cryosphere*, *13*(12), 3413–3434. doi: 10.5194/tc-13-3413-2019

Hands, A. D. P., Baird, F., Ryden, K. A., Dyer, C. S., Lei, F., Evans, J. G., . . . Henley, E. M. (2021). Detecting Ground Level Enhancements Using Soil Moisture Sensor Networks. *Space Weather*, *19*(8), e2021SW002800. doi: 10.1029/2021SW002800

Hawdon, A., McJannet, D., & Wallace, J. (2014). Calibration and correction procedures for cosmic-ray neutron soil moisture probes located across Australia. *Water Resources Research*, *50*(6), 5029–5043. doi: 10.1002/2013WR015138

Heidbüchel, I., Güntner, A., & Blume, T. (2016). Use of cosmic-ray neutron sensors for soil moisture monitoring in forests. *Hydrology and Earth System Sciences*, *20*(3), 1269–1288. doi: 10.5194/hess-20-1269-2016

Heidenreich, H., Boehrer, B., Kater, R., & Hennig, G. (1999). Gekoppelte Modellierung geohydraulischer und limnophysikalischer Vorgänge in Tagebaurestseen und ihrer Umgebung. *Grundwasser*, *4*(2), 49—54. doi: 10.1007/s767-1999-8604-4

Herbst, K., Kopp, A., & Heber, B. (2013). Influence of the terrestrial magnetic field geometry on the cutoff rigidity of cosmic ray particles. In *Annales geophysicae* (Vol. 31, pp. 1637–1643). doi: 10.5194/angeo-31-1637-2013

Hess, W. N., Canfield, E. H., & Lingenfelter, R. E. (1961). Cosmic-ray neutron demography. *Journal of Geophysical Research (1896-1977)*, *66*(3), 665–677. doi: 10.1029/JZ066i003p00665

Hubert, G., Pazianotto, M. T., Federico, C. A., & Ricaud, P. (2019). Analysis of the forbush decreases and ground-level enhancement on september 2017 using neutron spectrometers operated in antarctic and midlatitude stations. *Journal of Geophysical Research: Space Physics*, *124*(1), 661–673. doi: 10.1029/2018JA025834

Iwema, J., Rosolem, R., Rahman, M., Blyth, E., & Wagener, T. (2017). Land surface model performance using cosmic-ray and point-scale soil moisture measurements for calibration. *Hydrology and Earth System Sciences*, *21*(6), 2843–2861. doi: 10.5194/hess-21-2843-2017

Iwema, J., Schrön, M., Koltermann Da Silva, J., Schweiser De Paiva Lopes, R., & Rosolem, R. (2021, November). Accuracy and precision of the cosmic-ray neutron sensor for soil moisture estimation at humid environments. *Hydrological Processes*, *35*(11). doi: 10.1002/hyp.14419

Jakobi, J., Huisman, J. A., Fuchs, H., Vereecken, H., & Bogena, H. R. (2022). Potential of thermal neutrons to correct cosmic-ray neutron soil moisture content measurements for dynamic biomass effects. *Water Resources Research*, *58*(8), e2022WR031972. doi: 10.1029/2022WR031972

Jakobi, J., Huisman, J. A., Vereecken, H., Diekkrüger, B., & Bogena, H. R. (2018). Cosmic ray neutron sensing for simultaneous soil water content and biomass quantification in drought conditions. *Water Resources Research*, *54*(10), 7383–7402. doi: 10.1029/2018WR022692

Kobelev, P., Belov, A., Mavromichalaki, E., Gerontidou, M., & Yanke, V. (2011). Variations of barometric coefficients of the neutron component in the 22-23 cycles of solar activity. *CD Proc. 32nd ICRC, id0654, Beijing*.

Kodama, M. (1980). Continuous monitoring of snow water equivalent using cosmic ray neutrons. *Cold Regions Science and Technology*, *3*(4), 295–303. doi: 10.1016/0165-232x(80)90036-1

Kodama, M., Kawasaki, S., & Wada, M. (1975). A cosmic-ray snow gauge. *The International Journal of Applied Radiation and Isotopes*, *26*(12), 774–775.

Kodama, M., Kudo, S., & Kosuge, T. (1985). Application of atmospheric neutrons to soil moisture measurement. *Soil Science*, *140*(4), 237–242.

Köhli, M., Schrön, M., & Schmidt, U. (2018). Response functions for detectors in cosmic ray neutron sensing. *Nuclear Instruments and Methods in Physics Research Section A: Accelerators, Spectrometers, Detectors and Associated Equipment*, *902*, 184–189. doi: 10.1016/j.nima.2018.06.052

Köhli, M., Schrön, M., Zacharias, S., & Schmidt, U. (2023). URANOS v1.0 – the Ultra Rapid Adaptable Neutron-Only Simulation for Environmental Research. *Geoscientific Model Development*, *16*(2), 449–477. doi: 10.5194/gmd-16-449-2023

Köhli, M., Schrön, M., Zreda, M., Schmidt, U., Dietrich, P., & Zacharias, S. (2015). Footprint characteristics revised for field-scale soil moisture monitoring with cosmic-ray neutrons. *Water Resources Research*, *51*(7), 5772–5790. doi: 10.1002/2015wr017169

Köhli, M., Weimar, J., Schrön, M., Baatz, R., & Schmidt, U. (2021). Soil moisture and air humidity dependence of the above-ground cosmic-ray neutron intensity. *Frontiers in Water*, *2*. doi: 10.3389/frwa.2020.544847

Korotkov, V. K., Berkova, M. D., Belov, A. V., Eroshenko, E. A., Kobelev, P. G., & Yanke, V. G. (2011). Effect of snow in cosmic ray variations and methods for taking it into consideration. *Geomagnetism and Aeronomy*, *51*(2), 247–253. doi: 10.1134/S0016793211020095

Krüger, H., & Moraal, H. (2010). A calibration neutron monitor: Statistical accuracy and environmental sensitivity. *Advances in Space Research*, *46*(11), 1394–1399. doi: 10.1016/j.asr.2010.07.008

Krüger, H., Moraal, H., Bieber, J. W., Clem, J. M., Evenson, P. A., Pyle, K. R., ... Humble, J. E. (2008). A calibration neutron monitor: Energy response and instrumental temperature sensitivity. *Journal of Geophysical Research: Space Physics*, *113*(A8). (A08101) doi: 10.1029/2008JA013229

Kudela, K. (2012). Variability of Low Energy Cosmic Rays Near Earth. In *Exploring the Solar Wind.* IntechOpen. doi: 10.5772/37482

Laken, B., Kniveton, D., & Wolfendale, A. (2011). Forbush decreases, solar irradiance variations, and anomalous cloud changes. *Journal of Geophysical Research: Atmospheres*, *116*(D9). doi: 10.1029/2010JD014900

Lingri, D., Mavromichalaki, H., Belov, A., Abunina, M., Eroshenko, E., & Abunin, A. (2019, June). An Extended Study of the Precursory Signs of Forbush Decreases: New Findings over the Years 2008-2016. *Solar Physics*, *294*(6), 70. doi: 10.1007/s11207-019-1461-3

López-Comazzi, A., & Blanco, J. J. (2020). Short-term periodicities observed in neutron monitor counting rates. *Solar Physics*, *295*(6). doi: 10.1007/s11207-020-01649-5

López-Comazzi, A., & Blanco, J. J. (2022). Short- and mid-term periodicities observed in neutron monitor counting rates throughout solar cycles 20–24. *The Astrophysical Journal*, *927*(2), 155. doi: 10.3847/1538-4357/ac4e19

Mavromichalaki, H., Papaioannou, A., Plainaki, C., Sarlanis, C., Souvatzoglou, G., Gerontidou, M., ... others (2011). Applications and usage of the real-time neutron monitor database. *Advances in Space Research*, *47*(12), 2210–2222. doi: 10.1016/j.asr.2010.02.019

McJannet, D. L., & Desilets, D. (2023). Incoming Neutron Flux Corrections for Cosmic-Ray Soil and Snow Sensors Using the Global Neutron Monitor Network. *Water Resources Research*, *59*(4), e2022WR033889. doi: 10.1029/2022WR033889

McJannet, D. L., Franz, T. E., Hawdon, A., Boadle, D., Baker, B., Almeida, A., ... Desilets, D. (2014). Field testing of the universal calibration function for determination of soil moisture with cosmic-ray neutrons. *Water Resources Research*, *50*(6), 5235–5248. doi: 10.1002/2014WR015513

Mishev, A. L., Kocharov, L. G., & Usoskin, I. G. (2014). Analysis of the ground level enhancement on 17 May 2012 using data from the global neutron monitor network. *Journal of Geophysical Research: Space Physics*, *119*(2), 670–679. doi: 10.1002/2013JA019253

Montzka, C., Bogena, H. R., Zreda, M., Monerris, A., Morrison, R., Muddu, S., & Vereecken, H. (2017). Validation of spaceborne and modelled surface soil moisture products with cosmic-ray neutron probes. *Remote sensing*, *9*(2), 103.

National Centers for Environmental Information. (2015). *Magnetic field calculators.* Retrieved 2023-12-17, from https://www.ngdc.noaa.gov/geomag/calculators/magcalc.shtml#igrfwmm

Nuntiyakul, W., Sáiz, A., Ruffolo, D., Mangeard, P.-S., Evenson, P., Bieber, J. W., ... Humble, J. E. (2018). Bare neutron counter and neutron monitor response to cosmic rays during a 1995 latitude survey. *Journal of Geophysical Research: Space Physics*, *123*(9), 7181–7195. doi: 10.1029/2017JA025135

Oh, S., Bieber, J. W., Evenson, P., Clem, J., Yi, Y., & Kim, Y. (2013). Record neutron monitor counting rates from galactic cosmic rays. *J. Geophys. Res. Space Physics*, *118*, 5431-5436. doi: 10.1002/jgra.50544

Paschalis, P., Mavromichalaki, H., Yanke, V., Belov, A., Eroshenko, E., Gerontidou, M., & Koutroumpi, I. (2013). Online application for the barometric coefficient calculation of the nmdb stations. *New Astronomy*, *19*, 10–18.

Patil, A., Fersch, B., Hendricks-Franssen, H.-J., & Kunstmann, H. (2021). Assimilation of Cosmogenic Neutron Counts for Improved Soil Moisture Prediction in a Distributed Land Surface Model. *Frontiers in Water*, *3*. doi: 10.3389/frwa.2021.729592

Rasche, D., Köhli, M., Schrön, M., Blume, T., & Güntner, A. (2021). Towards disentangling heterogeneous soil moisture patterns in cosmic-ray neutron sensor footprints. *Hydrology and Earth System Sciences*, *25*(12), 6547–6566. doi: 10.5194/hess-25-6547-2021

Rasche, D., Weimar, J., Schrön, M., Köhli, M., Morgner, M., Güntner, A., & Blume, T. (2023). A change in perspective: downhole cosmic-ray neutron sensing for the estimation of soil moisture. *Hydrology and Earth System Sciences*, *27*(16), 3059–3082. doi: 10.5194/hess-27-3059-2023

Rockenbach, M., Dal Lago, A., Schuch, N. J., Munakata, K., Kuwabara, T., Oliveira, A., ... others (2014). Global muon detector network used for space weather applications. *Space Science Reviews*, *182*, 1–18. doi: 10.1007/s11214-014-0048-4

Rosolem, R., Shuttleworth, W. J., Zreda, M., Franz, T. E., Zeng, X., & Kurc, S. a. (2013, October). The Effect of Atmospheric Water Vapor on Neutron Count in the Cosmic-Ray Soil Moisture Observing System. *Journal of Hydrometeorology*, *14*(5), 1659–1671. doi: 10.1175/JHM-D-12-0120.1

Ruffolo, D., Sáiz, A., Mangeard, P.-S., Kamyan, N., Muangha, P., Nutaro, T., ... Munakata, K. (2016). Monitoring short-term cosmic-ray spectral variations using neutron monitor time-delay measurements. *The Astrophysical Journal*, *817*(1), 38. doi: 10.3847/0004-637x/817/1/38

Sapundjiev, D., Nemry, M., Stankov, S., & Jodogne, J.-C. (2014). Data reduction and correction algorithm for digital real-time processing of cosmic ray measurements: NM64 monitoring at Dourbes. *Advances in Space Research*, *53*(1), 71–76. doi: 10.1016/j.asr.2013.09.037

Schmidt, T., Schrön, M., Li, Z., Francke, T., Zacharias, S., Hildebrandt, A., & Peng, J. (2024). Comprehensive quality assessment of satellite- and model-based soil moisture products against the COSMOS network in Germany. *Remote Sensing of Environment*, *301*, 113930. doi: 10.1016/j.rse.2023.113930

Schrön, M. (2017). *Cosmic-ray neutron sensing and its applications to soil and land surface hydrology* (phdthesis, University of Potsdam). Retrieved 2023-05-10, from https://publishup.uni-potsdam.de/frontdoor/index/index/docId/39543 (Thesis)

Schrön, M., Köhli, M., & Zacharias, S. (2023). Signal contribution of distant areas to cosmic-ray neutron sensors – implications for footprint and sensitivity. *Hydrol. Earth Syst. Sci.*, *27*(3), 723–738. doi: 10.5194/hess-27-723-2023

Schrön, M., Zacharias, S., Köhli, M., Weimar, J., & Dietrich, P. (2016, August). Monitoring environmental water with ground albedo neutrons from cosmic rays. In *Proceedings of the 34th international cosmic ray conference — pos(icrc2015).* Sissa Medialab. doi: 10.22323/1.236.0231

Schrön, M., Zacharias, S., Womack, G., Köhli, M., Desilets, D., Oswald, S. E., ... Dietrich, P. (2018). Intercomparison of cosmic-ray neutron sensors and water balance monitoring in an urban environment. *Geoscientific Instrumentation, Methods and Data Systems*, *7*(1), 83–99. doi: 10.5194/gi-7-83-2018

Sentelhas, P. C., Dalla Marta, A., & Orlandini, S. (2008). Suitability of relative humidity as an estimator of leaf wetness duration. *Agricultural and Forest Meteorology*, *148*(3), 392–400. doi: 10.1016/j.agrformet.2007.09.011

Simpson, J. A. (1983). Elemental and isotopic composition of the galactic cosmic rays. *Annual Review of Nuclear and Particle Science*, *33*(1), 323-382. doi: 10.1146/annurev.ns.33.120183.001543

Stevanato, L., Baroni, G., Oswald, S. E., Lunardon, M., Mares, V., Marinello, F., … Rühm, W. (2022). An Alternative Incoming Correction for Cosmic-Ray Neutron Sensing Observations Using Local Muon Measurement. *Geophysical Research Letters*, *49*(6). doi: 10.1029/2021gl095383

Tian, Z., Li, Z., Liu, G., Li, B., & Ren, T. (2016). Soil water content determination with cosmic-ray neutron sensor: Correcting aboveground hydrogen effects with thermal/fast neutron ratio. *Journal of Hydrology*, *540*, 923–933. doi: 10.1016/j.jhydrol.2016.07.004

Usoskin, I. G., Bazilevskaya, G. A., & Kovaltsov, G. A. (2011). Solar modulation parameter for cosmic rays since 1936 reconstructed from ground-based neutron monitors and ionization chambers. *Journal of Geophysical Research: Space Physics*, *116*(A2). doi: 10.1029/2010JA016105

Väisänen, P., Usoskin, I., & Mursula, K. (2021). Seven decades of neutron monitors (1951–2019): Overview and evaluation of data sources. *Journal of Geophysical Research: Space Physics*, *126*(5), e2020JA028941. doi: 10.1029/2020JA028941

Weber, M., Rinke, K., Hipsey, M., & Boehrer, B. (2017). Optimizing withdrawal from drinking water reservoirs to reduce downstream temperature pollution and reservoir hypoxia. *Journal of Environmental Management*, *197*, 96—105. doi: 10.1016/j.jenvman.2017.03.020

Weimar, J. (2022). *Advances in Cosmic-Ray Neutron Sensing by Monte Carlo simulations and neutron detector development* (phdthesis, Heidelberg University). Retrieved 2023-01-17, from `https://archiv.ub.uni-heidelberg.de/volltextserver/32046/` (Thesis)

Weimar, J., Köhli, M., Budach, C., & Schmidt, U. (2020). Large-scale boron-lined neutron detection systems as a 3he alternative for cosmic ray neutron sensing. *Frontiers in Water*, *2*. doi: 10.3389/frwa.2020.00016

Zhang, X., Wang, K., Frassl, M. A., & Boehrer, B. (2020). Reconstructing six decades of surface temperatures at a shallow lake. *Water*, *12*(2), 405. doi: 10.3390/w12020405

Zreda, M., Desilets, D., Ferré, T. P. A., & Scott, R. L. (2008). Measuring soil moisture content non-invasively at intermediate spatial scale using cosmic-ray neutrons. *Geophysical Research Letters*, *35*(21). doi: 10.1029/2008GL035655

Zreda, M., Shuttleworth, W. J., Zeng, X., Zweck, C., Desilets, D., Franz, T. E., & Rosolem, R. (2012). COSMOS: The COsmic-ray Soil Moisture Observing System. *Hydrology and Earth System Sciences*, *16*(11), 4079–4099. doi: 10.5194/hess-16-4079-2012